Design and production of a candidate universal influenza A vaccine in *Nicotiana benthamiana* plants

Francisco De Figueiredo Pinto Gomes Pêra

University of Cape Town

Dissertation presented for the degree of Master of Science

Department of Molecular and Cell Biology

University of Cape Town

February 2017

The copyright of this thesis vests in the author. No quotation from it or information derived from it is to be published without full acknowledgement of the source. The thesis is to be used for private study or non-commercial research purposes only.

Published by the University of Cape Town (UCT) in terms of the non-exclusive license granted to UCT by the author.

University of Cape Town

Name: Francisco De Figueiredo Pinto Gomes Pêra

Student Number: DFGFRA001

Course: MCB5005W

Declaration

I know that plagiarism is wrong. Plagiarism is to use another's work and pretend that it is one's own.

I have used the **Harvard** convention for citation and referencing. Each contribution to, and quotation in, this **Dissertation** from the work(s) of other people has been attributed, and has been cited and referenced.

This **Dissertation presented for the degree of Master of Science in the Department of Molecular and Cell Biology** is my own work.

I have not allowed, and will not allow, anyone to copy my work with the intention of passing it off as his or her own work.

Signature Signature removed

Date: 13 February 2017

Acknowledgments

I would like to take a moment to acknowledge the following people:

- To my supervisor, Dr. Inga Hitzeroth and co-supervisors, Prof. Ed Rybicki and Dr. Suzanne Huddy, I wish to express my profound gratitude for giving me this opportunity and also for giving me the intellectual freedom to explore and develop my project. You have served as exemplary role models and thanks to you, I have learned tremendously from this journey.
- To Dr. Ann Meyers and Aleyo Chabeda, despite not being my formal supervisors, you have always given me advice and guidance when I needed, and for this I am truly grateful.
- To all the team in the Biopharming Research Unit for being extraordinary colleagues and people. You have made me come to work every day with a smile.
- To all the team in the Microscopy Unit, specially to Dr. Mohammed Jaffer for being extremely patient and providing excellent (much needed) technical assistance when using the transmission electron microscope.
- To Rodney Lucas and the UCT Animal Unit, for the advice with regards to the animal study and for taking care of the rabbits used in this study.
- The Lomonossof lab for providing the pEAQ-HT expression vector and the Fraunhofer IME for providing the pTRAc expression vector.
- To the Medical Research Council of South Africa (MRC) for funding this project as well as the Poliomyelitis Research Foundation (PRF) and the Biopharming Research Unit (BRU) for financial support.
- To my friends and family for your continuous love and support; specially to my parents, Isabel Pinto and Fernando Pêra, my brother Miguel and sister Laura; my brothers from another mother: Alan Liao (廖翔宇), Scott De Beer, Matthew Kiddingsh, Nick Passerin and Hendrik Els; and of course, to my love, Lise Baraton because none of this could be possible without you.

"The best time to plant a tree was 20 years ago. The second best time is now."

Chinese Proverb

Abstract

The influenza A virus is responsible for 250,000 to 500,000 deaths every year worldwide and millions more could die in the event of a serious pandemic. Vaccines against influenza have existed for long, but until today they have been limited by extensive production times and reduced cross-protection between different strains of the virus. This leads to a recurrent need to update the vaccine composition every year, which is both costly and inadequate to fight pandemics.

An innovative approach that could improve the vaccine efficacy has been recently developed based on the selection of conserved influenza epitopes with potential to induce broader immune responses. The 23-amino acid extracellular domain of the M2 protein (M2e) is highly conserved among different influenza A strains and thus it seems like an ideal candidate for a universal influenza vaccine. However, due to its small size, it is a poor immunogen when used on its own.

The aim of this project was to produce M2e-presenting virus-like particles (VLPs) in *Nicotiana benthamiana* plants via Agrobacterium-mediated transient expression. Plants are increasingly being examined as alternative recombinant protein expression systems due to their safety, scalability and rapid production times. Moreover, numerous studies suggest the use of recombinant virus-like particles (VLPs) to increase the immunogenicity of antigens. Therefore, to obtain VLPs presenting the M2e epitope, I genetically engineered several different M2e-HA fusion proteins by replacing the hemagglutinin (HA) globular head and main epitope with five tandem repeats of M2e epitope sequences (5xM2e) from human, swine, and avian origin influenza A viruses. To increase the chances of obtaining VLPs, M2e-HA fusions either contained the HA stalk domain (5xM2e-HAstalk) or simply the transmembrane region (5xM2e-HAtrans). Furthermore, the tetramerizing leucine zipper derived from the General Control Protein (GCN4) was also included in some of the constructs to promote particle formation. In total, six different M2e-HA fusions were created: 5xM2e-GCN4-HAstalk, 5xM2e-GCN4-HAtrans, 5xM2e-HAstalk, 5xM2e-HAtrans, 1xM2e-HAstalk and 1xM2e-HAtrans. The expression of these proteins was optimized in plants by testing different conditions and using three different expression vectors. Overall, I was able to show expression after only 3 days post-infiltration for most of the M2e-HA

fusion proteins utilizing the pEAQ-HT and pRIC 3.0 expression vectors whereas expression levels with pTRAc were low or non-detectable.

Once the expression of the M2e-HA fusions was optimized, the two proteins with the highest potential to form VLPs were selected for further characterization (5xM2e-HAstalk and 5xM2e-HAtrans). Using transmission electron microscopy to analyse purified proteins, both 5xM2e-HAstalk and 5xM2e-HAtrans were shown to assemble into VLPs resembling the shape and size of native HA VLPs. These VLPs could also be observed in the apoplastic fractions of infiltrated leaves. However, due to the low number of particles observed, the successful incorporation of the M2e peptide on the surface of the particles was inconclusive, as shown by M2e-specific immuno-gold labelling experiments. Furthermore, contrarily to previous studies, co-expression of the M2e-HA fusions with the M1 protein resulted in a decrease in recombinant protein accumulation and VLP formation in our plant system. A possible inhibition mechanism by the M1 protein is discussed.

In summary, this research provides preliminary data to produce universal influenza vaccines in plants. I report here for the first time that M2e fused to either the stalk or transmembrane domain of the HA protein, can self-assemble into VLPs without any other proteins, in *N. benthamiana* plants. Future work on the immunogenicity of the VLPs produced in this study is required to confirm their potential as a universal influenza vaccine that can be rapidly produced.

Table of contents

Abbreviations

A	alanine
bp	base pairs
BCIP	5-bromo, 4-chloro, and 3-indolylphosphate
BSA	bovine serum albumin
CAMV	Cauliflower mosaic virus
CPMV	Cowpea mosaic virus
DNA	deoxyribonucleic acid
dNTP	deoxy-ribonucleoside triphosphates (dATP, dCTP, dTTP and dGTP)
dpi	days post infiltration
E	glutamic acid
EDTA	ethylenediaminetetra-acetic acid
ELISA	enzyme linked immunosorbent assay
ER	endoplasmic reticulum
g	gram(s)
GCN4	general control nondepressible 4
H	histidine
HA	haemagglutinin
hr(s)	hour(s)
IIV	inactivated influenza vaccines
IPTG	isopropylthio-β-D-galactoside
K	lysine
kb	kilobase(s)

kDa	kilodalton(s)
L	litre(s)
LAIV	live attenuated influenza vaccine
LB	Luria broth
LPS	lipopolysaccharide
M	molar
M1	matrix protein 1
M2	matrix protein 2
mA	milli-amperes
MES	2-morpholinoethanesulfonic acid
mg	milligram(s)
min	minute(s)
mL	millilitre(s)
mM	millimolar
NA	neuraminidase
ng	nanogram(s)
nm	nanometre(s)
O/N	overnight
OD	optical density
PAGE	polyacrylamide gel electrophoresis
PBS	phosphate buffered saline
PCR	polymerase chain reaction
PTGS	post-transcriptional gene silencing
RNA	ribonucleic acid
RNP	ribonucleoprotein complex

rpm	revolutions per minute
RT	room temperature
s	second(s)
SDS	sodium dodecyl sulphate
TB	terrific roth
TBE	Tris-borate-EDTA buffer
T-DNA	transfer-DNA
TEM	transmission electron microscopy
TSP	total soluble protein
TSWV	Tomato spotted wilt virus
Tris	tris(hydroxymethyl)aminomethane
UTR	untranslated region
UV	ultraviolet
V	volts
v	volume
VLP(s)	virus-like particle(s)
w	weight
wt	wild type
µF	microfarad
µg	microgram(s)
µL	microlitre(s)
µm	micrometre(s)
%	percentage
°C	degrees Celsius
Ω	resistance

Chapter 1: Literature review

1.1. Introduction

Influenza is a highly infectious virus that has been causing acute respiratory illness in humans for thousands of years. Infections are often characterised by the sudden onset of fever, muscle pain, headache, and severe malaise, together with a sore throat, and nasal inflammation (Ayllon et al. 2012). Modern historians hypothesize that the first "flu-like" disease outbreak was reported in 412 BC by Hippocrates (Ghendon 1994). Since then, influenza viruses have caused some of the most devastating pandemics that humankind has ever faced. The most well-known example is the famous "Spanish flu" which infected about one third of the world's population (± 500 million) and killed between 50-100 million people around the world during 1918 and 1919 (Johnson & Mueller 2002; Taubenberger & Morens 2006). The Spanish flu pandemic killed more people than during the First World War, and it is estimated to have reduced life expectancy in the United States by 10 years (Howley 2013). Influenza pandemics have been taking place randomly every 10 to 40 years; adding up to a total of 32 (including the 2009 H1N1 "swine flu" pandemic) since the first influenza pandemic was documented in 1580 (Kendall 2007).

More routinely, influenza viruses also cause smaller outbreaks called "epidemics" or "seasonal flu"; their cumulative burden on human societies is sometimes more devastating than pandemics (Cox et al. 2004). It has been estimated that each year, influenza infects about 10 - 20% of the total worldwide population and is responsible for 250,000 to 500,000 deaths (De Filette et al. 2005). In the United States alone, the total economic burden of annual influenza epidemics has been evaluated to $87.1 billion dollars. This takes into account an average of 610,660 life-years lost, 3.1 million hospitalized days, and 31.4 million outpatient visits (Molinari et al. 2007).

Nowadays, the two major strategies to fight influenza infections are with the use of antiviral drugs and vaccines. Antivirals can be effective but they can quickly become obsolete against recurrent resistant strains. Also, antivirals are typically costly (since they need to be taken daily) and they can only be used for therapeutic purposes. On the other hand, vaccines can be made to preventively combat a specific influenza strain, and vaccination is generally required only once

or twice for a particular strain. For these reasons, vaccination is considered the most cost-effective way of controlling and preventing influenza infection (Saluja 2010).

There are many types of flu vaccines on the market, with inactivated vaccines made of purified spike proteins and disrupted virus particles being the most common; however, currently every type of influenza vaccine only offers strain-specific immunogenicity. And so, as influenza viruses can very rapidly undergo unpredictable antigenic drifts/shifts, it is required to re-design vaccines based on varying strains for every seasonal, epidemic and pandemic immunization (Krammer et al. 2014).

Apart from the lack of protection against variant strains, the use of traditional inactivated vaccines is also constrained by the need for specialized egg-based production facilities and long production times required for the creation of a new vaccine. Currently, inactivated influenza vaccines are made from viruses grown in the allantoic cavity of embryonated hens' eggs. Efficient vaccine production in embryonated eggs requires selection of a high yield, reassorted virus strain that can replicate in the egg without killing it. All this makes production expensive, time-consuming and potentially dangerous, as live viruses have to be handled (D'Aoust et al. 2010; D'Aoust et al. 2008). For instance, during the recent 2009 H1N1 pandemic, health authorities only released a candidate vaccine more than six months after the first outbreak was reported. This was already in the second wave of the pandemic. Luckily the 2009 pandemic turned out to be only of mild severity with a low case-fatality rate. However, it is clear that an alternative to current vaccines needs to be found.

Emerging and re-emerging influenza A infections in humans and animals have been reported with increased frequency in recent years (Morens et al. 2004). The threat of highly virulent avian influenza, such as H5N1 and swine-origin H1N1 viruses, emphasizes an urgent need to develop a universal influenza vaccine, which could provide cross-protection against different influenza virus strains, and longer-lasting and more universal protection.

1.2. Classification and structure

1.2.1. Classification

Influenza A viruses belong to the *Orthomyxoviridae* family which according to the International Committee on Taxonomy of Viruses (ICTV), consists of six genera: these are *Influenzavirus A, Influenzavirus B, Influenzavirus C, Isavirus, Thogotovirus*, and the recently added *Quaranjavirus* (International Committee on Taxonomy of Viruses 2014). All of the *Orthomyxoviridae* viruses have segmented single-stranded negative sense RNA genomes. However only viruses in the *Influenzavirus* genera are known to infect humans; with the exception of a few reported cases of thogotovirus human infections (Kosoy et al. 2015; Butenko et al. 1987). Despite being able to infect humans, the three types of influenza viruses are significantly different from each other; such differences include (but are not limited to): the number of RNA segments, pathogenicity, antigenic differences in the major internal proteins of the virus, morphological features, protein-encoding mechanisms, and host range infectivity (Knipe 2001).

Influenza B and C viruses were first isolated in 1940 and 1949 respectively (Francis 1940; Taylor 1949). Both of these viruses normally only infect humans, but there have been some reports of influenza B isolated from seals and influenza C from pigs and dogs (Osterhaus et al. 2000; Guo et al. 1983). Type A influenza viruses, on the other hand, have a natural host in aquatic birds, and can infect a wide variety of mammals including humans, horses, swine, domestic and wild birds and other mammals (Suarez & Schultz-Cherry 2000). All influenza A types can infect birds, with the exception of the two newly discovered subtypes H17N10 and H18N11 which have only been found in bats (Wu et al. 2014). Only types A and B cause human disease of any concern, with type A being responsible for every pandemic and most epidemics (Deng et al. 2015). Accordingly, only the type A will be discussed in detail in this review.

The influenza A virus was first isolated from humans in 1933 by Wilson Smith, Sir Christopher Andrewes, and Sir Patrick Laidlaw at the National Institute for Medical Research (NIMR) outside of London. They showed that the virus could infect ferrets and used them to propagate the virus in the laboratory (Smith et al. 1933). It was only in 1975 that the virus was first successfully maintained in MDCK cells after the discovery that the addition of trypsin to culture media was

necessary (Tobita et al. 1975). Since then, influenza A has been one of the most studied human viruses in the last century.

The nomenclature given to different influenza strains is done firstly according to their genus (type), the species from which the virus was isolated (except for humans), location of the isolate, the number of the isolate, the year of isolation, and, for influenza A viruses, the haemagglutinin (H) and neuraminidase (N) subtypes is given in parentheses at the end. For example, A/Vietnam/1194/2004 (H5N1), is the 1194th isolate of an H5N1 subtype virus isolated from humans in Vietnam in 2004. According to the US Centers for Disease Control and Prevention (CDC) there are currently 18 different haemagglutinin (H1 to H18) subtypes and 11 different neuraminidase (N1 to N11) subtypes for influenza A viruses (CDC, 2013).

1.2.2. Structure

The influenza A virion has a pleomorphic shape: it is typically spherical or elliptical (Figure 1A), ranging from 80-120 nm in diameter but it can occasionally be filamentous (Figure 1B), reaching more than 20 µm in length. Surprisingly, most laboratory-adapted strains of influenza A virus are primarily spherical or elliptical, whereas clinical isolates are generally filamentous and their

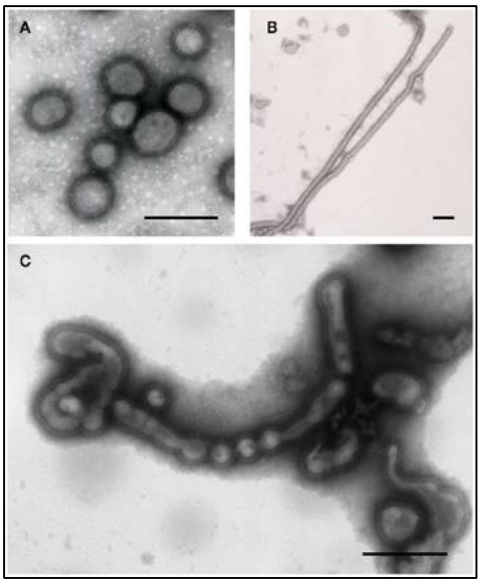

Figure 1| Different shapes of influenza A virions captured by Transmission Electron Microscopy. A) Spherical and eliptical-shaped virions from the strain [A/WSN/33 (H1N1)]. B) Filamentous-shaped virions from [A/Udorn/307/72 (H3N2)]. C) Irregular-shaped virions from [A/Puerto Rico/8/34 (H1N1)]. Bars represent 200nm (Noda 2012).

adaptation in eggs results in the loss of this filamentous phenotype (Noda 2012). The significance of the filamentous morphology for virus replication and pathogenesis remains unclear, but it is thought to be a genetic trait that is essential for virus survival in nature. There have also been reports of influenza virions with irregular shapes (Figure 1C), but this has been associated with artefacts introduced during sample preparation procedures that involve ultracentrifugation and storage (Almeida & Waterson 1967; Stevenson & Biddle 1966).

Besides its complex shape, influenza A virions possess a lipid envelope that is derived from the host plasma membrane during budding. From this membrane, two surface glycoproteins bulge out: the rod-shaped haemagglutinin (HA) assembled in trimers, and tetramers of the mushroom-shaped neuraminidase (NA) (Figure 2). These surface proteins form 10-14nm "spikes" on the surface of the virion, which are readily observable using negative stain electron microscopy. It is estimated that there are four HA subunits for each NA (Howley 2013). Embedded within the membrane is the relatively small matrix protein 2 (M2), whilst the matrix protein 1 (M1) is underneath the envelope. Within the matrix lies the influenza A segmented genome: eight negative-sense RNA strands, each wrapped up into a rod-shaped, double-helical ribonucleoprotein complex (RNP). Each RNP can be between 30-110nm (corresponding with the size of its associating vRNA) and contains a viral RNA bound to multiple copies of the nucleocapsid

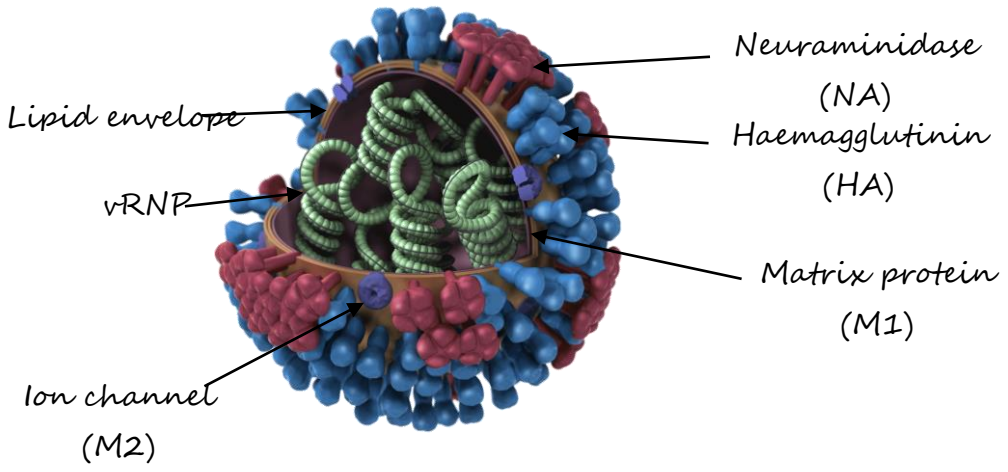

Figure 2| Schematics of influenza A virion structure. HA, NA and M2 are the outer envelope proteins. M1 forms the core of the virion which protects the genomic material: eight negative-sense RNA strands, each wrapped up into a viral ribonucleoprotein complex (vRNP). Adapted from the CDC webpage - http://www.cdc.gov/flu/images.htm.

protein (NP) and the heterotrimeric viral polymerase, consisting of PA, PB1, and PB2 proteins (Zheng & Tao 2013). The estimated composition of influenza virus particles is about 1% RNA, 5% to 8% carbohydrate, 20% lipid, and approximately 70% protein (Howley 2013).

1.2. Replication

Influenza virus attachment to the cell host is mediated by the specific binding of the HA spikes to sialic acid residues present on host cell surface glycoproteins or glycolipids. Two major linkages exist between sialic acids and the carbohydrates they are bound to: these are α(2,3) and α(2,6). Epithelial cells in the human trachea have predominantly the α(2,6) linkage whereas gut epithelial cells from ducks have the α(2,3) linkage (Knipe 2001). Receptor specificity to sialic acid linkages is thought to be an important determinant of host range (Cox & Subbarao 2000). In agreement with this is that human influenza viruses preferably bind to sialic acids with an α(2,6) linkage, whereas avian and equine influenza viruses bind to an α(2,3) linkage (Knipe 2001). There have been relatively few reports of direct natural human infections with avian influenza, with the notable exceptions of the 1997 and 2004 Hong Kong H5N1 outbreaks and continuing sporadic transmissions of H5N1 in several countries worldwide (Kandun et al. 2006; Chan 2002; Tran et al. 2004; Beigel et al. 2005; Gao et al. 2013; Butt et al. 2005).

Exceptionally, the trachea of pigs possesses both sialic acid linkages, making them susceptible to both avian and human influenza (Naffakh & van der Werf 2009; Brown 2000; Hass et al. 2011; Ma et al. 2008). Because of the segmented nature of the influenza genome, pigs that are infected with both avian and human influenza viruses can be seen as “mixing vessels” for avian and human influenza viruses to exchange or reassort whole fragments of their genome; thus, giving rise to novel influenza strains. This event is called “antigenic shift” and it can potentially result in the production of new dangerous pathogenic viruses by introducing a new HA or NA from another subtype, one that had not circulated in humans for a long time or even one that had never circulated in humans before. The most recent example of this, was the appearance of the reassortant 2009 H1N1 pandemic strain known as “swine flu”. This strain of influenza contained three classical swine genes (HA, NP, and NS1), one human gene (PB1), two North American

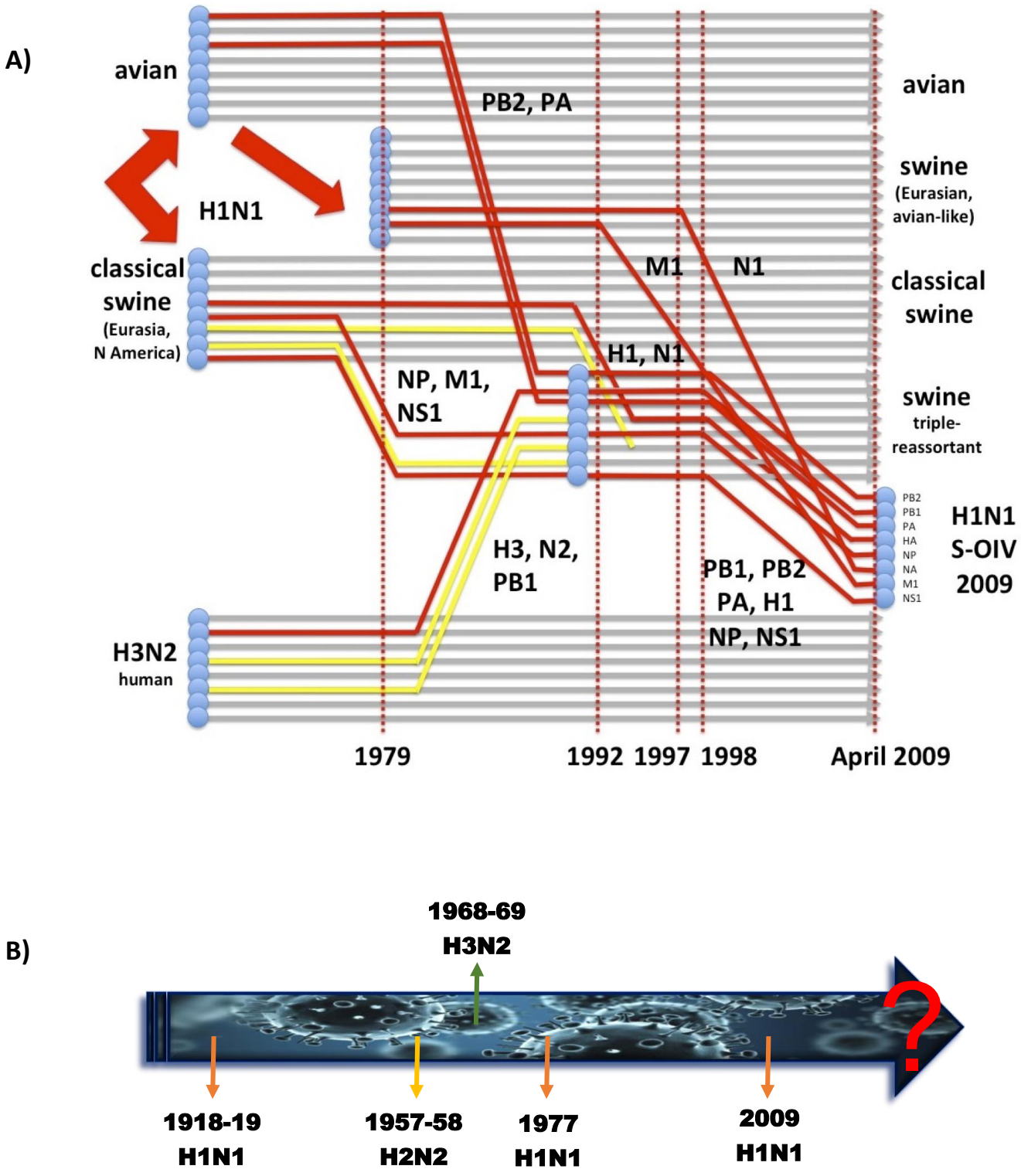

Figure 3| A) Origin of the Swine Influenza H1N1pdm 2009 strain. Blue circles represent complete influenza A virus genomes; grey lines are genes that remained unchanged; yellow lines are genes that reassorted but did not end up into the 2009 H1N1 strains; red lines show origins of specific genetic components. Reprinted with permission from Prof. Ed Rybicki. Copyright (Rybicki & Kightley 2015). B) Influenza A pandemics of the 20th century.

avian genes (PB2 and PA), and two Eurasian avian-like swine genes (N1 and M1) (Figure 3A); it was unrelated to the human seasonal H1N1 viruses that have been in general circulation among people since 1977 (del Rio & Guarner 2010; Rybicki & Kightley 2015).

Since the beginning of the 20th century there have been five major antigenic shifts that resulted in viruses that caused pandemics (Figure 3B): in 1918 the appearance of H1N1 started the "Spanish Influenza"; in 1957, the H1N1 subtype was replaced with H2N2, which caused the "Asian Influenza"; in 1968 the H2N2 replacement with H3N2 led to the beginning of the "Hong Kong Influenza", in 1977 the H1N1 reappeared in Russia thus starting the "Russian Influenza" and finally the "Swine Flu" in 2009 with the new triple reassortant H1N1, antigenically distinct from previous strains, that caused a mild pandemic and largely replaced previous seasonal H1N1 viruses in the human population (Kilbourne 2006; Taubenberger 2006; Brown 2000; Lagacé-Wiens et al. 2010). It is important to note that these shifts occurred sporadically and after irregular periods of time, making predictions for the next shift effectively impossible. It has further been postulated that pigs could even act as reservoirs for avian influenza, allowing them to slowly adapt to humans without the need of reassortment (Ito et al. 1998).

Besides the ability to easily reassort with other subtypes, the influenza virus is also incredibly susceptible to mutations in its genome. This is because the influenza RNA-dependent RNA polymerase lacks proofreading, resulting in replication errors at a rate of about one in every 10^4 bases (Holland et al. 1982). Given that the influenza A genome is about 13.6 kb long, this equals to about 1 base pair mutation per genome (Holland et al. 1982). Not surprisingly, most of these mutations are not viable and end up killing the virus. However sometimes, key mutations in the antigenic regions of the HA or NA proteins allow the virus to escape antibody neutralization and even create anti-viral drug resistance (as explained in the next section) (Wilson et al. 1981; Samson et al. 2013; Hayden & de Jong 2011; Rambaut et al. 2008; Scholtissek et al. 1993). These mutations typically cause epidemics that can prevail for 1 to 5 years before being replaced by a different variant (Howley 2013). More importantly, other than mutations in the antigenic regions, mutations in functional regions can drastically increase the pathogenicity of the virus.

For example, upon binding to the sialic acid residues, the HA precursor must be cleaved for endocytosis to occur. In its precursor conformation, the HA molecule is named HA0. HA0 is made up of two subunits linked by disulfide bonds: HA1, which contains the sialic acid receptor binding domain, and HA2, which contains the fusion peptide. For viral activation and internalization, HA0 must be cleaved by a trypsin-like serine endoprotease at the specific cleavage site, between the HA1 and HA2 domains of the protein. In mammals like humans and swine, this specific protease is only expressed in the epithelial cells of the upper and lower respiratory tract, which restricts the replication of the virus to those areas. On the other hand, in aquatic birds normal influenza replication takes place in the intestinal tract, because it is the only location where the protease is produced. In both cases these are considered to be “normal” regions for influenza replication, and usually only cause mild symptoms.

However, in some cases, influenza viruses can undergo mutational changes in the HA cleavage site, thus making them able to be cleaved by ubiquitous cellular proteases. Consequently, the virus can then replicate in different organs including the spleen, liver, lungs, kidneys, and brain, making it highly pathogenic. This is the case for some of the H5 and H7 HA proteins that have multiple basic amino acid residues at the HA1-HA2 cleavage site. Any type of mutation in the influenza genome that affects immunogenic proteins is commonly called “antigenic drift”.

1.3. Influenza treatments

1.3.1. Antiviral drugs

At present, there are two classes of drugs approved and on the market against influenza, the adamantanes and the neuraminidase inhibitors.

The two adamantane derivatives in use for influenza treatment since the mid-to-late 1960s are amantadine and rimantadine (Kato & Eggers 1969). These drugs are effective against all subtypes of influenza A virus, but not against influenza B or C viruses (Howley 2013). They work by specifically targeting and blocking the proton channel formed by the influenza A virus M2 protein, thereby inhibiting the acidification of the virion interior and thus, viral uncoating. Treatment of most influenza A strains with amantadine or rimantadine results in symptomatic improvements, including accelerated clearance of local symptoms and fever; the overall duration of illness is

estimated to be reduced by about 1.5 - 2.5 days (Stiver 2003). Until 2004, the proportion of resistance to adamantane-derived dugs among seasonal influenza viruses remained low. However, during the 2003 to 2004 season, the rate of resistance in seasonal H3N2 viruses increased to 12.3% and one year later more than 90% of all H3N2 viruses were resistant to adamantane compounds. This is typically attributed to a S31N point mutation in the M2 gene that makes the virus resistant to both adamantane drugs (Wathen et al. 2013; Nelson et al. 2009). Nowadays, most circulating human H3N2 viruses, the 2009 swine-origin H1N1 pandemic virus, and some highly pathogenic avian H5N1 influenza viruses are resistant to ion channel inhibitors (Govorkova et al. 2013; Malik Peiris et al. 2009; Bright et al. 2006; Bright et al. 2005). In fact, resistance to amantadine and rimantadine is so frequent that most health authorities worldwide recommended that neither be used anymore for the treatment and prevention of influenza A infections (WHO 2015; Walaza & Cohen 2015). This situation has resulted in a heavy reliance on the neuraminidase inhibitors.

Neuraminidase inhibitors were only approved in the late 90's and are mainly composed of two drugs: oseltamivir (Tamiflu®) and zanamivir (Relenza®). Like the name indicates, these drugs act by targeting the neuraminidase protein. However, contrarily to ion channel inhibitors that act in the early stages of replication, NA inhibitors have an effect towards the end of the replication cycle. They bind to the NA protein of the virus and inhibit the budding viruses from being released from cellular surfaces. If treatment is started early they can statistically reduce symptoms, the duration of illness and the amount of virus shed; however, treatment later in infection may still be beneficial (Jefferson et al. 2009; Monto et al. 1999; Laver et al. 1999; Louie et al. 2010). Drug resistant mutant strains are less common than those seen with the ion channel inhibitors, but have been reported (Hurt et al. 2009; Baranovich et al. 2010; Sheu et al. 2008). Nevertheless, NA inhibitors are recommended by the WHO as the primary treatment for human HPAI H5N1 virus infections (WHO 2015).

In conclusion, antiviral drugs can be efficiently used for treatment to potentially shorten the duration and decrease the severity of influenza infections. They can also be a useful tool in the early stages of a new outbreak when vaccines are not available. However, due to the increased appearance of mutant resistant strains, their use for chemoprophylaxis is currently not

recommended by the WHO (Walaza & Cohen 2015). Even though additional antiviral drugs with novel mechanisms of action are currently being tested, vaccination remains the solely accepted method to prevent influenza infections (Shaw 2011; Darwish et al. 2011).

1.3.2. Current vaccines

Vaccination is the most cost-effective means to prevent influenza virus infections and complications. It can significantly reduce and lessen the symptoms associated with influenza disease, especially for groups at risk including young children and the elderly. During the 2012 - 13 period, the CDC estimates that in the USA 42.4 million people were vaccinated against influenza, which prevented an estimated 6.6 million illnesses, 3.2 million medically attended illnesses, and 79,260 hospitalizations (Centers for Disease Control and Prevention (CDC) 2013).

There are three different classes of vaccines that have been licensed against seasonal influenza, which are inactivated, live attenuated, and recombinant HA vaccines (Centers for Disease Control and Prevention (CDC), 2013). All three vaccine types focus on the production of neutralizing antibodies against the HA protein and in some cases against the NA protein as well, to neutralize the virus and prevent infection (Gerhard 2001). These vaccines are generally trivalent, containing H1N1 and H3N2 subtypes of influenza A along with the predicted dominant lineage of influenza B (Belshe et al. 1998; Houser & Subbarao 2015). Recently, several quadrivalent formulations containing two distinct lineages of influenza B have been licensed and are also currently on the market (Traynor 2012).

Inactivated vaccines

Inactivated influenza vaccines (IIVs) are generally produced by propagation of the virus in the allantoic fluid of embryonated hens' eggs and then purifying and concentrating it by zonal centrifugation or column chromatography. The first influenza inactivated vaccines administered to humans consisted of whole-inactivated virus treated with either formalin or β-propiolactone for inactivation (Logrippo 1960). However, even though whole virus vaccines were shown to be highly immunogenic, they were later correlated with severe reactogenicity and adverse effects among the vaccinated, and so are no longer widely used (Gross et al. 1977). To reduce adverse reactions, vaccine virus preparations are now further disrupted by treatment with a nonionic

detergent (for example, Triton X-100) to make so-called “split vaccines” which may be partially purified by ultracentrifugation (subunit vaccines) to remove viral ribonucleoprotein complexes. The end product for subunit vaccines is composed of membrane vesicles that mostly contain the HA glycoprotein.

The amount of immune-reactive HA recommended by the Advisory Committee on Immunization Practices to confer protection for adults and older children is 15 µg of each purified HA protein administered intramuscularly, or 9 µg of each purified HA protein administered intradermally (Center for Disease Control and Prevention (CDC) 2013). This dose is approximately equivalent to the amount of purified virus obtained from the allantoic fluid of one to three infected embryonated eggs, depending on the strain of the virus. A higher dose of 60 µg for each HA is also available for the elderly population aged 65 years and older to increase immunogenicity (DiazGranados et al. 2014).

While inactivated vaccines do elicit strong type-specific antibody responses dominated by circulating IgG against the HA and NA proteins, they have been shown to induce poor levels of mucosal IgA antibody and cell-mediated immune responses (Cox et al. 2004; Blazevic et al. 2000).

The degree of protection conferred by inactivated vaccines is highly dependent on the age of the vaccinee and his or her history of influenza, and also on the antigenic match between the vaccine strains and those circulating in the population (Cox et al. 2004). Overall, IVs are 50 - 90% effective among young adults and children, but have lower efficacy in elderly populations (Jackson et al. 2010; Goodwin et al. 2006; DiazGranados et al. 2012; Jefferson et al. 2005; Osterholm et al. 2012; Cox et al. 2004)

Live-attenuated vaccines

The second type of licensed influenza vaccine is the live attenuated influenza vaccine (LAIV). Current approved LAIV vaccines are all quadrivalent, and composed of live, cold-adapted attenuated viruses. LAIV were developed by several passages of a wild-type virus at progressively lower temperatures in primary chicken kidney cell cultures and embryonated eggs. This approach results in cold-adapted, temperature-sensitive, and highly attenuated master donor strains with low infectivity in humans. In the United States, the two master donor strains used are the A/Ann

Arbor/6/60 and B/Ann Arbor/1/66, while in Eastern Europe (first approved LAIV vaccines), the two strains used are the A/Leningrad/134/17/57 and B/USSR/60/69 (Howley 2013; Shcherbik et al. 2016). These mutant donor strains differ by only seven or eight amino acids from the respective wild-type viruses. Although it has never happened, it is theoretically possible that they could undergo genetic reversion into a pathogenic, transmissible influenza strain (Soema et al. 2015; Cox et al. 2004).

Seed viruses for vaccine production are generated by combining, via reassortment or reverse genetics, the six internal segments from the master donor strains, with the HA and NA surface proteins from the strain against which vaccination is desired (Snyder et al. 1988; Maassab & Bryant 1999). These are referred to as 6/2 cold reassortant vaccines, and as for IIVs, they are also produced in embryonated hens' eggs. However, unlike IIVs, LAIVs are administered intranasally by spray. This results in limited viral replication in the upper and lower respiratory tract of the recipient. Shedding of live attenuated viruses on days 1 to 2 post-vaccination is frequent in young children and has been shown to sometimes cause wheezing in infants under 2 years old (Belshe et al. 2007). For these reasons, LAIVs are generally not recommended for children under 2 years of age, the elderly, and those caring for people with high risk of severe influenza infection. In the US and Canada, LAIVs are approved only for children and adults between the age of 2 to 49 and 59 respectively; whereas in Europe regulations restrict the vaccine to children of 2 to 18 years of age (Sridhar et al. 2015).

In contrast to IIVs, LAIVs induce a longer-lasting, broader immune response (humoral and cellular) with induction of neutralizing antibodies, local IgA and antigen-specific cytokine-secreting T-cells (Sridhar et al. 2015). Meta-analyses have shown that LAIV are generally more efficacious in children when compared to IIVs (Belshe et al. 2007; Jefferson et al. 2008; Jefferson et al. 2012; Howley 2013; Osterholm et al. 2012). This can in most part be explained by the fact that LAIVs mimic a more natural influenza infection.

Recombinant vaccines

In 2013, the FDA announced the approval of the first (and to date, the only) licensed recombinant influenza vaccine, FluBlok®. FluBlok® is produced in an insect cell expression system and is

composed of three full-length HA proteins derived from the WHO recommended strains. This vaccine has a three-fold higher total protein content (45 µg for each subtype) than inactivated virus vaccines (Yang 2013). Although FluBlok® has demonstrated a significant immunogenic capacity in young and older adults, its efficacy in children and the elderly has not yet been completely evaluated (Cox et al. 2015). Therefore, FluBlok® is only recommended for people between 18-49 years of age (Houser & Subbarao 2015).

One great advantage that FluBlok® has compared to IIVs and LAIVs, is that it is not produced in eggs: this allows people with egg allergies to be vaccinated safely. Also, production steps can be achieved in shorter periods of time because they are not dependent on an egg supply, limited by the selection of viruses that are adapted for growth in eggs, and additionally do not require high-level biocontainment facilities since production is based on recombinant technology (cloning and expression of recombinant proteins). All this can be extremely useful in the event of a pandemic or vaccine supply shortage.

Main disadvantage of current vaccines

Despite the fact that influenza vaccines have been developed and tested since the late 1930s, several limitations still exist involving both their availability and their effectiveness (Stokes et al. 1937).

One clear limitation that all current licensed vaccines have, with the exception of FluBlok®, is that they are produced in eggs. Egg-based production can take up to 8 months to produce a functional vaccine, and is critically dependent on continuous supply of expensive fertilized eggs - which would certainly be limited in case of a pandemic (Wong & Webby 2013). Moreover, egg-based vaccine facilities need to be under strict sterile conditions because eggs are highly susceptible to avian or microbial contaminants which could jeopardize vaccine supplies. This was observed during 2004 - 05, when one of the major manufacturers of egg-based vaccine in the US, Chiron (Emeryville, CA, US), announced that none of its trivalent inactivated influenza vaccine (TIV) would be available for distribution because of bacterial contamination; this caused major shortages in the vaccine supply (McQuillan et al., 2009). Furthermore, there is a possibility that unregulated levels of egg protein contaminants in the vaccines could cause anaphylactic

responses in egg-allergic individuals (Goldis, Bardina, Lin, & Sampson, 2010). Finally, in a time where research is heading towards universal vaccines made from recombinant protein expression, it is simply unfeasible and unpractical to use eggs to produce these molecules when there are many other more modern and productive systems that have been extensively used for similar purposes.

Another limitation of current vaccines, concerns using HA and NA antigens to elicit immune responses. As it was seen previously, the HA and NA genes are highly susceptible to antigenic shifts and drifts; this results in current vaccines requiring bi-annual revision and reformulation of their antigenic content (once for each influenza season of the northern and southern hemisphere). For this, the WHO has to conduct several surveillance studies on the immune status of the populations and on antigenic information about circulating viruses, before recommending a predicted vaccine composition for the upcoming season's vaccine (Ampofo et al. 2012). Since this decision must take place 7 to 8 months in advance of ''flu season'' to accommodate the steps of vaccine production, the predicted vaccine strains have a high chance of differing from the actual viruses circulating during the subsequent influenza season. Between 1999 and 2009, there were four vaccine compositions selected by the WHO for application in the northern hemisphere that failed to effectively match the epidemic strain because a new antigenic variant emerged after the vaccine formulation decision was made (Jackson 2009). It is estimated that these mismatches occur at a similar frequency in the southern hemisphere (Richard et al. 2010).

Not surprisingly, vaccine mismatches can result in suboptimal vaccine efficacy. A meta-analysis study of healthy young adults has shown that vaccine efficacy against influenza was 80% (95% CI 56 - 91%) during years with a good match versus 50% (95% CI 27 - 65%) during years with a poor antigenic match (Jefferson et al. 2007). Another analysis has also found from a 10 - year observational study of influenza vaccine effectiveness in community-dwelling elderly persons, that vaccine effectiveness dropped to 37% (95% CI 31 - 43%) during poor match seasons versus 52% (95% CI 49 - 54%) during good match seasons (Nichol et al. 2007).

Moreover, as it was discussed previously, it is nearly impossible to predict antigenic shifts that will cause pandemic-size infections. With the current egg-based technology, it would take around

5-6 months before a vaccine based on a new influenza strain can be produced on a large scale. This was clearly demonstrated during the 2009 H1N1 pandemic, where vaccine production and distribution organizations were not rapid enough to prevent the second wave of the pandemic (Broadbent & Subbarao 2011). Moreover, considering the current world egg-based manufacturing capacity estimated at 1,420 million doses, it seems that this system is not feasible for worldwide vaccine distribution (Partridge & Kieny 2013).

Even though it is well-known that influenza A virus is highly susceptible to mutations in its genome, especially on the antigenic segments of the HA and NA protein, every single influenza vaccine currently on the market is still designed primarily to elicit an immune response to these same main antigenic segments of the HA and NA proteins. This poses an obvious short-fall in the way current vaccines are being designed that leads to many different problems. After the 2009 pandemic, and with the increase in sporadic zoonotic avian influenza infections in humans with pandemic properties, researchers are moving towards new "universal" vaccines that induce broader cross-protection against a wide range of strains compared to currently licensed vaccines.

1.4. Future vaccines

From previous experiences with influenza epidemics and pandemics, the efficacy of current commercialized vaccines has become a topic of debate (Osterholm et al. 2012). Health authorities are finally realizing that next-generation influenza virus vaccines are urgently needed. Novel approaches to current vaccination against influenza have been focusing on two major improvements:

- inducing more broadly cross-protective immune responses (universal vaccines)
- decreasing the time of production of vaccines (other manufacturing methods)

In the next section, I will address the prospects and challenges of these two key points.

1.4.1. Universal vaccines

An ideal universal influenza A vaccine would not only have to induce a robust protective immunity against intrasubtypic drift variants, but also against various subtypes of influenza A virus, including those that have pandemic potential. This vaccine would not need to be administered

or updated every year and it would buy time in a pandemic scenario by reducing morbidity/mortality until a tailor-made vaccine would become accessible (de Vries et al. 2015). To produce universal vaccines, researchers have been targeting conserved epitopes that exist across different influenza virus subtypes and trying to make them sufficiently immunogenic to induce protective immunity. Although influenza has a wide variety of conserved sequences, most of these are located on the internal proteins and the mechanism of protection conferred by these proteins remains unclear or is not considered significant (Staneková & Varečková 2010; Wiersma et al. 2015). On the other hand, the stalk domain of the HA and the extracellular domain of the matrix protein 2 have been extensively studied and are considered the most promising conserved targets for a universal influenza vaccine.

HA stalk domain

The HA protein is the largest and most abundant envelope protein of the influenza virion. During viral replication, HA is first synthesized as a single precursor (HA0) that then undergoes trimerization and post-translational modifications via the ER and the Golgi apparatus before being transferred to the cell surface. Once it is exported to the cell surface, HA0 is cleaved by cellular host proteases into HA1 and HA2 which remain cross-linked by a disulfide bond.

The HA comprises two distinct domains: these are the globular head domain and the stalk domain (Figure 4). The former is situated entirely in HA1 and contains the sialic acid receptors necessary for virus binding to host cells. Due to its size and position, most virus-neutralizing antibodies are directed against this region, making it highly immunogenic. The stalk domain is located in both HA1 and HA2. It is situated proximal to the membrane region and forms a stem-like structure that mediates the essential fusion of viral and endosomal membranes once the virus is taken up into the cell (Jang & Seong 2014; Howley 2013).

Although the HA molecule is highly susceptible to antigenic drift, the stalk domain presents relatively more highly conserved regions (48 - 85% homology between subtypes) (Table 1) compared to the globular head (34 - 59% homology between subtypes) (Gerhard et al. 2006); presumably because neutralizing antibodies are primarily targeted against the globular head in natural infection, thus building evolutionary pressure for mutations in this region. For this reason,

Table 1| Percent identity comparison between the stalk domains of HA from different strains. Sequences were obtained from Genbank and alignement was performed using the CLCBio software (Qiagen).

		1	2	3	4	5	6	7	8
H2 (A_mallard duck_Netherlands_2011 (H2N2)) ARX94201.1.	1		84.95	80.00	77.09	60.36	61.96	48.75	48.56
H5 (A_VietNam_2004 (H5N1)) ACR48874.1	2	84.95		78.14	74.55	60.93	61.79	48.40	48.21
H1 (A_New Mexico_2016 (H1N1)) ASU06945.1	3	80.00	78.14		74.18	61.09	61.23	49.47	52.16
H6 (A_Anser fabalis_China_Anhui_2014 (H6N1)) ALG00537.1.	4	77.09	74.55	74.18		61.09	63.41	47.33	49.28
H8 (A_northern pintail_Alaska_2008 (H8)) ACY67463.1	5	60.36	60.93	61.09	61.09		61.96	46.98	49.64
H11 (A_blue-winged teal_Ohio_2012 (H11)) AHZ43563.1	6	61.96	61.79	61.23	63.41	61.96		47.16	51.61
H7 (A_duck_Japan_2017 (H7N9)) BBA21752.1.	7	48.75	48.40	49.47	47.33	46.98	47.16		60.22
H3 (A_Nicaragua_2014 (H3N2)) ASU47781.1	8	48.56	48.21	52.16	49.28	49.64	51.61	60.22	

researchers have been focusing on the stalk domain as a candidate for a universal influenza vaccine.

Broadly neutralizing antibodies directed against the stalk domain can be found in people after vaccines or after virus infections (Miller et al. 2013; Krammer et al. 2012; Nachbagauer et al. 2014; Throsby et al. 2008). These antibodies have a broad inhibitory spectrum and bind to highly conserved epitopes in diverse influenza viruses from Group 1 (H1, H2, H5, H6, H8, H9, H11, H12, H13, and H16), Group 2 (H3, H4, H7, H10, H14, and H15), or both groups of the HA protein (Hashem 2015; Krammer & Palese 2013; Wong & Webby 2013). In contrast to antibodies directed against the globular head, which act by obstructing the binding of the virus to the host cells, stalk-directed antibodies are thought to reduce influenza virus replication by inhibiting the fusion of viral and endosomal membranes (Edwards & Dimmock 2000). In theory, antibodies would bind to the stalk domain outside of the cell, enabling them to be endocytosed together with the virus (Krammer et al. 2014); this then either prevents the conformational change of HA during acidification of the endosome (Imai et al. 1998; Brandenburg et al. 2013), or blocks the insertion of fusion peptide into the endosomal membrane (Varecková et al. 2003).

However, these antibodies are produced in quantities that are not significant because of the bulky and highly immunogenic globular head domain that gives limited access to the stem, and is frequently immune-dominant. To try directing the immune response primarily to the stem region, vaccine experts have designed various vaccination strategies in which the HA globular

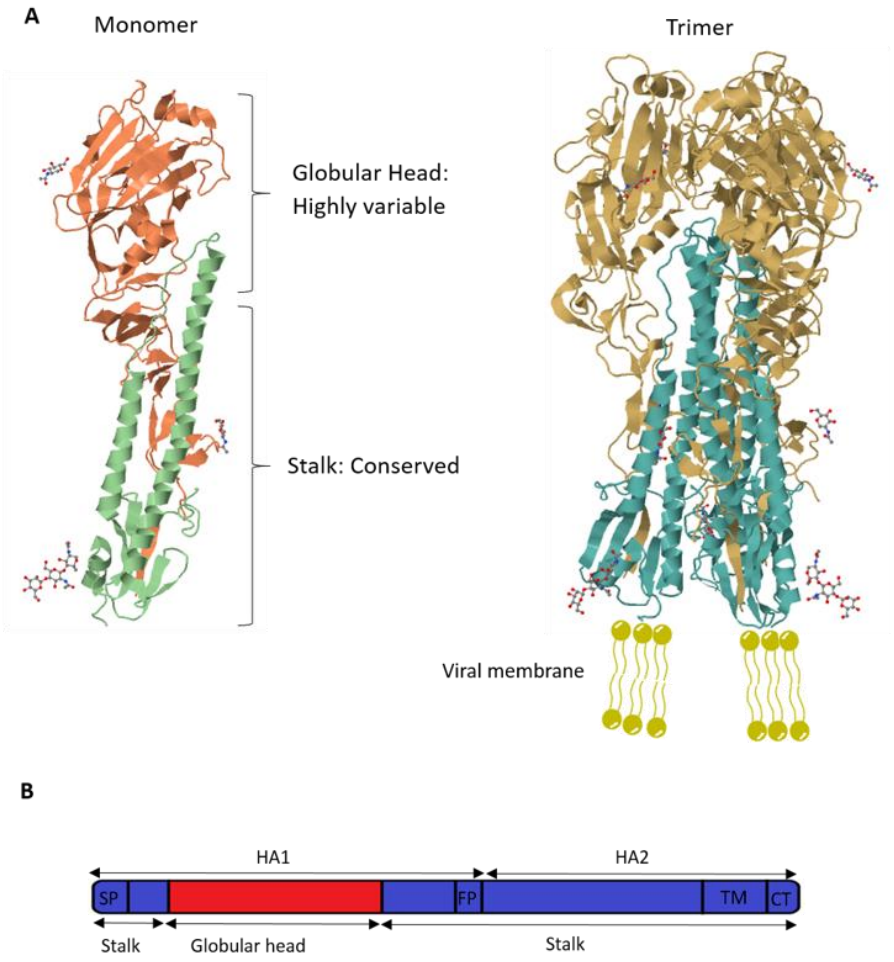

Figure 4| Three-dimensional structure and schematic representation of the influenza HA protein. A) The HA monomer (left) and trimer (right). Each monomeric HA is comprised of two functional domains. The highly variable globular head domain contains a receptor binding site and major antigenic epitopes. The stalk domain is located in membrane proximal region and is significantly conserved among different influenza viruses. The HA structure was produced using JSmol, on basis of the file from the Protein Data Bank, code 4YY9. B) Schematic representation of the HA primary structure. The globular head domain is exclusively formed by the HA1 subunit whereas the stalk domain is composed by the rest of the HA1 subunit and the entire HA2 subunit. SP: signal peptide, FP: fusion peptide, TM: transmembrane domain, CT: cytoplasmic domain.

head domain has been removed. The first true success using headless HA happened with vaccination of mice with a mammalian expressed virus-like particle (VLP) composed of HIV Gag protein fused to headless HA construct based on the A/Puerto Rico/8/34 (H1N1) HA. These VLPs generated antisera that were cross-reactive against multiple subtypes of haemagglutinin and protected against lethal influenza virus challenges (Steel et al. 2010). Another group then obtained the same results using an *E. coli* produced truncated HA2 protein, although it

demonstrated a lessen breadth of reactivity compared to the VLPs (Bommakanti et al. 2010). More recently, there have been several studies that show successful homologous and/or heterosubtypic protection after vaccination with different headless HA (Mallajosyula et al. 2014; Impagliazzo et al. 2015; Wohlbold et al. 2015; Yassine et al. 2015).

An alternative strategy to induce stalk-specific immunity is to repeatedly vaccinate with chimaeric HA proteins that have the same stalk domain but a variable globular head region. The reasoning for this is that with each vaccination, the immune response against the stalk domain is boosted, whereas the response to the globular region remains a primary response. This approach has been demonstrated by Krammer et al. (2013) where, either H1 or H3 stalk domains were combined with several different globular heads and used for sequential vaccinations in mice and ferrets. They found that these vaccinations induced high titres of stalk reactive antibodies and protected both animal types against homologous and heterotypic challenges including lethal H5N1 challenges (Krammer et al. 2013). These approaches show considerable potential for including the HA stalk domain in a universal influenza vaccine candidate.

Extracellular domain of matrix protein 2

Although the HA stalk domain has great prospects as a universal vaccine, perhaps the most explored universal influenza vaccine candidate remains the extracellular domain of the M2 protein (M2e). M2 is a small transmembrane protein that forms tetramers and functions as a pH-dependent proton channel. It regulates the pH inside the virion core, which is essential for virus maturation and uptake into the host cell (Gerhard et al., 2006). It is the smallest protein of influenza virus being only 97 amino acids long and its structure can be divided into three parts (Figure 5): the extracellular N-terminal domain (M2e, positions 2 - 24), the transmembrane (TM) domain (positions 25 - 46) and the intracellular C-terminal cytoplasmic domain (positions 47 - 97) (Deng et al. 2015). M2 tetramers can be found in the plasma membrane of infected cells in large numbers, with an approximate ratio of two M2 tetramers for each HA trimer in CV-1 cells (Lamb et al. 1985); however, only a few copies get incorporated into the envelope of mature virions (ratio of 1:10 - 100 M2:HA) (Zebedee & Lamb 1988).

In the late 1980s-90s, several groups demonstrated for the first time that anti-M2 immunity responses could confer protection and inhibit homologous and heterologous virus replication both in vitro and in vivo models (Zebedee & Lamb 1988; Treanor et al. 1990; Slepushkin et al. 1995). The mechanisms of the immune responses induced by M2 remain to this day unclear and

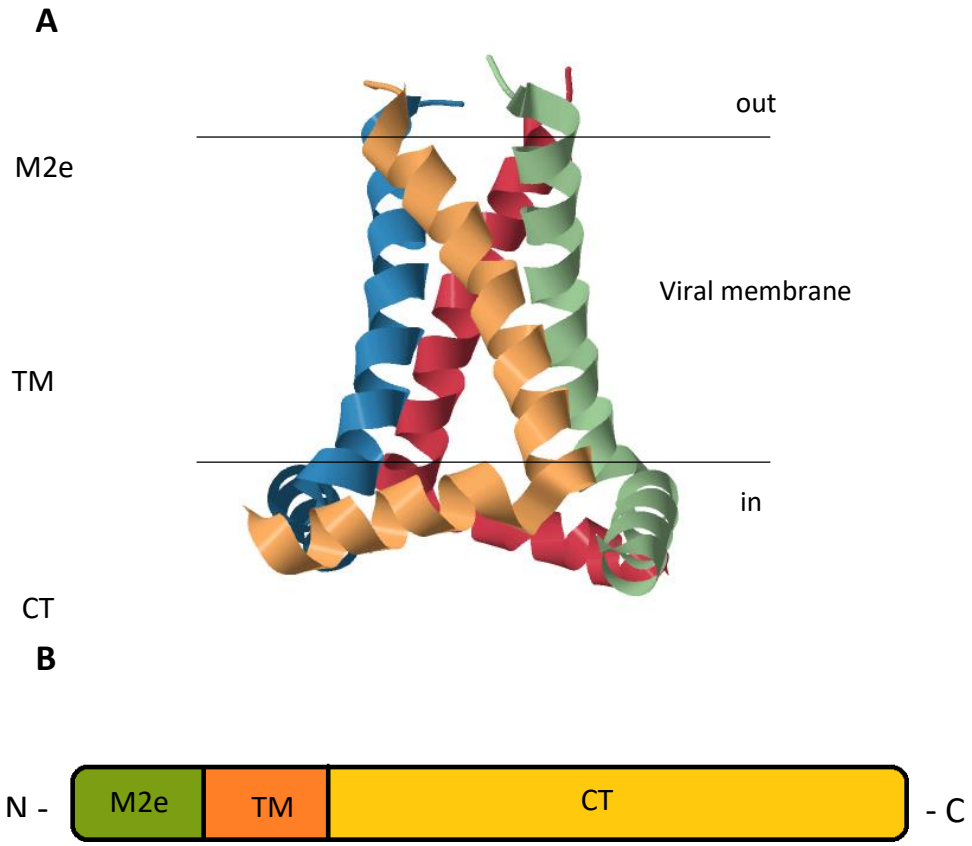

Figure 5| Three-dimensional structure and schematic representation of the influenza M2 protein. A) Lateral view of the M2 tetramer in context of the viral membrane. The M2 structure was produced using JSmol, on basis of the file from the Protein Data Bank, code 2L0J. B) Schematic representation of the M2 primary structure. M2e: extracellular domain, TM: transmembrane domain, CT: cytoplasmic domain.

require future studies. Presumably, protection is conferred by anti-M2 IgG antibodies, which, contrarily to neutralizing antibodies elicited by seasonal vaccines, reduce virus replication by binding to infected cells (higher amounts of M2 compared to virions) and mediating antibody dependent cell-mediated cytotoxicity (ADCC) and antibody dependent cell-mediated phagocytosis (ADCP) (Deng et al. 2015).

The interest in using the M2 protein to produce a universal vaccine comes from its extracellular domain M2e. In multiple sequence alignments, M2e has been shown to be incredibly conserved among different influenza strains, especially for human strains (Fiers et al. 2004). For example, residues 2-9 (SLLTEVET) of M2e were found to be 100% conserved among human influenza A isolates and approximately over 99% among all influenza A subtypes (Liu et al. 2005). This high level of conservation can be attributed to the lack of selective pressure caused by the low incorporation levels of M2 molecules into the virion and steric hindrance from the much larger HA and NA surface proteins (Rappazzo et al. 2016).

These two factors also result in low levels of immunity against the M2 protein. Studies have shown that natural virus infections or vaccination with current vaccines induce weak immune responses against the M2e fragment (Feng et al. 2006). Presumably, most immunogenic bodies generated in the course of natural infection are directed to HA and NA, making the frequency of M2e-specific precursor B cells lower than those of HA- and NA-specific B cells (Gerhard et al. 2006). Hence, to produce an effective vaccine, researchers have developed a plethora of different methods to enhance anti-M2e immune responses.

One very efficient way to make M2e immunogenic is by presenting it on the surface of VLPs by chemically or genetically fusing it to a variety of carriers that form VLPs. VLPs are composed of structural viral proteins that can self-assemble to make multiprotein particle structures resembling the morphology of live virions. VLPs allow for the presentation of desired epitopes in a ordered way, which has been shown to increase immune responses (Bachmann et al. 1993). This technique was first adopted for influenza in an early study by Neirynck et al. (1999), where M2e was genetically fused to the hepatitis B virus core protein. When expressed in *E. coli*, the M2e-HBc fusion would “spontaneously associate to form VLPs” because of the HBc backbone. These VLPs elicited high levels of anti-M2e IgG antibodies and conferred broad protection in mice against challenge with H1N1 and H3N2 viruses; passive immunization with sera from immunized mice was also successful (Neirynck et al. 1999). Since then, similar results have been obtained using different VLP carriers, such as Malva mosaic virus (MaMV) nanoparticles (Leclerc et al. 2013), Tobacco mosaic virus coat protein (Petukhova et al. 2013), Potato virus X (Tyulkina et al. 2011), Papaya mosaic virus (Denis et al. 2008), Human papillomavirus (Matić et al. 2011),

Woodchuck hepatitis virus-like particle (Ameiss et al. 2010), bacteriophages T7 and Qβ (Hashemi et al. 2012; Bessa et al. 2008) and even the transmembrane domain of haemagglutinin combined with the matrix protein M1 (Kim et al. 2013). Immunogenic VLPs can also be obtained by co-expressing the matrix protein M1 with the native, full-length M2 protein (Song et al. 2011).

Other carriers that do not form VLPs, but which enhance immunogenicity by acting as adjuvants, have also been exploited (Deng et al. 2015). Recently, Mardanova et al. (2015) successfully expressed M2e fused to bacterial flagellin in tobacco plants. These adjuvated molecules induced high, titres of anti-M2e antibodies by redirecting the response from the carrier flagellin towards the M2e epitopes; they also protected mice from lethal challenge with different strains of influenza A (Mardanova et al. 2015).

There is, however, one important caveat to consider when designing universal vaccines based on M2e. In 2005, Liu et al. (2005), first reported after several M2e sequence analyzes across different species, that some regions on the M2e peptide can vary depending on the host species. They suggested that there is one specific M2e region that is consistent with host restriction specificities of human, avian and swine (underlined residues represent changes in amino acids): PIRNEWGCRCN (aa 10 - 20, human isolates), PTRNGWECKCS (aa 10 - 20, avian isolates), LTRNGWGCRCS (aa 10 - 20, avian origin/human isolates), and PIRNGWECRCN (aa 10 - 20, swine isolates) (Lee et al., 2014; Liu et al., 2005). These changes in sequences between different species could possibly reduce the spectrum and the efficacy of an M2e vaccine.

To prevent this, some groups have been using tandem repeats of M2e epitope sequences of human, swine, and avian origin instead of just one single version. For example, Kim et al. (2013) successfully expressed a chimaeric protein composed of five different versions of M2e fused to the HA transmembrane domain in an insect cell-based system. This construct, when co-expressed with M1, successfully formed VLPs that incorporated heterologous M2e epitopes at significantly higher levels than on native influenza virions or in wild type M2 VLPs (M2WT). Intramuscular immunization with the chimaeric construct also induced higher levels of anti-M2e antibodies that conferred a wider range of cross reactivity to influenza virus than natural live virus infections or homologous M2e VLPs (Kim et al. 2013).

However, protection levels conferred by anti-M2 immunity have been the topic of a long and delicate debate amongst influenza researchers. While there are uncountable different proof of concept studies that show that anti-M2 immunity offers some correlate of protection in mice, extending these studies to other animals (ferrets or primates) has not always been satisfactory (Fan et al. 2004). On the other hand, some companies have proceeded to phase 1 clinical trials in humans and most of them resulted in positive safety profiles and good immunogenicity reports (Soema et al. 2015). One particular study on M2e-flagellin-conjugated vaccines has just recently completed a successful phase 2 trial (Turley et al. 2011). Phase 3 trials should be conducted in the coming years, and will provide much insight on the possibilities of these vaccines.

Overall, it seems that the future is bright for universal influenza vaccines. Interestingly, the current opinion is that universal vaccines should be administered as a complement to seasonal vaccines, rather than as a replacement (Atsmon et al. 2014; Antrobus et al. 2014). However, with many other universal influenza vaccine candidates under development, it is possible that future influenza vaccines will be composed of a cocktail of different conserved epitopes that together may offer strong, long lasting, and broad immune protection.

1.4.2. Plant-made vaccines

Besides conferring broader protection, future influenza vaccines should be produced at a much higher rate and in greater amounts than what is achievable today. With an estimated world population exceeding 9 billion by 2050, and with African countries probably seeing the highest increase (1.1 to 2.3 billion), it is simply unfeasible to continue producing expensive influenza vaccines from hens' eggs. The recent H1N1 influenza outbreak in 2009 has showed us that an egg-based production system for influenza vaccines is not suitable for a quick large-scale response in face of a new highly pathogenic influenza strain and especially not for developing countries, who received vaccine stocks only in late 2010 (Mortimer et al. 2012). For these reasons, health authorities will have no choice but to completely reform the current influenza vaccine production system to a more modern one that can be easily and cheaply scalable to produce large amounts of influenza vaccines.

Over the past 20 - 30 years, plants have been extensively reviewed as production systems for various medically and industrially relevant proteins. The rationale for using plants relies on their safety, cost-effectiveness and scalability. Contrarily to egg, microbial, insect and mammalian cell-based systems, plants can be cheaply grown virtually anywhere without the requirement of dedicated facilities containing expensive equipment (Waheed et al. 2016; Pogue et al. 2010; Mortimer et al. 2012). Moreover, this process can be rapidly and easily scaled up in response to sudden virus outbreaks or bioterrorism events (D'Aoust et al. 2010). Plants also do not harbor any known human pathogens such as prions or viruses, which makes them safe, and contributes significantly to the reduction of costs in both upstream and downstream processes (Horn et al. 2004; Thuenemann et al. 2013). Finally, as eukaryotic organisms, plants are able to produce complex eukaryotic proteins with correct folding, glycosylation, and activity (Horn et al. 2004).

The first evidence that plants could produce pharmaceutically relevant proteins came from a study conducted by Barta et al. (1986), where transgenic tobacco plants where shown to be able to express human growth hormone (Barta et al. 1986). Shortly after this pioneering study, many therapeutics were produced for the first time in plants, including human monoclonal antibodies (During K. 1988), secretory antibodies (Hiatt et al. 1989), hepatitis B surface antigen (Mason et al. 1992) and various egg proteins (Zhong et al. 1999; Hood et al. 1997). These proteins were all produced by generating stable transgenic plant lines. It is important to note that transgenic plant technology is only suitable for the production of therapeutics once a seed bank has been established. Generating a de nova production of a seed bank is an exceptionally time-consuming and often costly process, not suitable for the discovery of new drugs. Nowadays, an alternative method using transient expression is favored for the rapid optimization of recombinant protein expression (Thuenemann et al. 2013; Sainsbury & Lomonossoff 2014).

Transient expression can be generally performed in two ways: these are by directly using viral vectors such as those derived from Tobacco mosaic virus (TMV), or by agroinfiltration. The virus infection method is dependent on the ability of plant viruses to deliver foreign genes into plants in a rapid and systemic way (Schillberg et al. 2005). However, these are limited to a narrow range of hosts and gene size, and administration can sometimes be difficult, especially for RNA viral vectors (Rybicki 2010). Agroinfiltration on the other hand, relies on whole-plant infiltration with

a suspension of recombinant *Agrobacterium tumefaciens* containing the desired plant expression construct. When injected into the plant leaves, *A. tumefaciens* mediates the transfer of its T-DNA to the nucleus of plant cells in a highly efficient manner, where it can express the transgene at very high levels without stable transformation. This process only takes a few days to complete, versus several months when using transgenic plants. Although agroinfiltration was initially developed to quickly test different gene constructs before more traditional approaches could be used, the recent development of silencing suppressors and industrial-scale vacuum equipment has made it possible to use agroinfiltration for large-scale production of recombinant proteins (D'Aoust et al. 2008). Moreover, agroinfiltration can also be used to deliver virus-based vectors, thus combining the advantages of both these methods of transient expression (Rybicki 2010).

A wide variety of recombinant proteins have been successfully expressed in plants via agroinfiltration, from which a significant proportion are currently at various stages of clinical trials or at the verge of being commercialized (Huafang Lai & Jake Stahnke 2013; Bhaskar et al. 2009; Obembe et al. 2011). Probably the most relevant example to this study comes from Medicago® Inc. and their plant-produced avian flu H5 pandemic vaccine candidate which is currently in phase 2 clinical trials. They showed that by adopting a large-scale agroinfiltration system, they could express recombinant HA with yields up to 50 mg⁄ kg of leaves. These recombinant HA molecules assembled correctly into highly immunogenic VLPs that budded at the plasma membrane and conferred complete protection against a lethal challenge with a heterologous (A⁄Vietnam⁄1194⁄04 (H5N1)) virus (D'Aoust et al. 2008). Moreover, they reported being able to obtain a purified product only 3 weeks after receiving the HA sequence, which is approximately 8 times faster than the response given by governments to the 2009 H1N1 pandemic (D'Aoust et al. 2010).

1.5. Aims of the study

The overall aim of this project, was to design a universal candidate vaccine for influenza that can be rapidly and cheaply produced. To achieve this, I compared several studies on universal influenza vaccines and vaccine production systems. Based on my research, I first hypothesized that, *N. benthamiana* plants could be used to rapidly express M2e-HA chimaeric proteins.

And secondly, that these chimaeric proteins would self-assemble into VLPs with potential to elicit broad immune responses.

The aim of the first part of this study was to produce antibodies against the influenza M1 and M2 proteins. These antibodies would be used for the remainder of the project as reagents, thus removing the necessity to buy expensive commercial antibodies. For this, both M1 and M2 were produced in *E. coli* and subsequently used to raise antibodies in rabbits. Moreover, the proteins expressed in *E. coli* were also used as positive controls on acrylamide gel and western blots.

The second part of the project involved designing chimaeric proteins using the M2e peptide and HA protein. This was based on previous work performed by Kim, Lee, et al. (2013), where tandem copies of the M2e peptide were genetically fused to the HA transmembrane domain and expressed in insect cells (Kim, Lee, et al. 2013). When supplemented with the core protein M1, these fusion proteins successfully assembled into immunogenic VLPs capable of conferring cross-protection in mice. After such promising results, I decided to test whether similar VLPs could be obtained for the first time using a plant expression system, which would be more adaptable to the current demand for influenza vaccines. To increase the chances of VLP formation in plants, I designed six variations of the M2e-HA chimaera. The expression of these fusion proteins was optimized in plants using different conditions and expression vectors.

Finally, after selecting the most promising constructs, I proceeded with density gradient purification of the fusion proteins and analyzing if they formed VLPs using transmission electron microscopy (TEM). Furthermore, the effect of M1 co-expression on VLP formation was also investigated.

Chapter 2: Expression of influenza A M1 and M2 proteins in *E. coli*

2.1. Introduction

For the last few decades, the gram-negative bacterium *Escherichia coli* has dominated bacterial expression systems and remained the preferred organism for early laboratory investigations (Chen 2012). One of the reasons for this is that *E. coli* has been extensively genetically characterized and manipulated. Many techniques to increase recombinant protein production in *E. coli* have been explored, and there are an increasingly large number of different cloning vectors and mutant host strains widely available from commercial sources and public repositories, allowing for the expression of a vast number of different proteins (Sivashanmugam et al. 2009). *E. coli* can also be easily transformed with minimal amounts of foreign DNA and has unparalleled growth kinetics, which permits easily reaching high recombinant cell density cultures in short periods of time (Pope & Kent 1996; Rosano & Ceccarelli 2014).

However, since it is a prokaryotic based system, heterologous eukaryotic proteins expressed in *E. coli* may not be correctly folded or have the correct post-translational modifications such as glycosylation and disulfide bridge formations, thus they may lack or have decreased biological activity (Kamionka 2011). Moreover, when expressed in large amounts, recombinant proteins in *E. coli* often precipitate and aggregate, forming inclusion bodies that are difficult to purify (Khow & Suntrarachun 2012). Finally, *E. coli* produces high amounts of lipopolysaccharide (LPS) endotoxins, which are pyrogenic in humans and other mammals. Hence if they are intended for animal testing, proteins must first be purified to become endotoxin-free (Terpe 2006).

Nevertheless, there are ways to combat the disadvantages mentioned above. Apart from correct protein folding, which can be lengthy and fastidious to solve, inclusion bodies and endotoxins can be easily circumvented in relatively small-scale expressions. Hence, when compared to the high costs and lengthy optimization processes involved in most eukaryotic expression systems, *E. coli*-based expression becomes a more attractive offer for small scale, laboratory-sized experiments.

In this section of the study, I set out to produce antibodies in rabbits against the two influenza matrix proteins M1 and M2. Since these antibodies would be used to detect recombinant protein

expression in plants only, I had to use antigens that were produced in a different organism (i.e. *E. coli*) to reduce cross-reactivity. To produce these antibodies, I had to express and purify M1 and M2 in sufficient amounts that would induce a significant immune response in rabbits. For this, I used the pPROEX-HT (Life Technologies, USA) prokaryotic expression vector which contains an isopropyl β-D-1-thiogalactopyranoside (IPTG) inducible *trc* promoter and *lacI*^{q} repressor gene. The synthetic *trc* promoter is commonly used for its ability to drive high-level transcription of genes (Tegel et al. 2011).

The serum from immunized rabbits would facilitate the detection of both influenza matrix proteins produced by different expression systems, including in plants. The sera derived from M2 immunization should also allow for detection of M2e-fused proteins, since the M2e region contains most immunogenic epitopes (Frace et al. 1999; Zou et al. 2005; Fu et al. 2009). At the same time the *E. coli* produced M1 and M2 proteins were also used as positive controls in western blots, as discussed in Chapter 3.

2.2. Methods

2.2.1. Construction of pPROEx-M1 and pPROEx-M2

Human codon optimized cDNAs coding for influenza matrix proteins M1 and M2 (Genbank accession number: AY651387.1; only one accession number because the M1 protein is encoded on the seventh RNA segment together with the M2 protein) were supplied by Genscript in the pUC57 vector. The bacterial expression vector pPROEx-HTb (Thermo Fisher Scientific, MA, USA) was chosen to express both proteins in *E. coli*. pPROEx-HTb is a T7 promoter-based expression vector that is frequently used to obtain high levels of recombinant proteins in *E. coli* (Ochocka et al. 2003). It contains the *lacI*^{q} repressor gene, which enables IPTG-induced expression of the inserted gene from the promoter and a 6-histidine tag that allows for easy protein detection via western blots.

To facilitate cloning into pPROEx-HTb, the M1 gene was designed with a 5’ AflIII and a 3’ XhoI restriction site. The M2 gene did not contain any 5’ restriction sites that allowed cloning into pPROEx-HTb. Therefore, the pUC57-M2 plasmid was used as template DNA in a subsequent PCR

DNA amplification to add an AlfIII restriction site at the 5' terminus to allow cloning into the pPROEx-HTb vector. The primers used for the PCR reaction are listed in Table 1.

Table 1| Primers for *E. coli* expression

Primer	Sequence	RE added	Orientation
M2F	5'-TTT ACA TGT CTC TGC TGA C-3'	AflIII	Forward
M2R	5'-TCT CGA GCT TAT TCC AGT TCA ATG T-3'	-	Reverse
M1F	5'-TGT CCT GAG TAT TAT CCC-3'	-	Forward
M1R	5'-GAC CCC CAT CCT TTT CTG-3'	-	Reverse

The PCR reaction mixes consisted of 50 ng of the appropriate template DNA, 200 µM dNTPs, 0.5 µM of each primer, 2 mM Mg2+, 1 x Accuzyme buffer and 1.25 units (U) Accuzyme™ DNA Polymerase (Bioline, Meridian Bioscience Inc., USA). The reactions were amplified with an initial denaturation step at 95 °C for 2.5 min. Followed by twenty-five cycles of denaturation at 95 °C for 30 s, annealing at 49 °C for 30 s and elongation at 72 °C for 1 min. A final elongation step at 72 °C for 2 min was carried out at the end of the PCR run. The amplified product was separated on 0.8% w/v TBE (89 mM Tris base, 89 mM boric acid and 2 mM EDTA [pH 8]) agarose gels containing 00.5 mg/mL ethidium bromide and visualized under short wavelength ultraviolet (UV) illumination. O'GeneRuler™1kb DNA ladder #SM1163 (Thermo Fisher Scientific, MA, USA) was used as molecular weight marker on all the agarose gels.

DNA was purified from the agarose gels using the QIAquick® Gel Extraction kit (Qiagen, USA) following the manufacturer's instructions. The purified DNA was ligated into the pJET®-TEasy Vector system (Thermo Fisher Scientific ©, USA) according to the manufacturer's instructions and incubated overnight (O/N) at 4 °C.

The ligated pJET-M2 and the original pUC57-M1 plasmids were used to transform DH5-α chemically competent *E. coli* cells (E. cloni™, Lucigen) according to the method described by Sambrook et al. (1989). The transformed cells were plated on Luria Bertani (LB) media agar plates (Luria-Bertani media (LB): 10 g Tryptone, 5 g Yeast Extract, 5 g NaCl in 1 litre water; 15 g of

Bacterial Agar was added for agar plates) supplemented with ampicillin (amp) (100 µg/mL). Plates were incubated at 37 °C, overnight.

Positive colonies were selected by colony PCR using gene-specific primers for pUC57-M1 and pJET specific primers for pJET-M2 as showed in Table 1. The pUC57-M1 PCR reactions of the appropriate template DNA consisted of 250 µM dNTPs, 0.2 µM of each primer, 1 x Kapa taq Buffer A and 0.5 U KAPA Taq DNA Polymerase (KAPA Biosystems). The reactions were amplified with an initial denaturation step at 95 °C for 4 min; followed by twenty-five cycles of denaturation at 95 °C for 30 s, annealing at 47 °C for 30 s and elongation at 72 °C for 30 s. Reactions finished with a final elongation step at 72 °C for 4 min. The pJET-M2 PCR reaction was done according to manufacturer's instructions using pJET specific primers.

Positive colonies containing either pUC57-M1 or pJET-M2 were inoculated into 10 mL LB broth supplemented with 50 µg/mL ampicillin and incubated with agitation for 16 hrs at 37 °C. Plasmid isolations were performed using the QIAprep® Spin Miniprep kit (Qiagen, USA) according to instructions provided by the manufacturer.

The plasmid DNA was sequenced (Macrogen Inc., Netherlands) using the gene-specific primers (Table 1). Sequencing data were analyzed using CLC MAIN WORKBENCH software (Qiagen, USA).

Subcloning into pPROEx-HTb

The M1 and M2 encoding sequences were first excised from the pUC57 and pJET backbone respectively, by digesting the plasmid DNA (~2000 ng) with 1U of AflIII and XhoI (Thermo Fisher Scientific, MA, USA) for 1 hr at 37 °C. Digested DNA was separated on a 0.8 % w/v TBE agarose gel and the corresponding band was gel-purified with the QIAquick® Gel Extraction kit (Qiagen). This digestion yielded recombinant DNA with 5' AflIII and 3' XhoI restriction sites.

The pPROEx-HTb expression vector was supplied by Thermo Fisher Scientific © and linearized by restriction digestion with 1 U of NcoI and XhoI (Thermo Fisher Scientific, MA, USA) for 1 hr at 37 °C. After digestion, the vector DNA was dephosphorylated using 1 U rapid alkaline phosphatase (Roche) according to the manufacturer's instructions.

Recombinant DNA sequences were then directionally sub-cloned into pPROEx-HTb according to their respective restriction sites using T4 DNA Ligase (Thermo Fisher Scientific, MA, USA).

Recombinant clones were transformed into DH5-α chemically competent *E. coli* cells (E. cloni™, Lucigen) (Sambrook et al. 1989). Transformed cells were plated on LB media plates supplemented with ampicillin (100 µg/mL) O/N at 37 °C. Positive clones were selected by colony PCR using the same settings and gene-specific primers (Table 1) as previously. Successful recombinants were grown overnight and stored at -80 ^{o}C in 50 % glycerol.

2.2.2. Protein expression

Small-scale induction

Single colonies of recombinant pProEX-HTb clones were placed in 10 ml LB media with 100 µg/ml ampicillin and incubated O/N at 37 ^{o}C. Overnight cultures were sub-cultured into 10 ml of either LB media or Terrific broth (Terrific broth (TB): 12 g tryptone, 24 g yeast extract, 9.4 g K_2HPO_4, 2.2 g KH_2PO_4, 4 mL of glycerol in 1 litre water, pH 7.2) media supplemented with 100 µg/ml ampicillin. The cultures were allowed to grow at either 28 ^{o}C or 37 ^{o}C until they reached an OD_{590} between 0.5 and 1. After removing a 1 ml uninduced aliquot from each culture, IPTG was added at various final concentrations (0.4 mM, 0.6 mM and 0.8 mM). After induction, aliquots (1 ml) of bacteria were removed every hour for 3 hours for each construct. An aliquot after 16 hrs induction (overnight) was also removed. The samples were centrifuged at 10,000 rpm for 10 min and each pellet harvested, pooled and weighed. Pellets were re-suspended in 4X BugBuster™ Protein Extraction Reagent and extraction protocol followed as per the manufacturer's instructions (BugBuster™, Novagen) to separate soluble/insoluble fractions.

Large scale induction

One liter of Terrific broth media (0.6 mM IPTG) or 1 L LB media (0.6 mM IPTG) was used to grow recombinant bacteria containing pPROEx-M2 or pPROEx-M1 respectively. These were allowed to grow for 16 hrs at 28 ^{o}C for M2 or at 37 ^{o}C for M1. After induction, cell pellets were harvested by centrifugation at 10,000 rpm for 10 min and insoluble fractions were collected using 4 X BugBuster™ Protein Extraction Reagent as previously. Endotoxin-free Dulbecco's Phosphate

Buffered Saline (PBS) D8662 (Sigma-Aldrich, Merck, Germany) was used in the final wash steps instead of the BugBuster™ reagent before protein sample analysis.

2.2.3. Coomassie stained SDS-PAGE gels and western blots

For SDS-PAGE analysis, 5 X loading dye containing β-mercaptoethanol was added to protein extracts, and samples were incubated at 95 °C for 10 min. These were then loaded at equal volumes (30 uL) on 10% SDS-polyacrylamide gels using the Mini-PROTEAN® Tetra SDS-PAGE system (Bio-Rad, CA, United States of America), and electrophoresed at 120V for approximately 120 minutes. To determine the sizes of the resolved proteins in Coomassie stained gels and on nitrocellulose membranes, a Color Protein Standard Broad Range Ladder #P7712S (New England Biolabs, USA) was used as a molecular weight marker.

For Coomassie, gels were stained with Coomassie Brilliant Blue R250 (Merck, Darmstadt, Germany) stain for 2 hrs at 37 °C and destained overnight with destain solution (45 % methanol, 45 % water, 10 % glacial acetic acid).

For western blots, gels and nitrocellulose membranes were pre-equilibrated for 10 minutes in transfer buffer (5.82 g Tris base, 2.93 g glycine, 200 mL methanol in 1 L water, pH 9.2) before being transferred to a nitrocellulose membrane at 15V for 90 minutes using a Trans-blot®SD semi-dry transfer cell (Bio-Rad, CA, USA). After electrophoretic transfer, the membranes were blocked in blocking buffer (5 % non-fat dairy milk and 1 x PBST (137 mM NaCl, 1.8 mM KH2PO4, 10 mM Na2HPO4, 2.7 mM KCl, pH 7.4and 0.1% Tween-20) for 30 min. The membranes were probed overnight at 4 °C with either 1:2000 anti-histidine MCA 1396 mouse monoclonal IgG antibody (ABD Serotec, Bio-Rad, CA, United States of America), 1:5000 anti-M2 14C2 mouse monoclonal IgG antibody (Abcam, UK), or rabbit serum (at the specified dilution) diluted in blocking buffer. The membranes were then washed four times with blocking buffer for 15 minutes each and afterward incubated in a 1:10,000 dilution of anti-mouse IgG (whole molecule) alkaline phosphatase conjugated antibody A3562 produced in goat (Sigma-Aldrich, Merck, Germany) or goat anti-rabbit IgG alkaline phosphatase conjugate (1:5000, Sigma) in blocking buffer for 1 hour at 37 °C. Membranes incubated in secondary antibody were washed four times with 1x PBST (without milk), with 15 minutes for each wash. Detection was performed with 5-

bromo, 4-chloro, and 3-indolylphosphate (BCIP) (KPL, MD, United States of America). The membranes were washed with distilled water once bands were visible after 1 hr to stop the developing reaction. Protein expression, extraction and western blot analysis was repeated at least three times to confirm the expression of the recombinant influenza proteins.

2.2.4. Protein quantification

Standard BSA curves were constructed by loading varying amounts of bovine serum albumin (BSA) (#23210, Thermo Fisher Scientific, MA, USA) ranging from 0.3 µg/uL to 1.0 µg/uL onto SDS-PAGE gels. Concurrently, the insoluble fractions containing M1 or M2 influenza proteins were loaded on the same gel with varying dilutions ranging from 1 to 1:10. The proteins were diluted with sterile PBS and protein loading dye for SDS-PAGE gels. The quantitation of bands was performed using GeneTools software (Synoptics Inc., UK).

2.2.5. Endotoxin assay

Levels of endotoxin were measured using a ToxiSensor^{TM} chromogenic LAL Endotoxin Assay Kit L00350 (Genscript, China) as per the manufacturer's instructions. The absorbance readings were performed using Immuno 96-microwell clear solid plates (Thermo Fisher Scientific, MA, USA) and a BioTek Powerwave XS plate reader (BioTek, USA).

2.2.6. Polyclonal antibody production in rabbits: inoculation schedule

Four female New Zealand White rabbits of approximately 3 months old were used (2 per antigen). The amount of protein was divided equally into 4 tubes for each antigen (for the initial and three booster injections; see below). Each tube contained 0.5 mL of a suspension of the inclusion bodies in PBS and 0.5 mL of Freund's incomplete adjuvant (IFA). The total amount of antigen injected in each dose was approximately 75 µg for M1 and 56 µg for M2. Each inoculation consisted of two injections of 0.5 mL in two different sites (making the total amount of protein injected per inoculation: 150 ug for M1 and 112 ug for M2).

Inoculations and handling of animals were performed by Rodney Lucas at the Research Animal Facility, UCT Health Sciences Faculty, as follows:

Pre-bleed: Ten milliliters pre-immune blood was collected from the central ear vein of each rabbit, 3 days prior to administration of the antigen.

Initial inoculation: Animals were injected subcutaneously on the back at two sites with 0.5 mL (per site) of the antigen in the presence of Freund's incomplete adjuvant (IFA).

1st Boost: The first boost was performed 14 days after the initial inoculation (as above) with IFA. Ten milliliters blood was collected before boost, from the central ear vein of each rabbit.

2nd Boost: The second boost was performed 7 days after the first boost (as above) with IFA. Ten milliliters blood was collected before boost, from the central ear vein of each rabbit.

3rd Boost: The third and last boost was performed 7 days after the second boost (as above) with IFA. Ten milliliters blood was collected before boost, from the central ear vein of each rabbit.

Collection of serum: Fourteen days after the last boost, rabbits where exsanguinated and blood was collected in coagulant tubes to harvest serum.

Animal ethics approval for this research was granted by the Health Sciences Faculty Research Ethics Committee at the University of Cape Town - AEC Reference number 013/008.

2.2.7. Pre-absorption of rabbit sera

Where specified, rabbit sera were pre-absorbed against cell lysate from uninduced *E. coli* to reduce background. Nitrocellulose membrane was covered with *E. coli* cell lysate and incubated at room temperature on an orbital shaker for 2 hours. The cell lysate was discarded and the membrane was washed 4 x 15 mins with blocking buffer. The membrane was then incubated with rabbit serum, diluted in blocking buffer, for 2 hours. The membrane was discarded and the pre-absorbed rabbit serum was then used for immunoblotting or stored at -20 °C

2.2.8. Indirect ELISA

The anti-M1 and anti-M2 response in rabbit sera was determined by indirect ELISA. 96-well Maxisorp® microtitre plates (Nunc) were coated with 100 µL/well of antigen diluted in coating buffer (10 mM Tris, pH 8.5). For anti-M1 tests, plates were coated with the following diluted

plant-produced proteins: M1 as experimental sample and 5xM2e-HAtrans as negative control (Chapter 3). For anti-M2 tests, plates were coated with the following plant produced proteins: 5xM2e-HAtrans as experimental samples and M1 as negative control. The anti-M2 serum was further tried against a synthetic M2e peptide – SLLTEVETPIRNEWGCRCNDSSD – (Genscript, China). After incubating the plates O/N at 4 °C, plates were blocked with TBS blocking buffer (5 % non-fat dry milk in 1 x TBS [50 mM Tris, 150 mM NaCl, pH 7.5]) for 2 hrs at RT after which they were washed four times with 1 x TST buffer (1 x TBS [pH 7.5], 0.05 % Tween®20). One hundred microliters of corresponding final bleed sera were then added at several dilutions in TBS, after which plates were left for 1 hr at 37 °C for incubation. For M2 plates, the anti-M2 14C2 monoclonal IgG antibody produced in mouse (Abcam, UK) was used as positive control. Blank wells containing no antibody were included as background control. After incubation, plates were washed four times with 1 x TST buffer and 100 µL of goat anti-rabbit IgG alkaline phosphatase conjugate (1:5000, Sigma) diluted in blocking buffer was added per well and incubated for 1 hr at 37 °C. After incubation, the plates were washed four times with 1 x TBS (pH 9) buffer and 200 µL SIGMAFAST™ p-Nitrophenyl phosphate (pNPP, Sigma) was added per well. The plates were developed in the dark for 30 min after which the absorbance was detected at 405 nm on a BIO-TEK® Powerwave XS microtitre plate reader.

To determine the anti-M1 binding titers, rabbit serum from pre-bleed, 1st boost, 2nd boost, and final bleed was diluted in TBS blocking buffer in a 5-fold series in triplicate ranging from a 1:50 dilution to 1: 12,150 and used in an indirect ELISA as described above.

2.2.9. Statistical analysis

A two-tailed, non-paired t-test using the Holm-Sidak method was employed to calculate statistical significance of the final bleed anti-M2 or M1 response, as compared to the negative control antigen ($p = 0.001$). Statistical analysis was carried out using GraphPad Prism v 7.01 (GraphPad Software, Inc.).

2.3. Results

2.3.1. Cloning into pPROEx-HTb

Both M1 and M2 genes were supplied from Genscript, China. Before subcloning into the bacterial expression vector pPROEx-HTb, M2 had to be modified by PCR using the M2 primers from table 1, to include a 5' AflIII restriction site (data not shown). After adding the necessary restriction sites, M1 and M2 were excised from the pUC57 backbone by digesting with AflIII and XhoI restriction enzymes. The bands corresponding to the genes of interest were gel-purified; yielding genes flanked with 5' AflIII and 3' XhoI restriction sites (data not shown). These were then subcloned into pPROEx-HTb, which had been previously linearized using NcoI and XhoI. After digestion and ligation, all recombinant clones were transformed into *E. coli.* Colony PCR allowed to detect positive clones as bands of ~0.3 kb and ~0.7 kb (corresponding to M2 and M1 respectively) were observed (figure 1A and B). The identity of recombinant DNA was further confirmed by sequencing (data not shown).

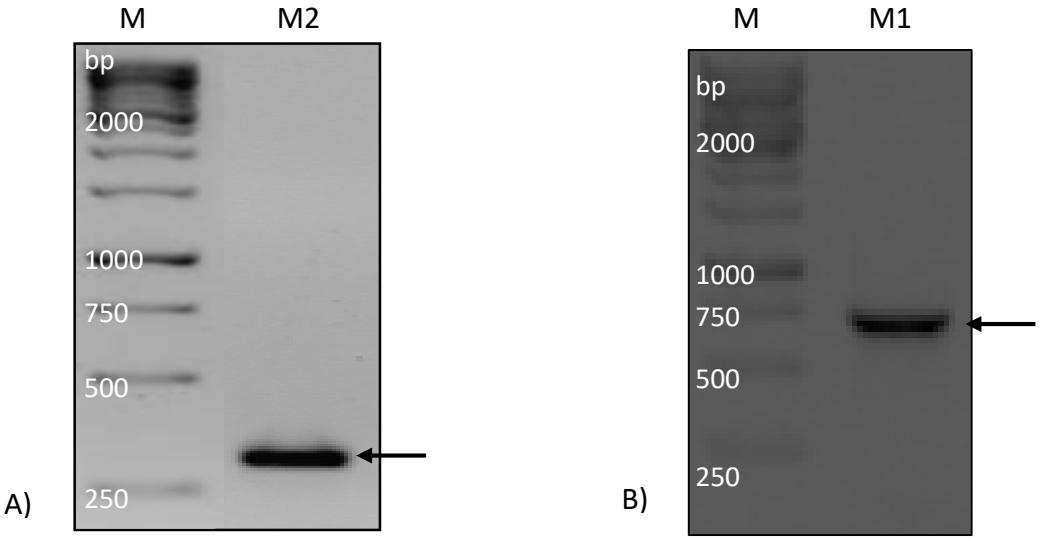

Figure 1| Colony PCR of pPROEX recombinant clones confirms the presence of inserts. A) PCR of recombinant pPROEx-HTb-M2 clones using M2 primers detailed in Table 1. The M2 gene is approximately 270 Bp. B) PCR of recombinant pPROEx-HTb-M1 clones using M1 primers detailed in Table 1. The M1 gene is approximately 670 Bp. M – Marker. Arrows indicate desired DNA band.

2.3.2. Optimizing M2 expression

Small-scale protein expression trials of recombinant bacteria containing pPROEx-M2 were conducted with harvesting of cell samples at 1, 2 and 3 hrs post-induction with 0.6 mM IPTG. The cells were sampled at different time points to determine the effect of incubation time on protein yield. Separation of soluble and insoluble fractions was also performed to analyze the solubility of the recombinant protein. This was performed using Bugbuster™, which is a mixture of detergents that achieves efficient lysis of bacterial cells. Immunoblotting of induced whole cells

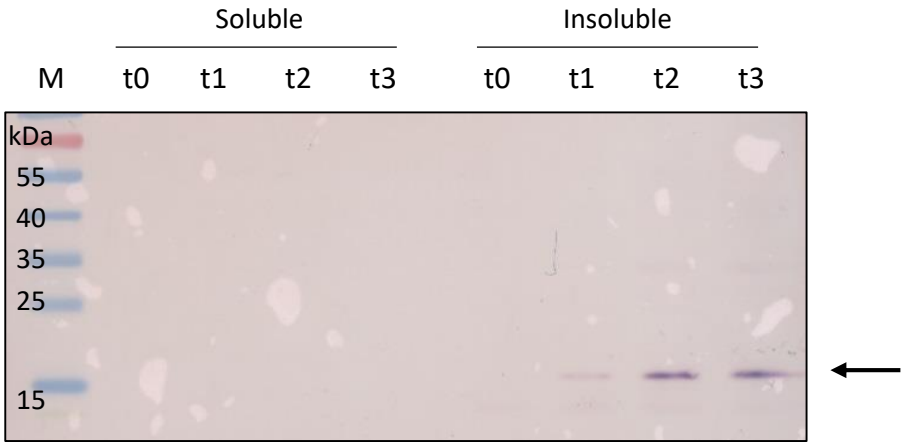

Figure 2| M2 expression in *E. coli*. Western blot of the soluble and insoluble fractions of recombinant *E. coli* expressing the M2 protein after IPTG induction. Anti-histidine tag antibody (1:2000) was used to detect the influenza protein. M – molecular marker; t0 - uninduced cells; t1 – 1 hour post-induction; t2 – 2 hours post-induction; t3 – 3 hours post-induction. Arrow indicates the position of the respective protein (± 17 kDa).

showed that M2 was only expressed after 2 hrs post induction and at low levels. Only the insoluble fraction showed bands corresponding to the M2 size (Figure 2). Moreover, the OD_{600} of recombinant *E. coli* rapidly decreased after induction; going from 0.65 (pre-induction) to 0.49 (3 hrs post-induction). Hence, expression was later optimized by using different IPTG concentrations (0.4 mM, 0.6 mM and 0.8 mM), longer periods (i.e. 16 hrs) and different temperatures (37 ^{o}C vs 28 ^{o}C) to try increase recombinant protein levels without killing the recombinant bacteria (data not shown). From these experiments, I observed an increase in protein levels as well as a decrease in bacterial lysis when the recombinant bacteria were induced at lower temperatures (i.e. 28 ^{o}C) and for longer periods (i.e. 16 hrs) (data not shown). The

combination of these two parameters yielded the best results. Lowering IPTG concentrations did decrease bacterial lysis but at the expense of lower protein levels. Hence it was determined that best expression could be obtained by inducing with 0.6 mM IPTG for 16 hrs at 28 ^{o}C; although protein levels remained relatively low as they could not be detected on a Coomassie stained SDS-PAGE gel. It is important to note that M2 was never observed in the soluble fraction.

To try and further increase protein levels, an enriched media (Terrific broth) was used during induction instead of LB. Immunoblot of induced cells in either LB or Terrific broth media, showed significantly increased levels of M2 in TB compared to LB (Figure 3) using the optimal conditions mentioned previously (i.e. 0.6 mM IPTG for 16 hrs at 28 ^{o}C). I also observed that the OD_{600} of recombinant bacteria increased when TB was used (0.81 to 0.92 in TB vs 0.8 to 0.69 in LB).

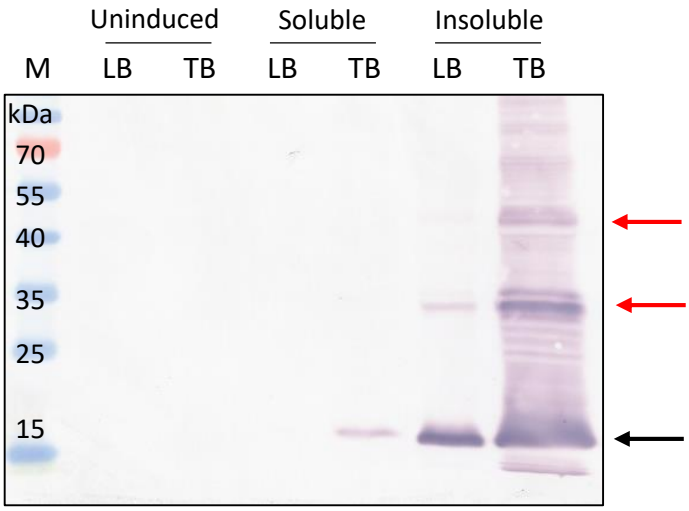

Figure 3| The effects of different induction media on M2 expression in *E. coli*. Western blot of recombinant *E. coli* grown in either LB or TB induction media. Soluble and insoluble fractions were extracted after induction with IPTG (0.6 mM) for 16 hrs at 28 ^{o}C. Anti-histidine tag antibody (1:2000) was used to detect the influenza protein. M – molecular marker; LB – Luria Broth; TB – Terrific Broth. Black arrow indicates the position of the respective protein (± 17 kDa), red arrows indicate the position of putative M2 multimers.

Moreover, soluble protein was observed for the first time using TB (Figure 3). Finally, it appears that M2 formed multimeric structures as observed from the increased molecular weight bands (Figure 3, red arrows). From these results, it was determined that the best conditions to express M2 in *E. coli* was by inducing in TB media supplemented with 0.6 mM IPTG for 16 hrs at 28 ^{o}C.

2.3.3. Optimizing M1 expression

As for M2 expression, small-scale protein expression trials of recombinant bacteria containing pPROEx-M1 were conducted to determine best expression conditions. Cell samples were harvested at 1, 3 and 16 hrs post-induction with 0.6 mM IPTG, and soluble/insoluble fractions were collected to analyze the solubility of M1 in *E. coli*. Unlike M2, M1 was present in both soluble and insoluble fractions; the most protein was found in the insoluble fractions after 16 hrs of induction (Figure 4). Only the insoluble fractions showed a band on Coomassie stained SDS-PAGE gels (data not shown). Also, from Figure 4, higher bands (kDa) can be observed in the insoluble fractions, which could correspond to M1 dimers.

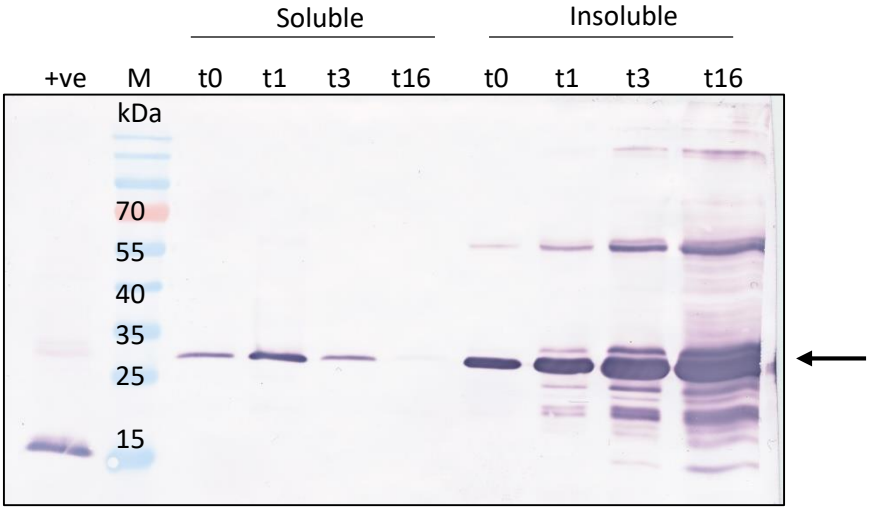

Figure 4| Small-scale expression of M1 in *E. coli*. Western blot of the soluble and insoluble fractions of recombinant *E. coli* expressing the M1 protein after IPTG induction. Anti-histidine tag antibody (1:2000) was used to detect the influenza proteins. +ve – M2 expressed in *E. coli*; M – molecular marker; t0 - uninduced cells; t1 – 1 hour post-induction; t3 – 3 hours post-induction; t16 – 16 hours post-induction. Arrow indicates the position of the respective protein (± 27 kDa).

To try increase the solubility of M1, expression was tried under different conditions (as for M2 expression). However, no significant change could be observed when using TB media, lower IPTG concentrations or lower incubation temperatures, with most of the protein still being in the insoluble fraction (data not shown). Hence, given the high levels of expression obtained using 0.6 mM IPTG, it was decided to continue using the insoluble fraction after induction with 0.6 mM IPTG for 16 hrs at 37 ^{o}C.

2.3.4. Large-scale expression of proteins for rabbit inoculation

To produce sufficient amounts of protein for rabbit inoculation, recombinant bacteria containing pPROEx-M2 and pPROEx-M1 were grown in 1 L media using the respective conditions mentioned in the sections above.

Before quantifying the proteins, an enrichment using nickel affinity purification was attempted by first denaturing inclusion bodies using 8M UREA (data not shown). However, this was not successful as the yields recovered were insufficient for rabbit inoculation. Since in both cases, most protein was found in inclusion bodies (insoluble fractions), I proceeded with using these for

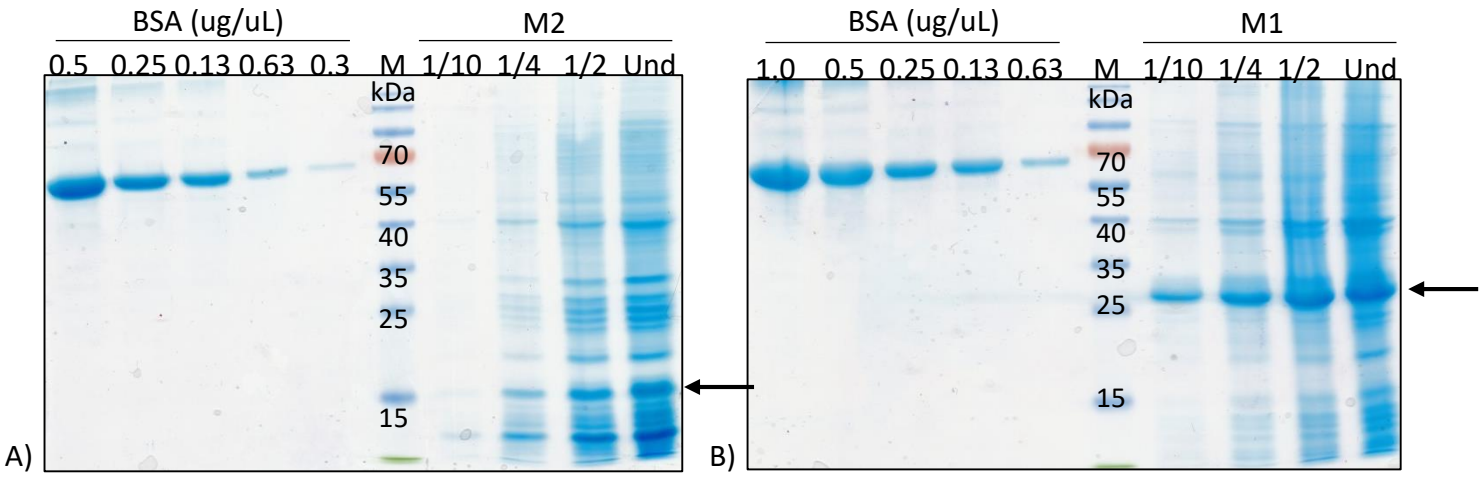

Figure 5| Quantification of proteins using BSA as a standard. Coomassie-stained SDS-PAGE gel of M2 (A) and M1 (B) serial dilutions after large-scale expression. M – molecular marker. Arrows indicate the position of the respective proteins.

the remaining of the experiments. Inclusion bodies were washed with Endotoxin-free Dulbecco's Phosphate Buffered Saline (PBS) to reduce bacterial endotoxins in the protein samples. After the washing steps, recombinant protein amounts were estimated using serial dilutions of bovine serum albumin (BSA) loaded for SDS-PAGE and stained with Coomassie Blue.

After quantification, the protein samples had to be tested for their levels of bacterial endotoxin using the ToxiSensorTM chromogenic LAL Endotoxin Assay Kit L00350 (Genscript, China). From this test, it was estimated that the inclusion bodies containing M2 had an average of 122 EU/mL whereas the M1 inclusion bodies had significantly higher levels at 613 EU/mL. Since

rabbits cannot take more than 100 EU/mL per inoculation (Malyala & Singh 2008), both samples had to be diluted in endotoxin-free Dulbecco's PBS to reduce the amount of endotoxins. The final antigen doses that were injected into rabbits were 112 ug per 0.5 mL injection for M2 and 150 ug per 0.5 mL injection for M1. The inoculation of rabbits was done by Rodney Lucas at the UCT's Research Animal Facility per the protocol detailed in the Methods section.

2.3.5. Testing of animal sera

After inoculation trials, I proceeded with extraction and testing of animal sera to check for the presence of specific antibodies against M2 and M1. For this, I firstly used the final serum (day 42) produced by the rabbits in immunoblots to probe against M2 and M1 produced in bacteria (Figure 6A and B). The specificity of the final serum was compared to serum obtained before antigen injection (pre-bleed) and to commercial monoclonal antibodies.

Western blot analysis of *E. coli* produced M2 with serum produced from rabbits

As can be observed in Figure 6A, probing with the anti-his monoclonal antibody resulted in detection of a band of approximately 15 kDa corresponding to M2 monomers, together with a higher band at round 30 kDa possibly corresponding to dimers. On the other hand, probing the membranes with rabbit final or pre-bleed serum resulted in a non-distinguishable band pattern (similar for both final and pre-bleed serum) that should correspond to *E. coli* host proteins (this was expected since the antigens used to inoculate rabbits were made in *E. coli*). Unfortunately, these non-specific bands made it very difficult to see if the M2 protein was being detected. To try and remove some of the non-specific bands I tried diluting the serum up to 1/20000, as well as pre-absorbing the serum against proteins from un-induced *E. coli;* however, none of these trials resulted in clearer band patterns (data not shown).

Western blot analysis of *E. coli* produced M1 with serum produced from rabbits

As previously demonstrated, detection of *E. coli*-produced M1 with an anti-his antibody resulted in a relatively clean band of approximately 27 kDa. However, as figure 6B shows, detection using serum from rabbits injected with M1 resulted in a complex band pattern. Nevertheless, it is possible to distinguish within the background signal, one band of

approximately the same size as M1 on the lane probed with the final serum. This band of approximately 27 kDa is not visible on the lane probed with pre-bleed serum indicating that there are probably M1-specific antibodies in the final serum. Serum pre-absorbing was also done to try to remove non-specific antibodies, however, this resulted in a loss of both background and M1 signal (data not shown).

Western blot analysis of M2 and M1 produced in different expression systems

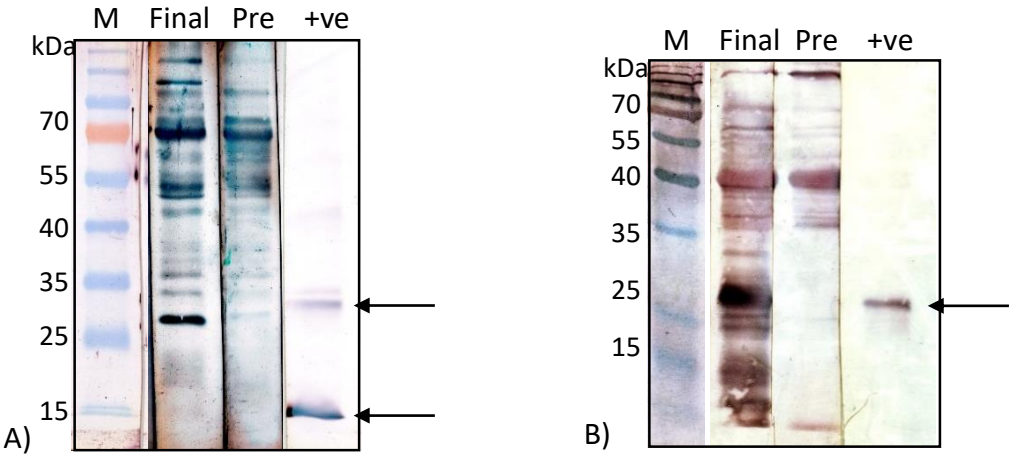

Figure 6| Detection of M2 and M1 proteins produced in *E. coli* with rabbit sera. Immunoblots of *E. coli*-produced M2 (A) detected with anti-M2 rabbit sera and *E. coli*-produced M1 (B) detected with anti-M1 rabbit sera. Both sera were at 1/2000 dilution. M – Molecular marker; Final – Final bleed serum; Pre – Pre-bleed serum; +ve – Proteins detected with commercial anti-histidine antibody. Arrows indicate the position of the respective proteins (± 17 kDa M2 and ± 27 kDa M1).

An additional immunoblot test of the rabbit sera was carried out to determine if it could detect proteins expressed in tobacco plants. For this, the plant-produced cytoplasm targeted 5xM2e-HAtrans and the M1 protein (both expressed using the pRIC vector, see Chapter 3) were used to test the anti-M2 and anti-M1 serum respectively.

As previously shown with *E. coli*-produced proteins, it was not possible to distinguish specific bands when using the anti-M2 sera (Figure 7A). The plant-produced 5xM2e-Hatrans runs at approximately 30 kDa (with higher molecular weight multimers of ± 60 and 120 kDa) as shown using the monoclonal 14C2 anti-M2 antibody; although the final M2 sera does pick up a band of

approximately 60 kDa on the lane loaded with plant produced 5xM2e-HAtrans, a band of this size is also visible in the pre-bleed lane (Figure 7A). Overall, it was not possible to confirm the presence of M2 specific antibodies using immunoblots.

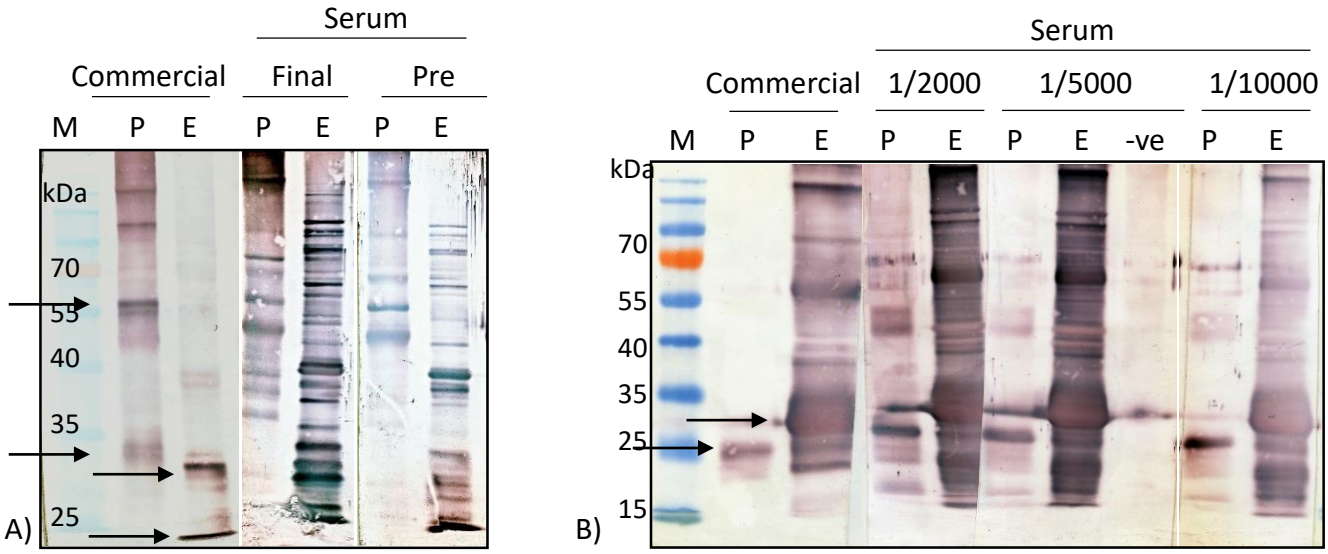

Figure 7| Reactivity of rabbit sera with proteins produced in different expression systems. Immunoblots with M2 (A) and M1 (B) rabbit sera. Lanes labelled E contain *E. coli*-produced M2 or M1 and lanes labeled P contain plant produced 5xM2e-HAtrans or M1. A) Proteins were detected with either commercial anti-M2 antibody (commercial; 1/5000); Final bleed anti-M2 rabbit serum (Final; 1/1000); or Pre-bleed anti-M2 rabbit serum (Pre; 1/1000). *E. coli*B) Proteins were detected with either commercial anti-M1 antibody (commercial; 1/5000); or anti-M1 rabbit serum at different dilutions. M – Molecular marker; -ve – Plants infiltrated with empty pRIC vector. Arrows indicate the position of the respective proteins (± 17 kDa M2, ± 30 kDa 5xM2e-HAtrans and ± 27 kDa M1).

On the other hand, it appears that the anti-M1 serum is able to pick up both bacterial and plant expressed proteins as shown by the 25 kDa and 27 kDa bands on Figure 7B corresponding to the plant-produced and bacterial-produced M1 protein respectively. It is worth noting that the plant-based M1 does not contain a Histidine tag which explains the lower molecular weight. Also, diluting the M1 serum resulted in fewer non-specific bands, especially for the plant produced protein.

Indirect ELISA for detection of anti-M2 and anti-M1 antibodies in rabbit sera

To more accurately confirm the presence (or absence) of specific antibodies in the rabbit sera, a

final test was carried out using an enzyme-linked immunosorbent assay (ELISA) as described in section 2.2.8.

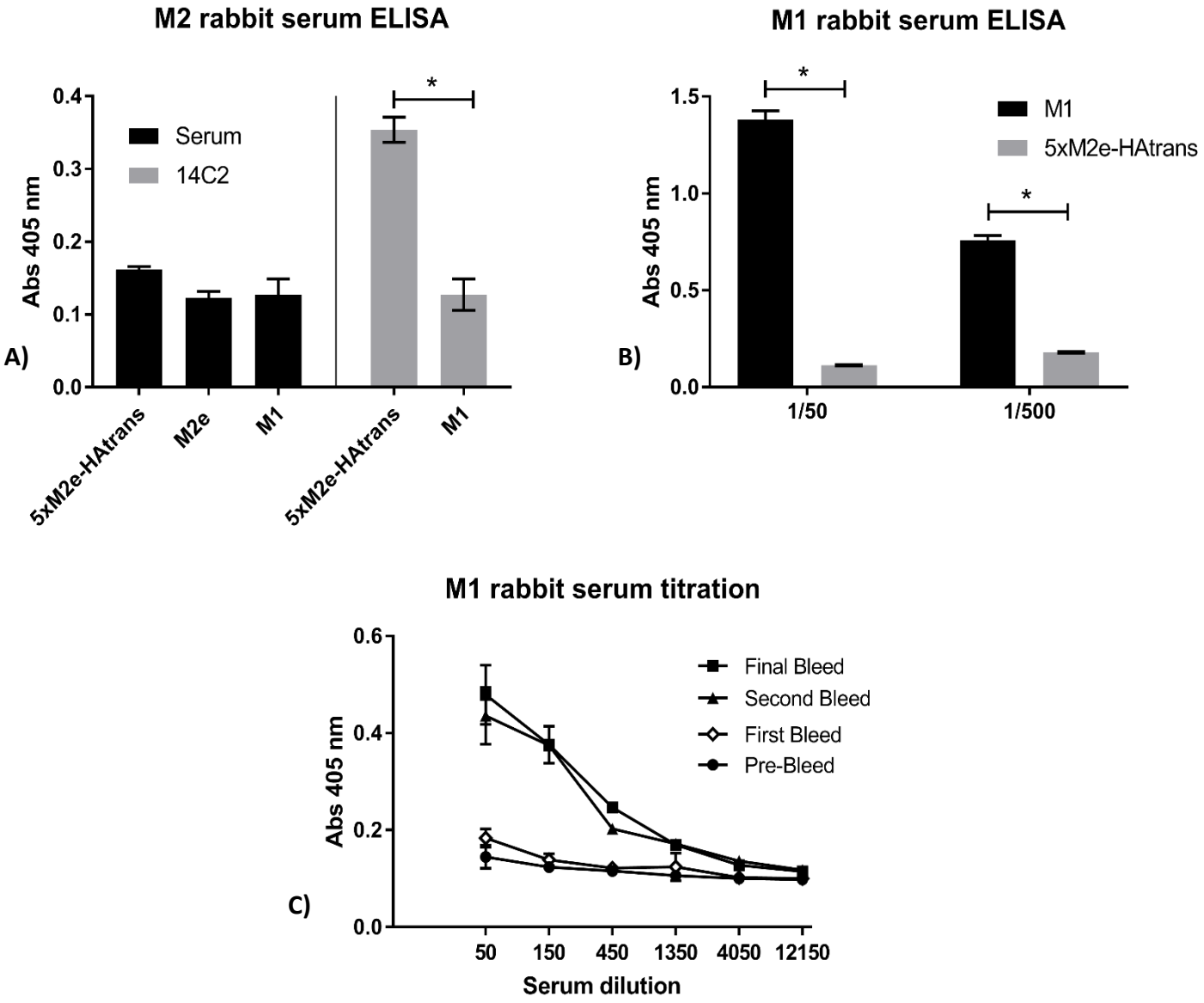

Figure 8| Testing of rabbit sera using indirect ELISA. (A) Indirect ELISA of anti-M2 rabbit sera at 1/50 dilution using either the plant produced 5xM2e-HAtrans and M1 (negative control) proteins or the synthetic M2e peptide (Genscript, China) as coating antigens. The commercial antibody 14C2 was used at a 1/5000 dilution as positive control to confirm the presence of recombinant proteins. (B) Indirect ELISA of anti-M1 rabbit sera at different dilutions using either the plant produced M1 or 5xM2e-HAtrans (negative control) proteins as coating antigens. (C) Reciprocal dilution values of the M1 rabbit sera collected after each bleed to validate immune responses against M1. The markers indicate the mean value of triplicate samples and error bars indicate the standard error of the mean (*p< 0.001).

Because bacterial-produced proteins gave high signal background on western blots with the rabbit serum, proteins expressed in plants instead of bacteria were used as coating antigens for ELISAs.

To probe for M2 specific antibodies in the M2 rabbit sera, plates were coated with either the plant-produced 5xM2e-HAtrans protein or with a synthetic M2e peptide as positive controls. The plant-produced M1 was used as a negative control. As shown in Figure 8A, detecting 5xM2e-HAtrans with a 1/5000 dilution of the commercial 14C2 monoclonal antibody serum resulted in a significant increase in absorbance compared to the M1 protein (negative control). However, when the rabbit serum was used, no differences in absorbance could be detected between the 5xM2e-HAtrans fusion protein, the M2e synthetic peptide or the M1 protein. Serial dilutions of the M2 serum lead to the same results (data not shown).

To test the M1 rabbit sera for M1-specific antibodies, ELISA plates were coated either with plant-produced M1 (positive control) or 5xM2e-HAtrans (negative control), and the absorbances compared. Detection of plant proteins with a 1/50 dilution of the anti-M1 rabbit serum resulted in an absorbance around 1.37 for wells coated with M1, whereas for wells coated with the negative control (5xM2e-HAtrans) the absorbance was around 0.11. This significant difference was also observed at a smaller scale, (0.77 for M1 and 0.18 for 5xM2e-HAtrans) when the serum was diluted by 100-fold (Figure 8B).

To evaluate the increase in anti-M1 specific antibodies in the rabbit serum after each injection, titration values were calculated for the pre-bleed (day 0), first boost (day 14), second boost (day 21), and final bleed (day 42) (Figure 8C). As it can be observed, the anti-M1 specific antibody concentration steadily increased after each boost, reaching a reciprocal endpoint titer value around 450 (Figure 8C).

2.4. Discussion

In this section of the study, I set out to produce antibodies against the two matrix proteins (M1 and M2) from Influenzavirus A, because current commercial antibodies against these proteins are exceedingly expensive, especially for ELISA applications. To create these antibodies,

the two proteins had to be produced in high amounts and in relatively short time. An *E. coli* based system was used for this effect due to its ease of manipulation and relatively short production times (Chen 2012; Terpe 2006; Rosano & Ceccarelli 2014).

Initial trials for M2 expression in *E. coli* using Luria Broth media were successful although expression levels were relatively low and the protein was found completely in the insoluble fractions. Previous studies have shown that exogenous expression of the M2 protein in bacteria resulted in decreased host cell viability (Prasetyoputri et al. 2010). I also reported a decrease in the OD_{600} of recombinant bacteria expressing M2 as soon as they were induced with IPTG suggesting that M2 might somehow be harmful to the bacterial cells. These results are consistent with previous studies which demonstrated that recombinant M2 is able to permeabilize cell membranes, causing cell lysis (Frace et al. 1999; Guinea & Carrasco 1994). M2 is a membrane-bound protein that acts as a proton pump in native influenza virions; its transmembrane portion contains highly hydrophobic amino acids which have been previously reported to compromise M2 solubility and yields in prokaryotic and eukaryotic cell systems (Frace et al. 1999; Czabotar et al. 2004; Mitraki et al. 1991). Some studies have even reported that efficient expression of M2 in recombinant cells can only be obtained in the presence of its target inhibitor, amantadine (Black et al. 1993).

In light of these constraints, I set to carry out different strategies to try increase the amounts of protein without killing the bacteria; these included: lower incubation temperatures, lower concentration of the inducer (IPTG), longer induction periods and different induction media (Khow & Suntrarachun 2012). Although inoculating the bacteria at a lower temperature (i.e. 28 ^{o}C) and for longer periods (i.e. 16 hrs), did reduce bacterial cell death while increasing protein levels, the most efficacious strategy was undeniably when bacteria were grown on the highly enriched media, Terrific broth. Terrific Broth, developed by Tartoff and Hobbs (1987), has been shown to increase bacterial growth and plasmid yields while slowing cell lysis (Tartof & Hobbs 1987; Collins et al. 2002; Collins et al. 2013). It contains high levels of tryptone, yeast extract and glycerol which provide amino acids, and carbohydrates necessary for high density growth. It also contains potassium phosphate which maintains optimal pH during growth. When induced on TB media, I observed a significant increase in recombinant M2 expression levels

compared to the traditional LB media. This increase was also accompanied by a reduction in cell death in TB induced cells. This effect has been demonstrated by several previous studies that used TB to express different proteins in *E. coli* (Manderson et al. 2006; Lim et al. 2000). What I did not anticipate was the appearance of low levels of soluble M2 in TB-induced cells. As previously discussed, M2 is an intrinsic membrane-bound protein and should therefore be insoluble. I suspect that the presence of glycerol in the TB media must have prevented "unfavorable" hydrophobic interactions in the M2 protein. It has previously been described that the addition of certain polyols (such as glycerol) to the incubation media can enhance the stability and solubility of membrane proteins in solution (Yasui et al. 2010). To the best of my knowledge, this is the first time that the full-length influenza A M2 protein has been expressed in *E. coli* in a soluble form without the addition of detergents.

M1 preliminary expression trials showed high levels of expression using LB which is in conformity with previous studies (Syed et al. 2012; Guo et al. 2009). Expression of full-length M1 with pPROEx yielded detectable protein levels in both soluble and insoluble fractions of induced *E. coli* cells, as determined by anti-His immunoblot. It is important to note that despite several attempts to try increase the solubility of M1 (by varying IPTG concentrations, induction media, incubation temperatures and durations), the insoluble fraction always showed significantly higher levels of protein compared to the soluble fraction; more interestingly, the presence of M1 multimers could only be observed in the insoluble fraction.

In its native environment, the influenza A M1 protein forms a coat inside the viral membrane envelope that maintains the structural integrity of the virion and encapsidates the viral genome complexed with the NP (vRNP). For this, the M1 protein is able to bind both vRNP and viral membrane envelope simultaneously (Ruigrok et al. 2000). Although the exact mechanisms of the M1 and lipid membrane binding are not fully understood, a recent study has showed that M1 dimerization is enhanced by the presence of lipid membranes and that once bound to the membrane, M1 dimers recruit additional M1 in solution to form large complexes at the surface of the membrane (Hilsch et al. 2014). Based on these findings, I can hypothesize that both the increased levels of M1 and the exclusive presence of multimers observed in the insoluble fraction can be in part explained by the membrane-binding properties of M1. I say "in part" because most

certainly, overexpression of the non-native M1 protein in *E. coli* also has a role in directing recombinant protein to inclusion bodies (i.e. insoluble fraction).

Since the highest amount of protein in both M1 and M2 trials was observed in inclusion bodies, I decided to proceed with these for rabbit inoculations. Inclusion bodies in *E. coli* are usually formed because of a defense mechanism that protect the cell when heterologous protein is overexpressed. If the expression levels of a non-native protein goes beyond 2 % of the total cellular proteins, it generally leads to inclusion body formation (Mitraki et al. 1991). Other factors such as hydrophobic regions, misfolding or disulfide bonds are also believed to play a role in inclusion body formation (Singh et al. 2015).

These inclusion bodies have been long considered as a waste product composed of non-active misfolded protein aggregates that were too time-consuming and cumbersome to solubilize (García-Fruitós 2010). However, recent studies on the formation and composition of inclusion bodies have shed light on new evidence that IBs, contrarily to what had been widely believed, are at least in part composed of biologically active proteins. This was first demonstrated when the green fluorescent protein (GFP) was shown to be highly fluorescent inside inclusion bodies (García-Fruitós et al. 2005) and later supported by other studies using different proteins that were also found to be active inside inclusion bodies (Morell et al. 2008; Huang et al. 2013; Jevsevar et al. 2005). Thus, combining these new findings with already known advantages from IBs (i.e. expression of a very high level of protein; easy purification of the inclusion bodies from cells; lower degradation of the expressed protein; resistance to cellular proteases; and lack of contaminants/high purity), researchers are now looking at IBs less as a “dead-end” by-product but more like “highly pure deposits of recombinant protein” (Huang et al. 2013; Singh & Panda 2005; García-Fruitós 2010). In agreement with this and in perspective with my work, a recent study has demonstrated that inclusion bodies containing the desired recombinant protein can be used as antigens to directly immunize animals and obtain polyclonal serum (Yang et al. 2011). Therefore, it was decided to partially purify M1 and M2-containing IBs from *E. coli* using successive washes in PBS which were then injected into rabbits for antibody production. Rabbits are the most widely used animal for antibody production because of its convenient size, ease of handling and large amounts of serum producing adequate volumes of high-titer antisera

(Stills et al. 2012; Hanly et al. 1995). Incomplete Freunds' adjuvant was used at a 1:1 ratio with the protein. This adjuvant is routinely used in polyclonal antibody production in animals and has been widely demonstrated to be efficient in improving the immune response to an antigen (Leenaars & Hendriksen 2005; Hanly et al. 1995).

Two weeks after the final injection, collected serum was used on immunoblots loaded with either bacterial or plant produced recombinant M2 and M1 proteins. Between the two sera used, only the anti-M1 serum showed visible results that confirmed detection of the M1 protein. This was observed for both bacterial and plant produced proteins, indicating that the serum was reactive against soluble and insoluble proteins. Moreover, since the plant proteins did not contain a Histidine tag, it can be assumed that the antibodies present in the serum were specific to M1. There was however, excessive background signal, especially when using the M2 serum. This was probably linked to the presence of non-specific antibodies in the serum, reactive to host proteins. Pre-absorption of the sera against proteins from untransformed *E. coli* cell lysate has been suggested to decrease background. However, in this case it did not improve band visualization (data not shown).

To confirm the presence (or absence) of specific antibodies, sera was used to detect plates coated with plant-produced proteins in an indirect ELISA test, as ELISAs are generally more specific and qualitative than immunoblots. Moreover, since the proteins used to coat the ELISA plates were made in plants, the background signal should be minimized.

To detect the M2 serum, a fusion protein presenting five tandem copies of the M2 extracellular domain was used (5xM2e-HAtrans; full details explained in Chapter 3). This was chosen as it was never possible to express the full M2 protein in plants and *E. coli*-produced M2 would give too much background. Nonetheless, since the antibodies desired had to detect the M2e domain for the continuity of the project, it should not pose an issue. A positive control was included using a commercial anti-M2 antibody (14C2) to exclude the possibility of protein degradation in the samples. As previously for immunoblots, ELISA experiments using the M2 serum did not show any increase in activity compared to negative samples. This indicates that either i) there were no

specific M2 antibodies in the serum or ii) the levels of specific M2 antibodies were too low to be detectable.

On the other hand, the M1 serum was able to react with plant M1. The antibody titration values showed a reciprocal endpoint titre around 450, although this value could be higher as no further dilutions were tried. M1-specific antibody levels seemed to increase after each boost, with the strongest values after the third immunization; this confirmed that the M1 protein efficiently induced rabbit immune responses.

Overall, by combining the immunoblotting and the ELISA results, I can conclude that between the two serums, only the M1 showed detectable levels of specific antibodies.

2.5. Conclusions

To summarize, Influenzavirus A M1 and M2 proteins were successfully expressed in *E. coli*, mostly in the form of insoluble inclusion bodies. In contrast to M1, which expressed at high levels in conventional LB media, M2 was only produced in low amounts and its expression had to be optimized. After several trials, the best M2 expression was obtained by growing recombinant bacteria in the enriched TB media for longer periods (i.e. 16 hrs) and at lower temperatures (i.e. 28 ^{o}C). Inclusion bodies containing M1 or M2 were then partially purified by successive washes in PBS and injected into rabbits to raise antibodies.

The anti-M1 serum could detect M1 protein produced in bacteria or plants as shown by immunoblot and ELISA experiments. This serum can be used for subsequent immunoblots and ELISA experiments, thus reducing greatly the costs of the project.

The anti-M2 serum, on the other hand, was never shown to react with any of bacterial M2, plant 5xM2e-HAtrans or with a synthetic M2e peptide. It seemed that the levels of anti-M2 antibodies in the serum were too low for detection. It could be possible that the M2 epitopes were obscured by other proteins in the insoluble bodies that made them inaccessible to the rabbits' immune system. There have been reports showing that the M2 protein is a poor immunogen and that M2-specific antibody responses remained low in the mammalian host (Deng et al. 2015). However, these reports were made after natural or experimental infection with influenza A viruses, never

after injection of a solution containing recombinant M2. In fact, most of the literature regarding the production of M2 serum for experimental analysis has used the M2e peptide as an immunization antigen, not the full M2 protein (Mardanova et al. 2015; Nikbakht et al. 2012; De Filette et al. 2011). Here I have shown that recombinant M2 produced in *E. coli* using the conditions described above, was not able to elicit detectable anti-M2 antibodies in the serum of injected rabbits. Nevertheless, I hypothesize that by increasing the amounts and the purity of recombinant M2 as well as the number and the time between each boost, should result in increased immune responses against the M2 protein. Feng et al. 2006 stated that although M2 induces poor immune responses, "primary infections elicit a degree of B cell immune memory against M2e that can be boosted by subsequent challenges". Due to time and cost constrains, I was not able to repeat immunization trials, but further trials must be conducted to verify these hypotheses.

Chapter 3: Design and optimization of several M2e-HA chimaeric protein expression in *N. benthamiana*

3.1. Introduction

Influenza has been infecting humans for many centuries and continues to be today one of the leading causes of human acute respiratory infections (Mayor 2010). With a global annual attack rate estimated at 5 - 10 % in adults and 20 - 30 % in children, which leads to more than 4 million severe infection cases and 250,000 - 500,000 deaths worldwide, researchers have ranked influenza (among other types of respiratory diseases) to be the fourth leading cause of death in the world (Anon 2014; Lozano et al. 2012). As a result, influenza vaccine development has been a priority for international health authorities.

Despite the reported efficacy of existing approved seasonal influenza vaccines (Foppa et al. 2015; Jefferson et al. 2014), long production times, limited capacity and the lack of broadly cross-protective immune responses have made it difficult for current vaccines to meet the global demand (Lee et al. 2014; Doherty & Kelso 2008; Shoji et al. 2008).

To address this point, alternative approaches to influenza vaccine formulations and production systems are being examined. To produce vaccines with broad efficacy, researchers have been targeting conserved epitopes that exist across different influenza virus subtypes. To this date, the most promising epitopes investigated are the M2e ectopic peptide and the HA stalk domain (de Vries et al. 2015; Doherty & Kelso 2008; Gerhard et al. 2006; Fiers et al. 2009; Yassine et al. 2015). However, given the low immunogenicity of these peptides in their native conformation, the challenge now relies on finding ways of increasing the immunogenicity of these conserved sequences. VLPs have shown promising results for presenting influenza surface proteins in a highly immunogenic form (Choi et al. 2013; D'Aoust et al. 2010; Kang et al. 2012; Song, Van Rooijen, et al. 2011). VLPs are generated upon expression and subsequent self-assembly of defined recombinant viral proteins. These nanoparticles present an external surface resembling that of their native virus with the benefit of not incorporating viral genomic material, making them safer than inactivated viral vaccines (Pêra et al. 2015). The presentation of antigens in a native conformation has been shown to achieve enhanced stimulation of humoral and cellular

immune responses (Lee et al. 2014; Kang et al. 2012). This is particularly true in the case of enveloped viruses, since enveloped VLPs should present the surface antigens in their natural membrane-bound state (Grgacic & Anderson 2006). VLPs have been produced using a variety of systems including insect cells (Choi et al. 2013), microbial cells (Denis et al. 2008), mammalian cells (Steel et al. 2010) and more recently, in plants (D'Aoust et al. 2010; Pillet et al. 2015).

For the last two decades, plant-based platforms have been gaining popularity as an important alternative to "conventional" fermenter-based systems for recombinant protein production. Major advantages supporting plants as bioreactors include, lower up-front investment required for commercial production, no risk of contamination with animal pathogens and high scalability potential (Sainsbury & Lomonossoff 2014; Thuenemann et al. 2013; Waheed et al. 2016).

Initially, modification of plants for recombinant protein expression relied on the generation of stable transgenic lines, which is both time-consuming and resource-intensive (Sainsbury & Lomonossoff 2014). However, with the development of new transient expression methods, it is now possible to produce commercially-relevant levels of recombinant proteins within days versus several months using stable transformation (D'Aoust et al. 2010). These recent advances in plant biopharming have made plants an excellent alternative to current egg-based platforms for influenza vaccine production.

The aim of the work presented here was to design HA-based M2e-containing chimaeric proteins with the potential to self-assemble into M2e-presenting VLPs in plants. It is still almost impossible to predict whether chimaeric proteins will be compatible with VLP assembly or whether they will be immunogenic in the resulting chimaeric VLP. And, although Kim, Lee, et al. (2013) demonstrated that immunogenic VLPs could be obtained in insect cells by fusing 5xM2e to the transmembrane domain of HA, differences in expression systems and protein sequences used between this and their study, make it difficult to extrapolate on VLP formation. Hence, to maximize the chances of obtaining immunogenic VLPs, I designed different M2e-HA fusions (see Figure 1).

The first variation involved fusing the M2e peptides to either the full HA stalk domain (5xM2e-HAstalk) or just the transmembrane domain (5xM2e-HAtrans). Besides having possible structural

properties that could enhance VLP formation, the HA stalk domain is extremely well conserved. In fact, apart from the M2e peptide, the HA stalk domain has been the most used peptide for the generation of candidate universal influenza vaccines (Staneková et al. 2011). Hence, by including the stalk domain in our M2e fusions, it could be possible to create VLPs that have increased cross-protection as compared to VLPs with only the HA transmembrane domain.

The second permutation of the M2e-HA fusions involved the addition of the tetramerizing domain of the yeast transcription factor, general control nondepressible 4 (GCN4). The idea of using GCN4 as a tetramerizing scaffold originated from a study conducted by De Filette et al. (2008), where the M2e peptide was fused to GCN4 (M2e-tGCN4) to obtain a structure that would closely mimic the tetrameric conformation of the native M2e peptide. Antibodies raised by M2e-tGCN4 immunization were shown to specifically bind to the surface of influenza-infected cells and to an M2-expressing cell line. Here, the incorporation of GCN4 into the M2e-HA chimaeras was investigated as a way to possibly enhance immunogenic responses against the M2e peptides. Introducing a tetramerizing domain might not be compatible with the natural trimerization induced by the HA stalk, therefore, two control constructs were created were the GCN4 domain was not added.

Finally, the last permutation of the M2e-HA fusions involved using only one copy of the M2e peptide (1xM2e-HAtrans and 1xM2e-HAstalk) instead of five. These constructs would allow to test whether multiple tandem copies of M2e in a vaccine construct would elicit higher M2e IgG titers than one M2e containing construct, as suggested by Deng et al. (2015).

In total, six different M2e-HA chimaeras were created: 5xM2e-GCN4-HAstalk, 5xM2e-GCN4-HAtrans, 5xM2e-HAstalk, 5xM2e-HAtrans, 1xM2e-HAstalk and 1xM2e-HAtrans. Injection agro-infiltration was used for the rapid optimisation of protein expression and several methods were analyzed to maximize yields in plants. Finally, most promising M2e-HA fusion proteins were selected for co-expression studies with the influenza matrix protein 1. This optimization work is the initial step towards creating the first plant-produced influenza VLP vaccine based on M2e-HA chimaeric proteins.

3.2. Methods

3.2.1. Fusion protein design

M2e alignment was performed using CLC Bio (Qiagen); a full list of the sequences used can be found in Appendix A. The gene construct for encoding the 5xM2e-GCN4-HAstalk fusion protein was genetically designed to contain the HA signal peptide (MEKIVLLFAIVSLVKS-A/Vietnam/1203/04, H5), five copies of different M2e sequences from the M2e consensus (SLLTEVETPTRNEWECRCSDSSD), human type (SLLTEVETPIRNEWGSRSNDSSD, (Kim, Lee, et al. 2013)), swine type (SLLTEVETPTRSEWESRSSDSSD, A/California/4/2009, H1N1), and two avian types (SLLTEVETPTRNEWESRSSDSSD, A/Vietnam/1203/04,H5N1 and SLLTEVETLTRNGWGCRCSDSSD, A/Hong Kong/156/97, H5N1) separated by a EAAAK linker peptide, a tetramerizing leucine zipper derived from GCN4 (De Filette et al., 2008), and the stalk, transmembrane and cytoplasmic domains of HA derived from A/Vietnam/1203/04, H5N1. Human codon optimized 5xM2e-GCN4-HAstalk fusion protein sequence was synthesized by Genscript (China) and delivered in the pUC57 vector.

The pUC57-5xM2e-GCN4-HAstalk vector was transformed into DH5-α (E. cloni™, Lucigen) and Dam^- (devoid of dam methylation) (BIO 85044, Bioline, Meridian Bioscience Inc., USA) chemically competent *E. coli* cells according to the method described by Sambrook et al. (1989).

The transformed cells were plated on Luria Bertani (LB) media agar plates (10 g Tryptone, 5 g Yeast Extract, 5 g NaCl in 1 L water; 15 g of Bacterial Agar was added for agar plates) supplemented with ampicillin (amp) (100 µg/mL). Plates were incubated at 37 °C, O/N. Single colonies were selected and inoculated in 10 mL LB broth supplemented with 50 µg/mL ampicillin and incubated with agitation for 16 hrs at 37 °C.

Plasmid isolations were performed using the QIAprep® Spin Miniprep kit (Qiagen) according to instructions provided by the manufacturer. Recombinant pUC57-5xM2e-GCN4-HAstalk clones were verified by restriction enzyme digestion. Recombinant DNA (~ 500 ng) was digested for 1 hr at 37 °C using 1 U XhoI and 1 U BamHI (Thermo Fisher Scientific, MA, USA) per reaction according to the manufacturer's instructions. Linearized DNA was separated on 1 % w/v TBE (89 mM Tris base, 89 mM boric acid and 2 mM EDTA [pH 8]) agarose gels containing 0.5 mg/mL ethidium

bromide. O'GeneRuler™ 1kb DNA ladder #SM1163 (Thermo Fisher Scientific, MA, USA) was used as molecular weight marker on all the agarose gels.

After verification of pUC57-5xM2e-GCN4-HAstalk in both DH5-α and Dam- cells, several restriction digests were performed to create five different permutations of 5xM2e-GCN4-HAstalk, as illustrated in Figure 1.

Briefly, recombinant DNA (~ 1000 ng) from DH5-α was digested using 1 U of either BamHI and BglII or XbaI and NheI to produce 1xM2e-HAstalk or 5xM2e-HAstalk respectively. DNA from Dam- cells (not methylated) was digested with 1 U of either BclI and BglII or BamHI and BclI to produce, 5xM2e-GCN4-HAtrans or 1xM2e-HAtrans respectively. All digests were performed for 1 hr at 37 °C. However, BclI / BglII and BamHI / BclI had to be first digested for 1 hr at 37 °C without BclI, followed by heat inactivation for 20 min at 80 °C. Only after inactivation, BclI was added to the reactions and incubated at its optimal temperature of 55°C for 1 hr.

Digested DNA was separated on 1 % w/v TBE agarose gels containing 0.5 mg/mL ethidium bromide and visualized under long wavelength ultraviolet (UV) illumination. Corresponding bands were identified and DNA was purified from the agarose gels using the QIAquick® Gel Extraction kit (Qiagen) following the manufacturer's instructions. Purified DNA was re-circularized with T4 DNA Ligase (Thermo Fisher Scientific, MA, USA) for 15 min at room temperature, per manufacturer's instructions and transformed into DH5-α as previously. pUC57-5xM2e-HAstalk was also transformed into Dam^- cells. All transformed cells were plated on Luria Bertani (LB) media agar plates supplemented with ampicillin (100 µg/mL).

Positive colonies were selected by colony PCR using gene-specific primers as showed in Table 1. The PCR reactions of the appropriate template DNA consisted of 250 µM dNTPs, 0.2 µM of each primer, 1 x Kapa taq Buffer A and 0.5 units (U) KAPA Taq DNA Polymerase (KAPA Biosystems). The reactions were amplified with an initial denaturation step at 92 °C for 2 min and 30 s; followed by twenty-five cycles of denaturation at 92 °C for 30 s, annealing at 47 °C for 30 s and elongation at 72 °C for 90 s. Reactions finished with a final elongation step at 72 °C for 4 min.

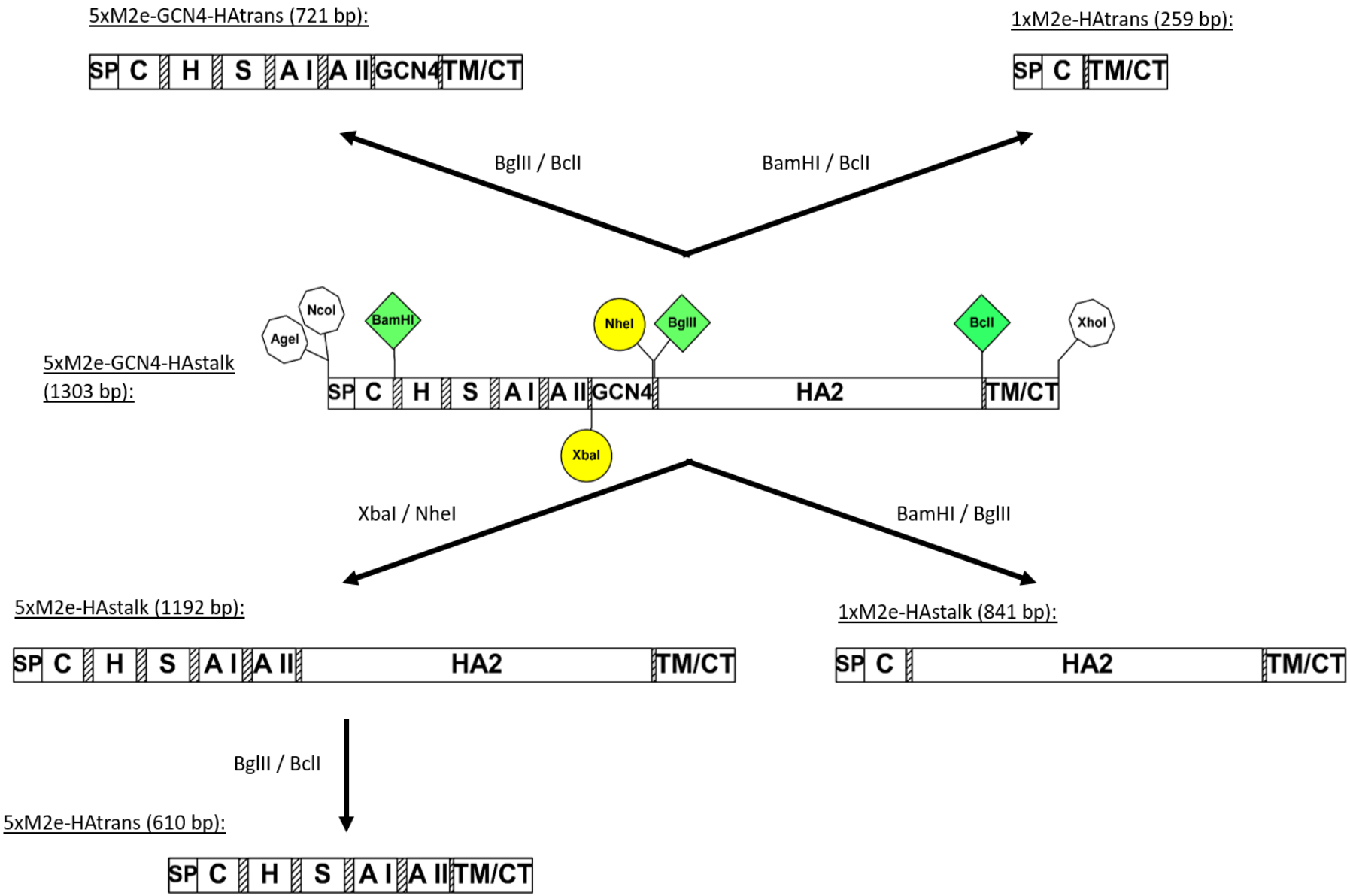

Figure 1| M2e-HA fusion protein design. Restriction enzyme digest strategy used to create the six different M2e-HA permutations as described in section 3.2.1. SP – Haemagglutinin signal peptide; C – consensus M2e sequence; H – M2e from human type (Kim, Lee, et al. 2013); S – M2e from swine type (A/California/4/2009, H1N1); A I – M2e from avian type (A/Vietnam/1203/ 04, H5N1); A II – M2e from avian type (A/Hong Kong/156/97, H5N1); ▨ – EAAAK linker; GCN4 – Leucine zipper of the yeast transcription factor GCN4 (oligomerization domain, 105 bp); HA2 – Haemagglutinin stalk domain; TM/CT – Haemagglutinin transmembrane and cytoplasmic domain. Figure not made to scale.

Positive Dam$^-$ colonies containing pUC57-5xM2e-HAstalk were inoculated into 10 mL LB broth supplemented with 50 µg/mL ampicillin and incubated with agitation for 16 hrs at 37 °C. Plasmid isolation was performed as previously described. Recombinant DNA (~ 1000 ng) was then digested for 1 hr at 37 °C, with BclI and BglII to create the last chimaeric protein: 5xM2e-HAtrans.

Table 1| Primers for plant expression

Primer	Sequence	Orientation
M2eF	5'-AAA ATC GTG CTG CTG TTC-3'	Forward
M2eR	5'-CTG CAG ACT TCC ATT TGA -3'	Reverse
M1F	5'-TGT CCT GAG TAT TAT CCC-3'	Forward
M1R	5'-GAC CCC CAT CCT TTT CTG-3'	Reverse

Digested DNA was then separated on a 0,8 % w/v TBE agarose gel and the corresponding band was purified and re-circularized as indicated previously. Re-circularized pUC57-5xM2e-HAtrans was then transformed into DH5-α cells as previously. Positive clones were identified by colony PCR using the same gene-specific primers (Table 1) and conditions as previously described.

After verification of every clone by colony PCR, the plasmid DNA was sequenced (Macrogen Inc., Netherlands) using the gene-specific primers (Table 1). Sequencing data was analyzed using CLC MAIN WORKBENCH (Qiagen®).

3.2.2. Sub-cloning of fusion proteins into different plant expression vectors

All fusion proteins were designed with AgeI and NcoI sites on the 5'end and an XhoI site on the 3' end to facilitate cloning into three different plant expression vectors (designed to target recombinant proteins to the cytosol): pTRAc, pRIC 3.0 and pEAQ-HT. The M1 sequence described in Chapter 1 was also used for plant expression since it contained an AgeI and AflIII site on the 5'end and an XhoI site at the 3'end. pTRAc was kindly provided by Dr Rainer Fischer, Fraunhofer Institute, Aachen, Germany. pRIC 3.0 is a novel autonomously replicating plant expression vector developed using elements of the replication machinery of Bean Yellow Dwarf Virus as described by Regnard et al. (2010). pEAQ-HT contains a P19 silencing suppressor and the 5'/3'-untranslated region (UTR) from the Cowpea mosaic virus (CPMV) RNA-2 which has been shown to greatly

enhance the translation efficiency of recombinant proteins (Sainsbury & Lomonossoff, 2008). The M1 and fusion protein sequences were excised from the pUC57 backbone by first digesting the plasmid DNA with XhoI and either NcoI (or AflIII for M1) or AgeI for 1 hr at 37 °C, after which the DNA was gel-purified with the QIAquick® Gel Extraction kit (Qiagen). This digestion yielded recombinant proteins with 5' AgeI (for cloning into pEAQ-HT) or NcoI (for cloning into pTRAc and pRIC 3.0) sites and 3' XhoI sites.

The pTRAc and pRIC 3.0 expression vectors were linearized by restriction digestion with AflIII and XhoI whereas pEAQ-HT was linearized with AgeI and XhoI. The vector DNA was dephosphorylated using 1 U rapid alkaline phosphatase (Roche) per the manufacturer's instructions.

Table 2|Different expression vectors and recombinant proteins that were tested

Expression vector	Vector restriction sites (5'/3')	Insert	Size (Kb)	Insert restriction sites (5'/3')
pTRAc	AflIII/XhoI	5xM2e-GCN4-HAstalk	~1.3	NcoI/XhoI
		5xM2e –HAstalk	~1.2	
		5xM2e- HAtrans	~0.6	
		5xM2e-GCN4-HAtrans	~0.7	
		1xM2e- HAstalk	~0.8	
		1xM2e- HAtrans	~0.3	
		M1	~0.8	AflIII/XhoI
pRIC3.0	AflIII/XhoI	5xM2e-GCN4-HAstalk	~1.3	NcoI/XhoI
		5xM2e –HAstalk	~1.2	
		5xM2e- HAtrans	~0.6	
		5xM2e-GCN4-HAtrans	~0.7	
		1xM2e- HAstalk	~0.8	
		1xM2e- HAtrans	~0.3	
		M1	~0.8	AflIII/XhoI
pEAQ-HT	AgeI/XhoI	5xM2e-GCN4-HAstalk	~1.3	AgeI/XhoI
		5xM2e –HAstalk	~1.2	
		5xM2e- HAtrans	~0.6	
		5xM2e-GCN4-HAtrans	~0.7	
		1xM2e- HAstalk	~0.8	
		1xM2e- HAtrans	~0.3	
		M1	~0.8	

Recombinant protein sequences were then directionally sub-cloned into all three expression vectors according to their respective restriction sites using T4 DNA Ligase (Thermo Fisher Scientific, MA, USA). All constructs are listed in Table 2.

Recombinant clones were transformed into DH5-α chemically competent *E. coli* cells (E. cloni™, Lucigen) as described by Sambrook et al. (1989). Transformed cells were plated on LB media plates supplemented with ampicillin (100 µg/mL) O/N at 37 °C. Positive

clones were selected by colony PCR using the same settings and gene-specific primers (Table 1) as previously.

3.2.3. *Agrobacterium* transformation

A. tumefaciens LBA4404 and *A. tumefaciens* GV3101::pMP90RK cells were made electrocompetent using the method described by Shen and Forde (1989). The pEAQ-HT or pTRAc and pRIC 3.0 recombinant plasmids were electroporated into *A. tumefaciens* LBA4404 or *A. tumefaciens* GV3101::pMP90RK, respectively. Transformation of the *A. tumefaciens* strains was carried out by electroporation according to the method described by Maclean et al. 2007. Briefly, 200 to 400 ng of recombinant plasmid DNA was added to a 1 mm chilled electroporation cuvette (Bio-Rad, CA, United States of America), along with 100 µl of electrocompetent cells. After 5 minutes of incubation on ice, cells were electroporated using a Bio-Rad GenePulser™ under the following conditions: 1.8 kV, 25 µF, 200 Ω. After electroporation, 900 µl of antibiotic-free Luria broth was added to the electroporated cells, which were incubated for 2 hrs at 27 °C.

Recombinant pEAQ-HT clones were selected on LB media agar plates at 27 °C containing 30 µg/mL kanamycin and 50 µg/mL rifampicin. The pTRAc and pRIC 3.0 clones were selected under the same conditions except that the plates were additionally supplemented with 50 µg/mL carbenicillin. Successful transformation was confirmed by colony PCR (as in Section 2.2.1) using the gene-specific primers listed in Table 1.

3.2.4. *A. tumefaciens*-mediated transient expression

Starter cultures of recombinant pEAQ-HT, pTRAc and pRIC 3.0 *A. tumefaciens* cells, including *A. tumefaciens* LBA4404 containing pBIN-NSs, the plasmid carrying the TSWV NSs silencing suppressor gene, were supplemented with the relevant antibiotics and grown in LB broth as described by Maclean et al. (2007). To prevent clumping of the recombinant LBA4404 *A. tumefaciens* cells, the medium was supplemented with 2 mM magnesium sulphate (MgSO4).

After making glycerol stocks, the starter cultures were used to inoculate induction medium (Maclean et al., 2007) with the addition of the appropriate antibiotics, including 20 µM acetosyringone. The cultures were incubated O/N at 27 °C with agitation to induce expression of the vir genes. The cells were harvested from the O/N cultures by

centrifugation at 4 000 x g for 5 min and re-suspended in infiltration medium (10 mM magnesium chloride [MgCl2], 10 mM 2-morpholinoethanesulfonic acid [MES], 3% sucrose and 150 µM acetosyringone in water, pH 5.6). The cell suspensions were incubated at 22 °C for 2 hrs to allow for additional expression of the vir genes prior to infiltration. After incubation, the cultures were diluted to the required optical density (OD_{600}) in infiltration medium. The cell densities (OD_{600}) used for infiltration of the constructs were varied to find the optimal cell concentration where all recombinant proteins were successfully co-expressed.

For each one of the expression vectors used, the relevant recombinant *A. tumefaciens* constructs were infiltrated into six-week-old *N. benthamiana* leaves as described by Maclean et al., 2007. *N. benthamiana* plants were grown from seed in a controlled plant growth room. The plants were grown at 22 °C, with 16 hrs of light per day for 6 weeks.

Small-scale infiltration was performed by injecting the Agrobacterium suspension into the abaxial spaces of the plant leaves, using a 1 mL needless syringe. After infiltration, the plants were grown at 22 °C under 16 hrs/8 hrs light/dark cycles until harvested.

As a negative control the plants were infiltrated with infiltration medium. Time-trials were conducted to evaluate and compare single and co-expression of fusion proteins with M1 in different vectors.

3.2.5. Crude leaf extract

For protein extraction, three leaf discs (cut by using the cap of a microcentrifuge tube) were harvested at desired days post infiltration (dpi). Leaves were then ground up using a micro-pestle in the presence of extraction buffer at an approximate ratio of 1:3 (weight: volume). Extraction buffer was composed of 1xPBS (PBS composition: 137 mM NaCl, 1.8 mM KH2PO4, 10 mM Na2HPO4, 2.7 mM KCl, pH 7.4) containing protease inhibitor (cOmplete, Mini, EDTA-free tablets, Roche) as specified.

Ground leaf extracts were clarified by a centrifugation step at 15,000 x g for 10 min. The supernatant representing the crude leaf extract was collected for further analysis.

Crude leaf extracts were incubated at 90 °C for 10 min in sample application buffer prepared for analysis by sodium dodecyl sulphate-polyacrylamide gel electrophoresis (SDS PAGE) (Sambrook et al., 1989) and stored at -20 °C until further analysis.

3.2.6. Coomassie Stained SDS PAGE gels and western blots

Recombinant proteins were resolved on 10 % SDS polyacrylamide gels, loading an equal volume of plant extract into each lane to separate proteins on the basis of their molecular weights (Sambrook et al. 1989). To determine the sizes of the resolved proteins in Coomassie stained gels and on nitrocellulose membranes, a Color Protein Standard Broad Range Ladder #P7712S (New England Biolabs, USA) was used as a molecular weight marker.

For Coomassie, gels were stained with Coomassie Brilliant Blue R250 (Merck, Darmstadt, Germany) stain for 2 hrs at 37 °C and destained overnight with destain solution (45 % methanol, 45 % water, 10 % glacial acetic acid).

For western blots, gels and nitrocellulose membranes were pre-equilibrated for 10 min in transfer buffer (5.82 g Tris base, 2.93 g Glycine, 200 mL methanol in 1 L water, pH 9.2) before being transferred to a nitrocellulose membrane at 15 V for 90 minutes using a Trans-blot®SD semi-dry transfer cell (Bio-Rad, CA, USA). After electrophoretic transfer, the membranes were blocked in blocking buffer (5 % non-fat dairy milk and 1 x PBST (137 mM NaCl, 1.8 mM KH_2PO_4, 10 mM Na_2HPO_4, 2.7 mM KCl, pH 7.4 and 0.1 % Tween-20) for 30 min. The membranes were probed overnight at 4 °C with either 1:10000 M1 rabbit serum, 1:5000 anti-M1 GA2B (Abcam, UK), 1:5000 anti-M2 14C2 (Abcam, UK) or anti-histidine MCA 1396 mouse monoclonal IgG antibodies (ABD Serotec, Bio-Rad, CA, United States of America) diluted in blocking buffer. The membranes were then washed four times with blocking buffer for 15 minutes each and afterward incubated in a 1:10000 dilution of anti-mouse or anti-rabbit IgG (whole molecule) alkaline phosphatase conjugated antibody produced in goat (Sigma-Aldrich, Merck, Germany) in blocking buffer for 1 hr at 37 °C. Membranes incubated in secondary antibody were washed four times with 1 x PBST (without milk), with 15 min for each wash. Detection was performed with BCIP (KPL, MD, USA). Protein expression,

extraction and western blot analysis was repeated at least three times to confirm the expression of the recombinant influenza proteins.

3.2.7. Analysis of post-translational modifications

N-glycosylation sites of fusion proteins were predicted using the NetNGlyc 1.0 software available at URL http://www.cbs.dtu.dk/ services/NetNGlyc/.

3.2.8. Indirect ELISA

Indirect ELISA was used to compare fusion protein expression levels. 96-well Maxisorp® microtitre plates (Nunc) were coated with 100 µL/well of antigen diluted in coating buffer (10 mM Tris, pH 8.5). After incubating the plates O/N at 4°C, plates were blocked with TBS blocking buffer (5 % non-fat dry milk in 1 x TBS [50 mM Tris, 150 mM NaCl, pH 7.5]) for 2 hrs at RT after which they were washed four times with 1 x TST buffer (1 x TBS [pH 7.5], 0.05 % Tween®20). The anti-M2 14C2 mouse monoclonal IgG antibody (Abcam, UK) was then diluted to 1:5000 in TBS and 100 µL was added to each well sera, after which plates were left for 1 hr at 37 °C for incubation. Blank wells containing no antibody were included as background control. After incubation, plates were washed four times with 1 x TST buffer and 100 µL of goat anti-mouse IgG alkaline phosphatase conjugate (1:10000, Sigma) diluted in blocking buffer was added per well and incubated for 1 hr at 37 °C. After incubation, the plates were washed four times with 1 x TBS (pH 9) buffer and 200 µL SIGMAFAST™ p-Nitrophenyl phosphate (pNPP, Sigma) was added per well. The plates were developed in the dark for 30 min after which the absorbance was detected at 405 nm on a BIO-TEK® Powerwave XS microtitre plate reader.

3.3. Results

3.3.1. Designing the M2e constructs

To cover a broader range of influenza A types and to increase the density of M2e epitopes, I designed a tandem repeat of five M2e sequences (5xM2e) derived from human, avian and swine origin influenza A viruses. In total, two avian-derived M2e sequences, one human, one swine and a consensus sequence derived from different species were used; all separated by a linker peptide (EAAAK). To determinate the consensus sequence (SLLTEVETPTRNEWECRCSDSSD), I aligned a total of 33 different

M2e sequences from several different Influenza A origins using the CLC bio software (Qiagen) (Figure 2).

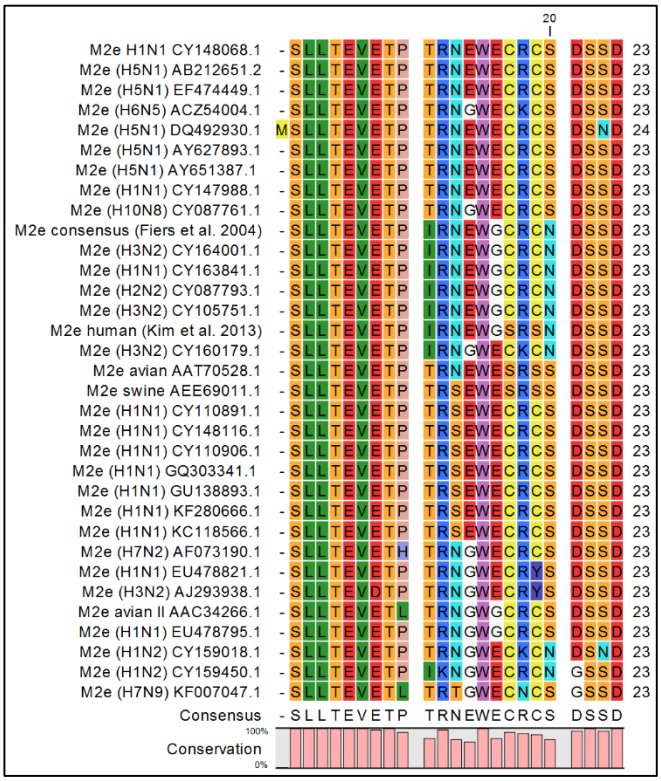

Figure 2 | M2e alignment of 33 sequences from different Influenza A strains.

To present the 5xM2e repeats on the surface of VLPs, I originally designed a chimaeric protein (5xM2e-GCN4-HAstalk) by replacing the HA globular head with the 5xM2e repeats. Additionally, a domain known to stabilize oligomer formation (general control non-depressible 4, GCN4) was inserted between the C-terminal part of M2e5x and the N-terminal part of the HA stalk domain. From this original 5xM2e-GCN4-HAstalk sequence, I constructed five permutations (5xM2e-GCN4-HAtrans, 5xM2e-HAtrans, 1xM2e-HAtrans, 5xM2e-HAstalk, 1xM2e-HAstalk), resulting in a total of six clones which were used to analyze the effect of each component on VLP formation and expression levels. A detailed structure of each construct can be found in Figure 1.

3.3.2. Verification of M2e chimaera clones

The M2e chimaeras, and the native M1 capsid protein were successfully cloned into the pTRAc-HT, pRIC 3.0 and pEAQ-HT plant expression vectors. These were then transformed into *E. coli* and subsequently into either *A. tumefaciens* GV3101::pMP90RK for pTRAc-HT and pRIC 3.0 or *A. tumefaciens* LBA4404 for the pEAQ-HT constructs.

Positive recombinant clones were screened by colony PCR using genes specific primers (Table 1).

All constructs produced fragments of the expected size, confirming the presence of recombinant genes in pRIC 3.0 (figure 3), pEAQ-HT and pTRAc-HT (data not shown). To verify the integrity of sequence for each individual gene, recombinant clones were sequenced with gene-specific internal primers (Table 1). The sequences were analyzed in CLC bio (Qiagen) by multiple alignment of the sequence data with theoretical sequences of the plasmid. Sequence analysis confirmed that the genes were intact and correct (data not shown).

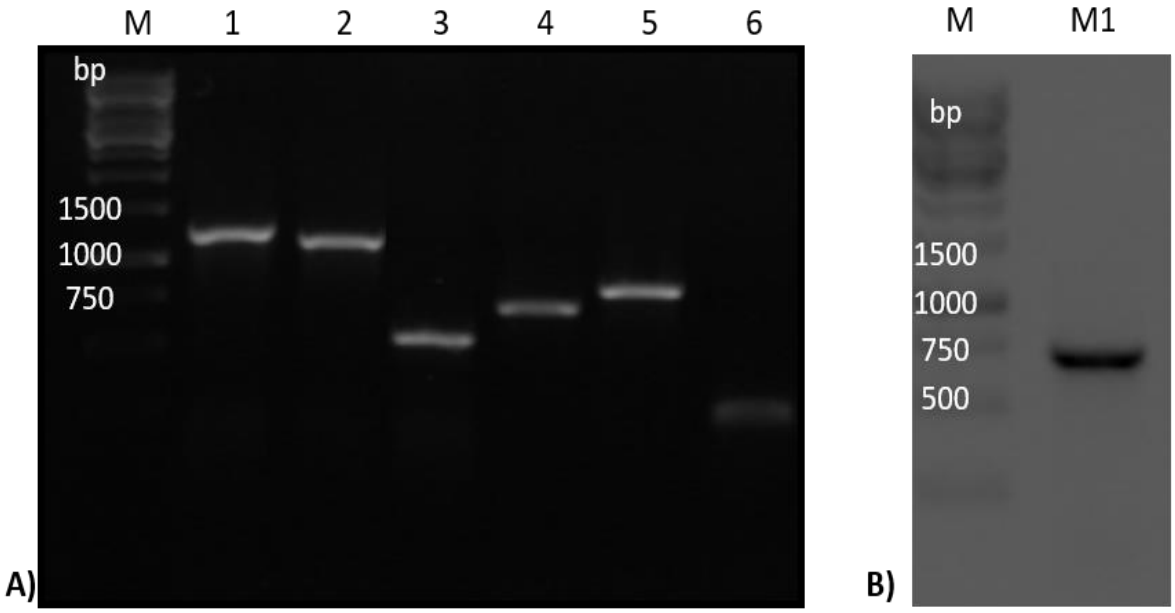

Figure 3| Colony PCR to verify the presence of recombinant genes in pRIC 3.0. A) M2e-HA fusion constructs. Lanes: 1 - 5xM2e-GCN4-HAstalk [~ 1.3 kb]; 2 - 5xM2e-HAstalk [~ 1.2 kb]; 3 - 5xM2e-HAtrans [~ 0.6 kb]; 4 - 5xM2e-GCN4-HAtrans [~ 0.7 kb]; 5 - 1xM2e-HAstalk [~ 0.8 kb]; 6 - 1xM2e-HAtrans [~ 0.3 kb]. B) M1 colony PCR; M1 [~ 0.7 kb]. The molecular marker is represented by lanes M.

3.3.3. Small-scale optimisation of M2e chimaera expression in *N. benthamiana*

The expression of every M2e chimaera in *N. benthamiana* was examined over 1 - 7 days post infiltration (dpi). Initial attempts were performed using the plant expression vector pTRAc-HT and an optical density of 0.5 for the recombinant *Agrobacterium*. Three 7 mm leaf disks per leaf were harvested and extraction was performed using 1 x PBS. EDTA-free protease inhibitor was added to PBS in initial trials, however its addition did

not improve significantly protein expression compared to PBS alone (data not shown). Hence, due to its high costs, protease inhibitor was not added throughout the remaining of the experiments. Total soluble protein was determined by Bradford assay. Expression levels were analyzed by western blotting, loading equal TSP amounts and using the monoclonal anti-M2 14C2 antibody which has been shown in previous studies to be able to bind to M2e epitopes.

As shown in Figure 4, of all the fusion proteins, only the 5xM2e-HAstalk presented detectable levels of expression using the pTRAc-HT vector. This protein was readily detectable using the anti-M2 antibody, after only 3 days post-infiltration (Figure 4, lane 1). Extracting proteins at days 5 and 7 resulted in decreased expression levels for 5xM2e-HAstalk, while the remaining proteins could never be detected (data not shown). Additional attempts of detection were tried using an anti-His antibody (the pTRAc-HT constructs add a Histidine tag on the N-terminus of the proteins). However, for all proteins, no difference could be observed between the anti-M2 and anti-His tag antibodies (data not shown).

Considering these results, I decided to retry expression trials using two additional expression vectors: these were pRIC 3.0 and pEAQ-HT (Figure 5 and 6). Initial attempts using these vectors were performed with the same conditions as for the pTRAc-HT trials,

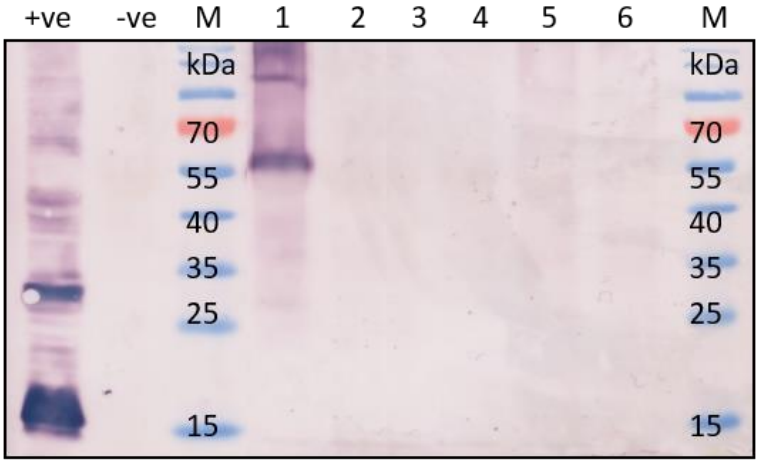

Figure 4| Immunoblot of fusion protein expression in *Nicotiana benthamiana* using the pTRAc-HT expression vector. Infiltration was performed at OD_{600} 0.5 and proteins were harvested at 3 d.p.i. and detected using the monoclonal anti-M2 antibody 14C2. +ve – M2 protein produced in *E. coli*; -ve – empty pTRAc-HT vector; M – Molecular marker; 1 – 5xM2e-HAstalk; 2 – 5xM2e-HAtrans; 3 – 5xM2e-GCN4-HAstalk; 4 – 5xM2e-GCN4-HAtrans; 5 – 1xM2e-HAstalk; 6 – 1xM2e-HAtrans.

except that using an anti-histidine antibody was not possible for pRIC 3.0 and pEAQ-HT because these vectors did not provide a histidine tag.

Table 3| Comparison between predicted versus observed recombinant protein sizes

Construct	Size (aa)	Predicted size (Kda)	Observed size (kDa)
5xM2e-GCN4-HAstalk	427 aa	48.1 kDa	58 kDa
5xM2e-GCN4-HAtrans	233 aa	25.7 kDa	33 kDa
5xM2e-HAstalk	390 aa	43.7 kDa	53 kDa
5xM2e-HAtrans	196 aa	21.3 kDa	30 kDa
1xM2e-HAstalk	273 aa	31.0 kDa	N/A
1xM2e-HAtrans	78 aa	8.4 kDa	N/A

Overall, using the two new vectors, I could detect the expression of 4 out of six chimaeras, namely 5xM2e-GCN4-HAstalk, 5xM2e-GCN4-HAtrans, 5xM2e-HAtrans and 5xM2e-HAstalk (Figure 5A and 6). Interestingly, all four proteins ran at higher molecular weights than what was predicted in silico. As showed in Table 3, an average of 10kDa increase was observed for both stalk fusions; whereas for the transmembrane fusions, the increase was slightly lower at about 7 - 8 kDa. Analysis of the M2e-HA fusion protein sequences using the NetNGlyc 1.0 program predicted three and two N-glycosylation sites for the fusions with and without the stalk domain, respectively. Moreover, although proteins were denatured prior to gel loading, 1 - 3 additional bands of higher molecular weight were detected for the constructs lacking the GCN4 domain (5xM2e-HAtrans and 5xM2e-HAstalk), corresponding approximately to the double, triple and quadruple size of the original band (Figure 6, red arrows). This was observed to a lesser extent for the proteins that included the GCN4 domain (5xM2e-GCN4-HAtrans and 5xM2e-GCN4-HAstalk) where only the dimer band could be clearly distinguished (Figure 5, red arrows). The two remaining proteins, 1xM2e-HAtrans and 1xM2e-HAstalk could never be detected on immunoblots (Figure 5B). It is important to note that these two

proteins only contain one copy of the M2e peptide which could be too small for reliable detection with an anti-M2 antibody.

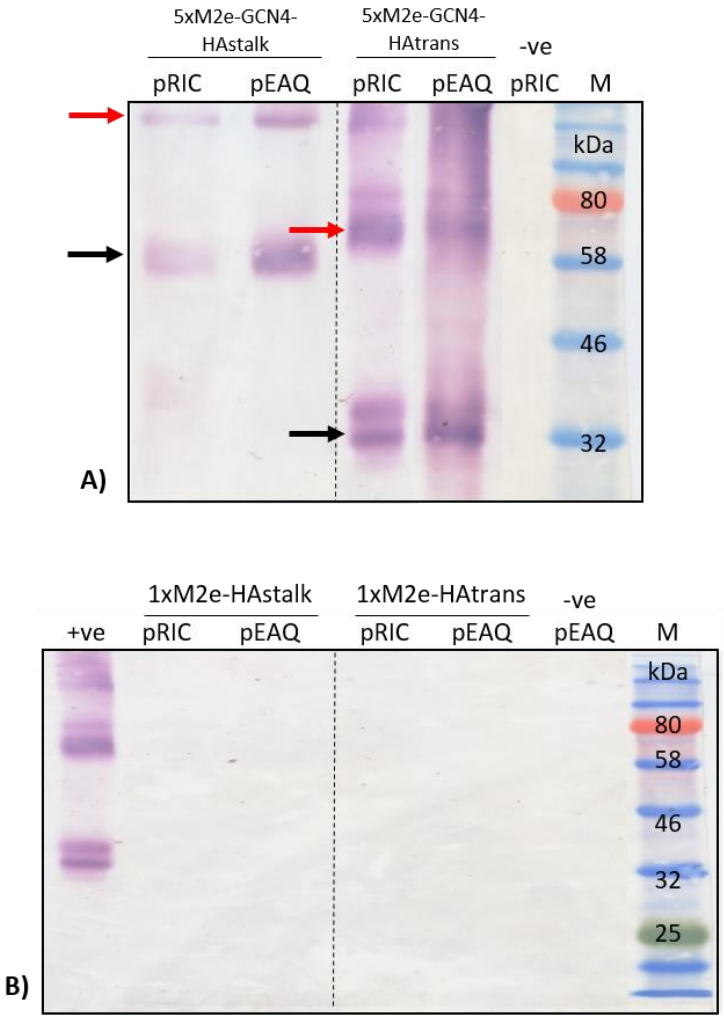

Figure 5 | Immunoblot of 5xM2e-GCN4-HAstalk, 5xM2e-GCN4-HAtrans, 1xM2e-HAstalk and 1xM2e-HAtrans expression in *Nicotiana benthamiana* using the pRIC 3.0 and pEAQ-HT expression vectors. A) Detection of 5xM2e-GCN4-HAstalk and 5xM2e-GCN4-HAtrans expression. B) Detection of 1xM2e-HAstalk and 1xM2e-HAtrans expression. Infiltration was performed at OD_{600} 0.5 and proteins were harvested at 3 d.p.i. and detected using the monoclonal anti-M2 antibody 14C2. -ve pRIC/pEAQ – empty expression vectors; +ve – pRIC-5xM2e-GCN4-HAtrans; M – Molecular marker. Black arrow indicates the position of the respective protein; red arrows indicate the position of putative multimers.

In view of the inability to detect the 1xM2e-HAtrans and 1xM2e-HAstalk, it was decided to abandon further experiments involving these two proteins. Moreover, after further investigation into the chimaeric proteins containing the GCN4 domain, it was found that the sequence coding for GCN4 used in this project had several nucleotide changes that promoted the formation of dimers instead of tetramers (Figure 7). Therefore, because wild-type M2 protein forms tetramers and not dimers on the surface of native influenza

virions, a decision was made to pursue experiments using only the chimaeric proteins that did not have a GCN4 domain (namely 5xM2e-HAstalk and 5xM2e-HAtrans).

For both 5xM2e-HAstalk and 5xM2e-HAtrans proteins, corresponding bands could be observed throughout days 3, 5 and 7; day 3 seemed to have the highest expression profiles (Figure 6). Moreover, changing the OD_{600} of recombinant Agrobacterium (0.25/0.5/1.0) did not have a significant effect on expression levels for both proteins

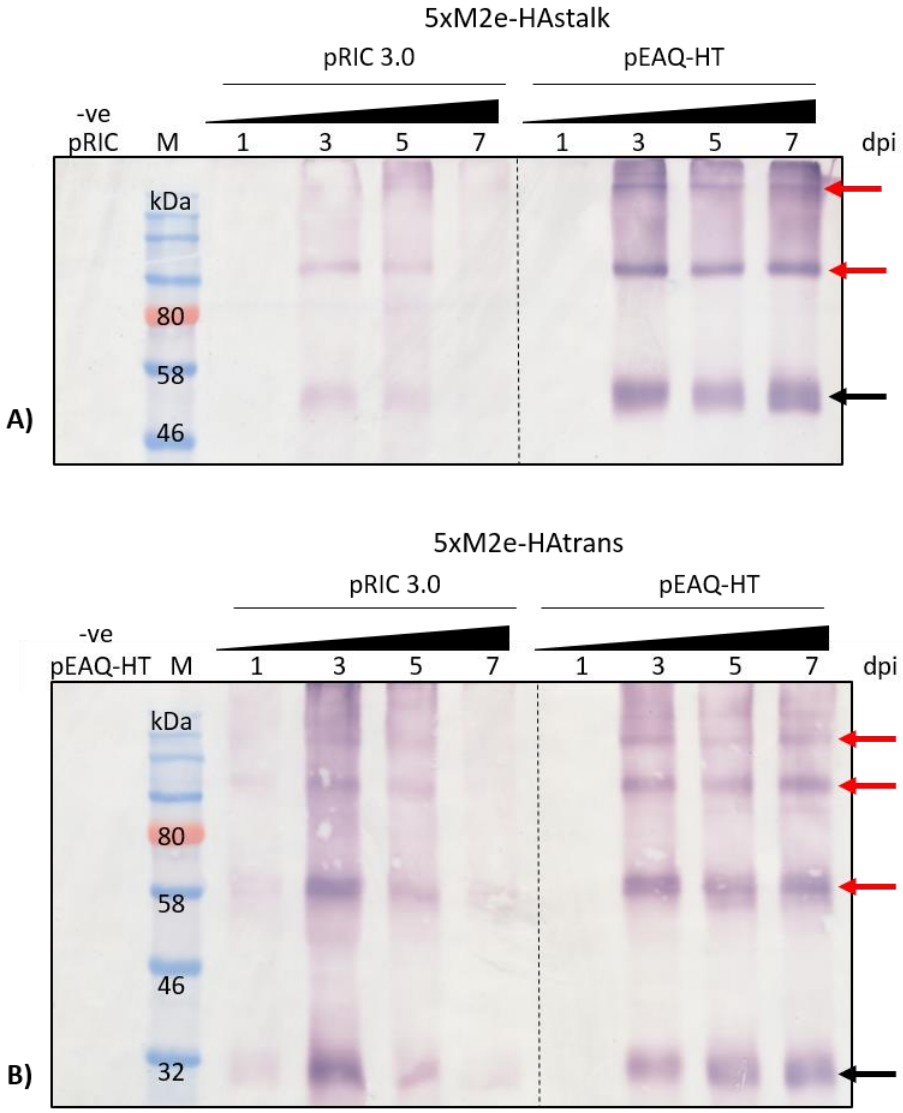

Figure 6 | Time trial of 5xM2e-HAstalk and 5xM2e-HAtrans expression in *Nicotiana benthamiana* using different expression vectors (pRIC 3.0 and pEAQ-HT). Western blots were performed to compare expression levels. A) 5xM2e-HAstalk in pRIC 3.0 and pEAQ-HT. B) 5xM2e-HAtrans in pRIC 3.0 and pEAQ-HT. Infiltration was performed at OD_{600} 0.5 and proteins were detected using the monoclonal M2 antibody 14C2. –ve pRIC/pEAQ-HT – empty expression vectors; dpi – days post infiltration; M – molecular marker. Black arrow indicates the position of the respective protein (~ 20 kDa), red arrows indicate the position of putative multimers.

(data not shown). Therefore, all further infiltrations were performed using recombinant *Agrobacterium* at an OD_{600} of 0.5.

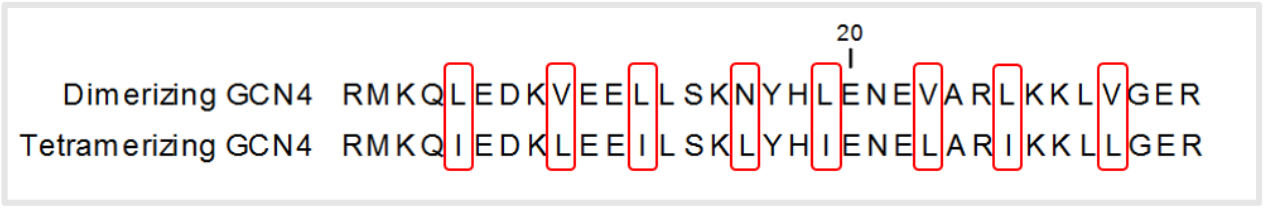

Figure 7| Changes in the primary sequence of GCN4 define its oligomerization. The dimerizing sequence corresponds to wild-type GCN4; tetramerizing sequence was obtained from the study by Harbury et al., 1993.

Direct comparison of expression levels between different vectors using densitometry on western blots showed that highest expression of 5xM2e-HAstalk was obtained using the pEAQ-HT vector, followed by pRIC 3.0 (Figure 6A). However, for 5xM2e-HAtrans, pRIC 3.0 seemed to result in higher expression levels than pEAQ-HT (Figure 6B). These results were also confirmed by indirect ELISA using the anti-M2 commercial antibody 14C2 (data not shown). Also, it is worth mentioning that it was not possible to detect bands corresponding to recombinant proteins on Coomassie stained SDS-PAGE gels (data not shown).

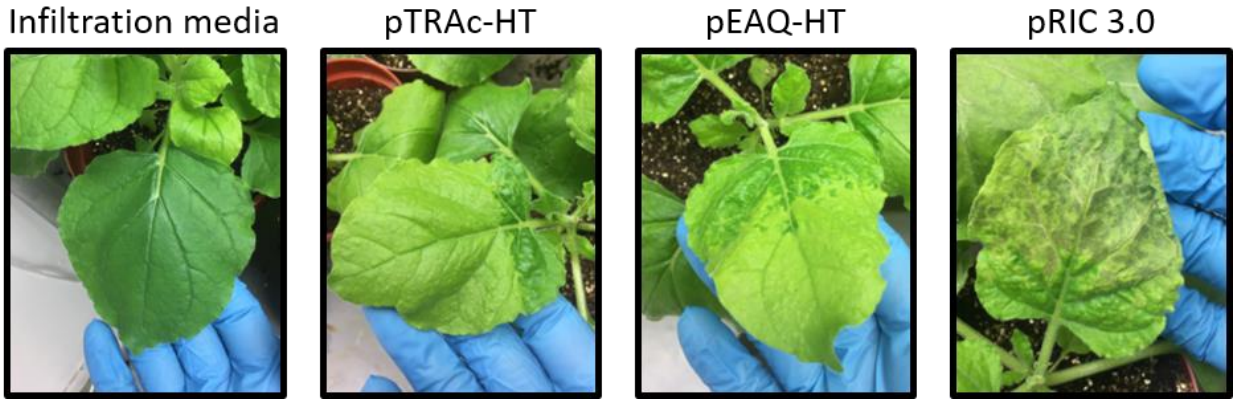

Figure 8| Photographs of leaves infiltrated with 5xM2e-HAtrans in three different expression vectors: pTRAc-HT, pEAQ-HT and pRIC 3.0. Leaves were infiltrated at an OD_{600} of 0.5 and photographed 3 days post infiltration. Plants infiltrated with infiltration medium served as a negative control.

Infiltrated leaves were examined for the visible effects caused by using different expression vectors. Plants infiltrated with infiltration medium only, served as a control for evaluating the effects caused by infiltration with the different recombinant

constructs. Leaves infiltrated with the pTRAc-HT or pEAQ-HT set of constructs developed slight signs of chlorosis at 3 dpi (Figure 8), with leaves progressively becoming more chlorotic over the last days of the time-trial (7 dpi), showing initial signs of necrosis at the injection sites (data not shown). On the other hand, leaves infiltrated with the pRIC 3.0 set of constructs showed severe signs of chlorosis at 3 dpi (Figure 8); these symptoms worsened progressively over the course of the time-trial, resulting in severely necrotic leaves at 7 dpi (data not shown).

3.3.4. Small-scale optimization of native M1 protein expression in *N. benthamiana*

Following optimization of fusion protein expression, I proceeded with expression of the native influenza matrix protein 1 (M1). M1 has been shown to promote VLP formation in other studies, hence I decided to evaluate its effect when co-expressed with the fusion proteins.

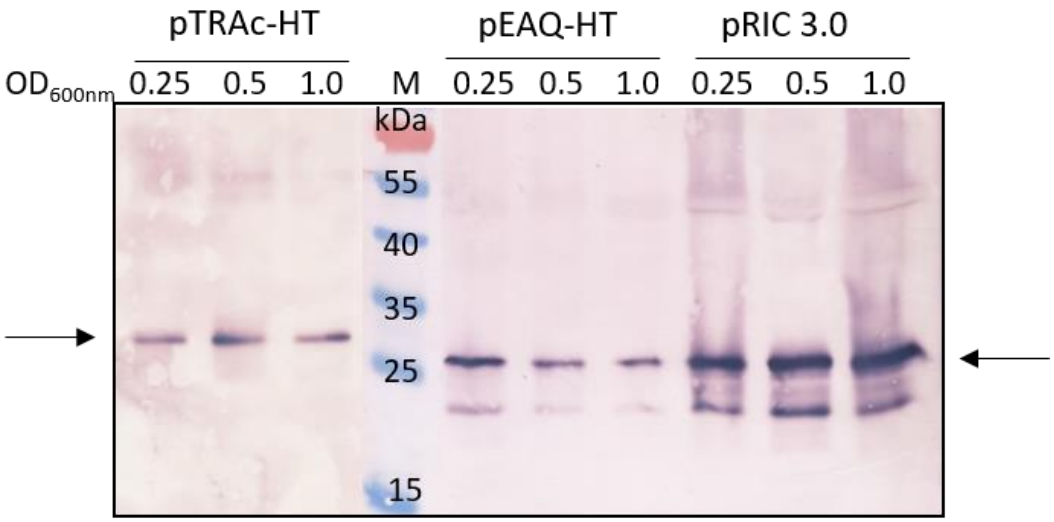

Figure 9 | Western blot of M1 expression in *Nicotiana benthamiana* using different Agrobacterium densities and expression vectors (pTRAc-HT; pEAQ-HT; pRIC 3.0). Infiltration was performed at OD_{600} 0.5 and proteins were harvested at 3 dpi and detected using the monoclonal anti-M1 antibody. M – Molecular marker. Black arrows indicate the position of the M1 protein.

As previously, initial expression trials with M1 involved the harvesting of leaf discs several days post infiltration (day 1, 3, 5 and 7) followed by PBS extraction and TSP determination. M1 expression levels were further compared between the three expression vectors pTRAc-HT, pRIC 3.0 and pEAQ-HT.

M1 protein expression in plants was readily detected at 3 dpi using all three expression vectors, as shown in Figure 9. As expected, a band of approximately 26 kDa was observed for both pRIC 3.0 and pEAQ-HT, whereas a slightly higher band was obtained using the pTRAc-HT due to the presence of a histidine tag. Overall, pRIC 3.0 seemed to give higher expression levels than the pTRAc-HT and pEAQ-HT vectors, as determined by densitometry (Figure 8). Increasing the optical densities of recombinant *Agrobacterium* had little effect on protein expression, but it did increase necrotic symptoms of infiltrated leaves (data not shown). Hence, I proceeded with an OD_{600} of 0.5 for large-scale infiltrations to be in conformity with the 5xM2e fusion proteins.

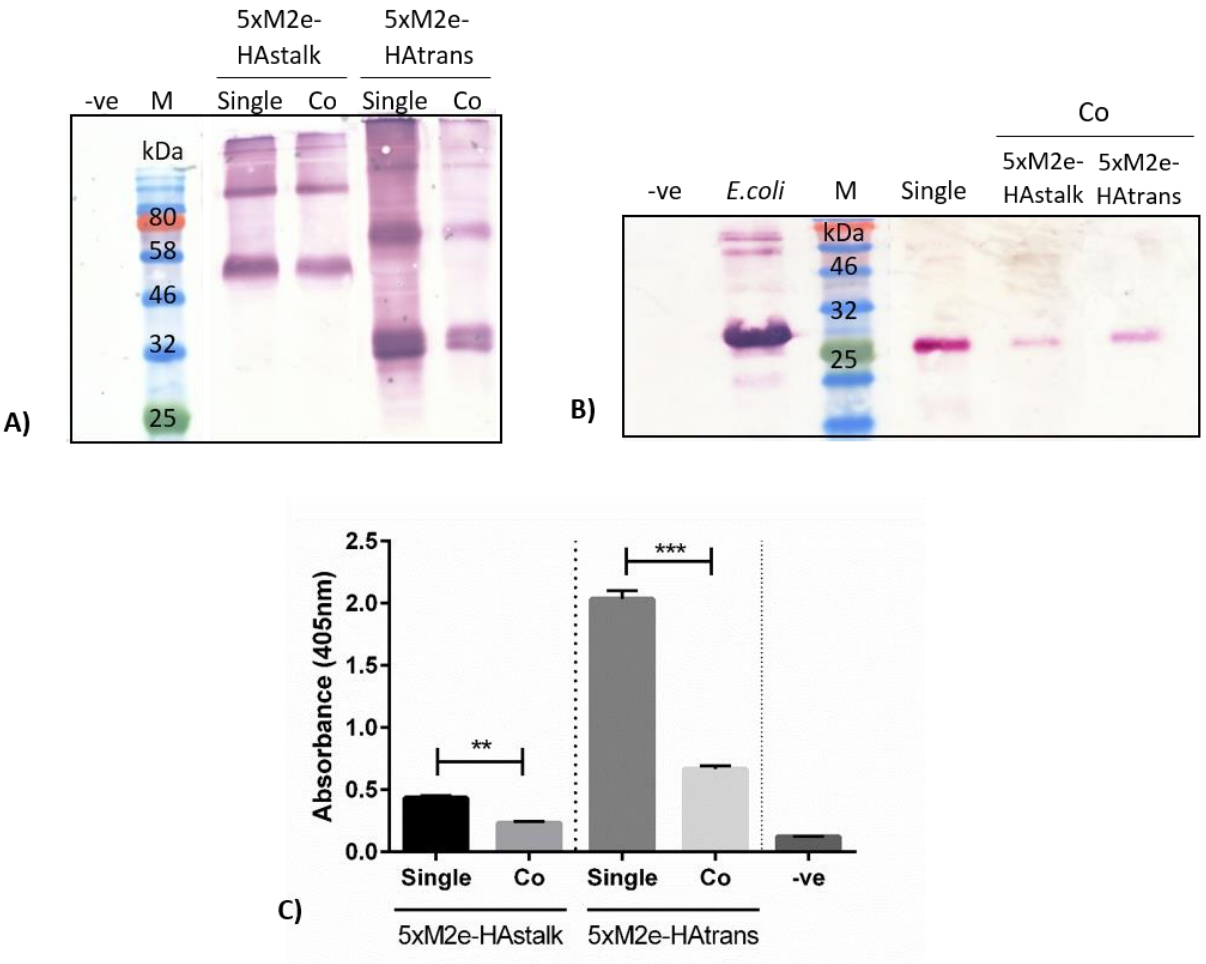

Figure 10| Analysis of fusion protein co-expression with the M1 core protein. Crude extracts were harvested at 3 dpi. A) Western blot of fusion proteins co-expressed with M1; fusion proteins were detected using the anti-M2 14C2 monoclonal antibody. B) Western blot of M1 co-expression; M1 was detected using the anti-M1 rabbit serum. C) Indirect ELISA of fusion proteins single and co-expressed with M1. The markers indicate the mean value of triplicate samples and error bars indicate the standard error of the mean (**p<0.001; *** p<0.0001). -ve – Empty pRIC vector; *E. coli* – M1 expressed in *E.* coli. M – Molecular Marker; Single – Single expression; Co – Co-expression.

It is worth noting that the plant M1 could also be detected with the rabbit serum produced in Chapter 2 (See chapter 2.3.3).

3.3.5. Co-expression of M1 with 5xM2e-HAstalk and 5xM2e-HAtrans

Once the optimal expression conditions for each protein were determined, it was possible to proceed with co-expression trials. Co-expression was performed by infiltrating plants with a mixture of recombinant agrobacteria containing pRIC-M1 and either pEAQ-5xM2e-HAstalk or pRIC-5xM2e-HAtrans; at a ratio of 1:1. All recombinant agrobacteria were used at a final OD_{600nm} of 0.5 and leaf material was harvested at 3 dpi. Western blot analysis of crude extracts confirmed the presence of both M1 (Figure 10B) and fusion proteins (Figure 10A); indicating that the proteins could be expressed together. However, for both fusion proteins and M1, co-expression resulted in fainter bands than expression alone (Figure 10). This was also observed when different expression vectors were used (data not shown). To confirm these results, crude extracts from plants either single or co-infiltrated with M1, were used to coat ELISA plates. Fusion proteins were then detected using the 14C2 monoclonal antibody and absorbances were compared between samples (Figure 10C). As shown in figure 10C, co-infiltrating 5xM2e-HAstalk and 5xM2e-HAtrans with the M1 protein resulted in significantly lower absorbance values compared to when both fusion proteins were expressed on their own. Also, between the two singly expressed chimaeric proteins, the absorbance corresponding to 5xM2e-HAtrans showed a 4-fold increase in signal compared to the 5xM2e-HAstalk protein (Figure 10C).

3.4. Discussion

Recent developments in the field of transient expression in plants have made plant-based manufacturing of influenza vaccines in particular, a promising alternative to more classical approaches based on egg- or cell-based systems (Thuenemann et al. 2013; Lomonossoff 2016). Several groups have been successful at the production of influenza structural proteins in plant expression systems, specifically whole-plant *N. benthamiana* (D'Aoust et al. 2008; Mardanova et al. 2015; Mortimer et al. 2012).

In this study, I focused on using *N. benthamiana* plants to rapidly and efficiently produce a new candidate vaccine for influenza A. For this, I designed and engineered several

chimaeric proteins with potential to present the M2e peptide in a membrane-anchored form on the surface of VLPs. Although the M2e peptide is relatively well conserved amongst different influenza strains, there are few amino acid changes between positions 10 - 23, depending on the host species where the virus was isolated from (Liu et al. 2005). Therefore, 33 M2e peptide sequences from different influenza A strains were aligned to create a new M2e consensus sequence. This consensus sequence was used on its own (1xM2e) or in fusion with four other M2e sequences from human, swine, and avian origin (5xM2e) to further enhance the breadth of cross-protection. In total, two avian, one human, one swine and the consensus M2e sequences were fused in tandem to create 5xM2e.

To enhance the immunogenicity of M2e sequences, several carriers have been previously used, such as the TLR5 ligand flagellin (Huleatt et al. 2008; Mardanova et al. 2015), hepatitis B virus core (HBc) particles (De Filette et al. 2005), or even recombinant adenoviruses (Price et al. 2010). However, here I used the HA glycoprotein as a scaffold to present the five M2e tandem repeats (5xM2e) on the surface of VLPs. Previously, D'Aoust et al. (2008) demonstrated that when expressed in *N. benthamiana*, the full-length HA protein formed highly immunogenic membrane-derived particles resembling the shape of native influenza virions. Hence, I investigated if similar particles could be obtained in *N. benthamina*, by replacing the immune-dominant globular head of the HA with the 5xM2e repeats. These M2e-HA VLPs, contrary to the case with other carriers, would present the M2e peptides in a highly immunogenic, membrane-anchored form, thus hopefully mimicking their native conformation. VLPs that resemble the native structure of the virus have been shown to induce CD4 T-cell proliferation and cytotoxic T-cell immune responses in vitro, and to stimulate CD8 T-cells via dendritic cell-mediated antigen cross-presentation (Song et al. 2010; Kang et al. 2012).

To maximize the chances of obtaining immunogenic VLPs, the 5xM2e peptide was fused to either the stalk domain or the transmembrane domain of the HA protein. Furthermore, the tetramerizing leucine zipper domain GCN4 was included in some of the chimaeras to possibly increase their immunogenicity as suggested by De Filette et al. 2008.

Six different chimaeric proteins were designed in total: 5xM2e-GCN4-HAstalk, 5xM2e-GCN4-HAtrans, 5xM2e-HAstalk, 5xM2e-HAtrans, 1xM2e-HAstalk and 1xM2e-HAtrans.

Because the 5xM2e-GCN4-HAstalk construct contained all necessary domains to create the remaining chimaeras, several compatible restrictions enzyme sites were introduced at strategic locations on the 5xM2e-GCN4-HAstalk sequence (Figure 1). This allowed me, through specific enzyme digestions, to rapidly clone all five other chimaeras from the 5xM2e-GCN4-HAstalk sequence.

Small-scale expression trials of the different M2e-HA fusion proteins in plants were first performed using the pTRAc-HT vector. Previously in our group, Mortimer et al. (2012) showed successful expression of both full-length and truncated HA proteins in plants using the non-replicating pTRAc vector system based on the cauliflower mosaic virus 35S promoter (Maclean et al., 2007). However, despite having used different expression conditions, the pTRAc-HT vector only showed detectable expression levels for one of the six M2e-HA fusion proteins (namely 5xM2e-HAstalk). These results were consistent either when the 14C2 antibody or an anti-histidine antibody was used, suggesting that the lack of expression observed was probably due to the vector used and not the detection method. Hence, I proceeded with expression trials using the two remaining vectors pEAQ-HT and pRIC 3.0.

Expression using the pEAQ-HT and pRIC 3.0 vectors resulted in detectable protein levels after only 3 dpi, for 4 out of 6 fusion proteins: 5xM2e-GCN4-HAstalk, 5xM2e-GCN4-HAtrans, 5xM2e-HAtrans and 5xM2e-HAstalk. Differences in the sequences between pTRAc-HT and pEAQ-HT or pRIC 3.0 could be attributed to the expression profiles observed. For instance, the pEAQ-HT vector includes the silencing suppressor gene p19 on the same T-DNA, which ensures that both the gene of interest and the silencing suppressor are transferred to the same plant host cells (Sainsbury et al. 2009). Alternatively, pRIC 3.0 possesses the Bean yellow dwarf virus replication-associated elements between the left and right borders for T-DNA integration that allows for the vector to self-replicate inside the plant cells resulting in increased protein expression (Regnard et al. 2010). Although using different approaches to enhance recombinant protein expression, both pEAQ-HT and pRIC 3.0 showed higher protein levels than pTRAc-HT (Figure 4, 5 and 6), which is in conformity with previous studies (van Zyl et al.

2016; Regnard et al. 2010). Therefore, the pEAQ-HT and pRIC 3.0 vectors were used for all further plant expression work.

As previously mentioned, only four out of the six M2e-HA fusion proteins could be detected on western blots. The two remaining proteins, 1xM2e-HAstalk and 1xM2e-HAtrans could never be detected despite several attempts (Figure 5B). Given the high expression profiles observed for the 5xM2e fusion proteins using pRIC 3.0 and pEAQ-HT, it is highly probable that the 1xM2e-HAstalk and 1xM2e-HAtrans protein were being expressed but could not be detected by the anti-M2 monoclonal antibody (14C2) because they only possessed the consensus M2e peptide. These results are in agreement with previous studies that suggested that repeated M2e tandem copies were more reactive to specific antibodies than wild-type M2 proteins. However, because 1xM2e-HAstalk and 1xM2e-HAtrans could never be detected, it was not possible to measure the difference in reactivity between the 1x and 5xM2e constructs. Detection using more broad antibodies, such as a polyclonal anti-M2 antibody, should therefore be investigated.

Interestingly, when detected on western blots, all four 5xM2e proteins ran at higher molecular weights than what was predicted in silico (Table 3). Analysis of the 5xM2e-HA sequences using the NetNGlyc 1.0 program predicted three N-glycosylation sites for 5xM2e-GCN4-HAstalk / 5xM2e-HAstalk; and two for 5xM2e-GCN4-HAtrans / 5xM2e-HAtrans, which would have contributed to the respective 10 kDa and 7.5 kDa increased molecular weight bands. These results are in agreement with previous reports which showed that full-length recombinant HA expressed in *Nicotiana benthamiana,* is glycosylated, and thus runs at higher molecular weights (Kanagarajan et al. 2012; Kalthoff et al. 2010). To confirm the predicted glycosylation, future work should focus on enzymatic de-glycosylation cleavage of recombinant proteins and subsequent western blot visualization of smaller bands.

In addition to the increase in molecular weight, several extra bands corresponding approximately to multiples of the size of the original band could be detected in denaturing SDS-PAGE gels. In agreement with previous observations that recombinant HA forms oligomers upon heterologous expression (D'Aoust et al. 2008; Weldon et al. 2010), I hypothesize that these bands correspond to dimer, trimer and possibly tetramer

formations of the respective M2e-HA proteins. This would suggest that denaturation by SDS was incomplete, which possibly corroborates previous reports that HA-based influenza particles are thermally stable under neutral pH (Kissmann et al. 2011).

It is important to note that, practically only the dimer band could be observed for the constructs containing the GCN4 domain, whereas for the proteins lacking the GCN4 domain, all three conformations (dimers, trimers and tetramers) were clearly visible (Figure 5 and 6). These results were surprising since the GCN4 domain used in this study was supposed to promote tetramer formation and not dimers. However, Harbury et al. (1993) reported that small changes in buried hydrophobic amino acid residues of the GCN4 sequence, are key factors in determining whether the GCN4 would form dimers, trimers or tetramers (Harbury et al., 1993). An alignment of these GCN4 sequences compared to the one used in this study revealed eight amino acid changes which promoted dimerization instead of tetramerization (Figure 7). Therefore, since neither the HA nor the M2 proteins form dimers in native virions, and that epitope conformation has been shown to be a crucial factor in the efficacy of anti-viral immune responses (Brunel et al. 2006; Blokhina et al. 2013; Staneková & Varečková 2010; Weldon et al. 2010); I decided to only focus on characterization of the two M2e-HA fusions lacking the GCN4 domain.

Expression profiles of 5xM2e-HAstalk and 5xM2e-HAtrans fusion proteins were compared by western blotting (Figure 5 and 6). Using the pEAQ-HT vector, both proteins could be detected at similar levels from days 3 to 7, whereas, when the pRIC 3.0 vector was used, protein expression peaked at 3 dpi and then gradually decreased over the following days, finally being undetectable at 7 dpi. These results seemed to coincide with the physical appearance of leaves, where, leaves infiltrated with pEAQ constructs showed little necrosis up to day 7, while leaves infiltrated with pRIC constructs already showed necrotic symptoms after day 3 (Figure 8). This difference in protein accumulation over time could be attributed to the presence of the p19 silencing suppressor in the pEAQ-HT sequence and not on pRIC 3.0.

Post-transcriptional gene silencing (PTGS) is a general plant response that can limit the efficiency of *Agrobacterium*-mediated transient expression (Voinnet et al. 2003). Numerous studies have shown that PTGS can be suppressed by co-expressing viral

silencing suppressors such as the p19 from the tomato bushy stunt virus. Another explanation could be that the self-replicating properties of the pRIC 3.0 vector, which lead to increased transgene copy number, end up exhausting the leaves resources after short periods of time, causing them to eventually die. If this is the case, it should follow that longer genes will have a more detrimental effect on infiltrated leaves than shorter ones. Hence, the difference in size of 582 bp between the 5xM2e-HAstalk and 5xM2e-HAtrans sequences could explain why plants infiltrated with pRIC-5xM2e-HAstalk showed decreased protein accumulation compared to pRIC-5xM2e-HAtrans. These results demonstrate the importance of testing several different expression vectors when expressing new constructs for the first time.

Once the best expression conditions for the two M2e-HA chimaeric proteins were determined, it was possible to investigate the effects of M1 co-expression. The matrix protein 1 (M1) is the most abundant influenza A protein, and forms the inside coat of the native influenza virion (Howley 2013). Lying just beneath the lipid envelope, M1 is able to interact with both the transmembrane domain of the glycoprotein spikes and the internal ribonucleoprotein particles, thus forming a bridge that allows other structural proteins to assemble and form a complete virion structure (Ali et al. 2000; Ruigrok et al. 2000). Most of the influenza-VLP production studies, including the Kim, Lee, et al. (2013) study on which I based the fusion protein design, consider that M1 is an imperative factor for correct VLP formation (Song et al. 2011; Tang et al. 2011; Thompson et al. 2015). Hence, I decided to evaluate its effect when co-expressed with the fusion proteins.

To obtain the highest expression conditions for co-expression, I first had to optimize M1 single expression. Although there is an extensive number of studies mentioning the successful expression of recombinant M1, D'Aoust et al. (2008) have been the only ones that showed it using a plant production system (D'Aoust et al. 2008). Here, when run on western blots, our plant-expressed M1 produced a band of approximately 26 kDa which corresponds approximately to the size of M1 from native virus (Theresa Latham & Galarza 2001). As expected, this band could be detected with either our anti-M1 rabbit serum or a commercial monoclonal anti-M1 antibody. I have shown that amongst the conditions tested, best accumulation of the M1 protein was found 3 days after

infiltrating leaves with pRIC-M1 at an OD_{600} of 0,5. Further increasing the cell density of the recombinant constructs to an OD_{600} of 1.0 did not have any effect on M1 expression; it did however cause necrosis of the plant leaves. *Agrobacterium* has been well characterized to cause necrosis in many plant species (Wroblewski et al. 2005), hence, it is possible that by increasing their concentration, *A. tumefaciens* cells may have played a detrimental part in normal plant regulatory functions. Therefore, by infiltrating with an OD of 0.5, I was able to find an equilibrium between protein expression and the necrotic effect of *Agrobacterium*.

In their study, D'Aoust et al. (2008) showed that the co-expression of HA and M1 in plants led to a substantial decrease in HA levels. Here, co-expressing the 5xM2e-HAstalk and 5xM2e-HAtrans fusions with M1 also resulted in a significant decrease in fusion protein accumulation, as shown by western blot and ELISA experiments. These findings are contradictory with previous studies in both insect and mammalian cells, where, co-expression of M1 and HA proteins increased VLP production, rather than HA expressed alone (Tang et al. 2011; Choi et al. 2013). Although the causes for these discrepancies remain unknown, it is possible that the production of M1-derived influenza VLPs is affected by the expression system used.

3.5. Conclusions

In summary, in this work I designed six M2e-HA fusion proteins with potential to form VLPs. From these six, I selected the most promising two proteins based on expression levels and sequence analysis; namely, 5xM2e-HAstalk and 5xM2e-HAtrans. These two proteins were readily expressed in *N. benthamiana* plants after only 3 days post infiltration. Although optimizations increased the accumulation of fusion proteins, expression levels were still low since recombinant proteins were never detectable on Coomassie-stained SDS-PAGE gels. This is similar to recombinant expression levels seen for plant-produced HIV p17 / p24 (Meyers et al. 2008). Further improvements in recombinant expression may be achievable by optimizing several parameters such as the G+C content of the coding genes, the extraction buffer used, the temperature of incubation after infiltration and also targeting the recombinant proteins to different cellular compartments, namely the apoplast (Jung et al. 2015; Maclean et al. 2007; Mortimer et al. 2012; D'Aoust et al. 2008).

Furthermore, despite observing a substantial drop in fusion protein accumulation levels after co-expression with M1, these proteins were still detectable on western blots. Hence, in views of the many contradictory conclusions regarding co-expression with the M1 protein, I decided to investigate the formation of M2e-HA VLPs with and without M1.

Chapter 4: Characterization and purification of M2e fusion VLPs

4.1. Introduction

Virus-like particles (VLPs) have recently emerged as a promising vaccine platform for influenza due to their non-infectious nature and effective presentation of antigens (Shoji et al. 2015; Kang et al. 2012). Because influenza viruses are constantly undergoing antigenic changes (antigenic drift and shift), the ease/speed of VLP production is another advantage over current live vaccines (Jain et al. 2015). Several different influenza vaccine candidates based on VLP technology, are under investigation and have shown promise in preclinical and clinical trials (Landry et al. 2010; Herzog et al. 2009; López-Macías et al. 2011; D'Aoust et al. 2010; Choi et al. 2013). Most of these VLP vaccines have been designed to fight against specific influenza strains because they were formulated using the full-length haemagglutinin (HA) and/or neuraminidase (NA) structural proteins as main antigens.

However, VLPs presenting more conserved antigens (such as the M2e or the HA stalk domain) capable of eliciting broader immune responses, have also been described (Ibañez et al. 2013; Kim, Lee, et al. 2013; Steel et al. 2010). To present these conserved antigens on the surface of VLPs, chimaeric VLPs can be engineered, where the target conserved epitopes are genetically incorporated within the primary sequence of the VLP structural subunits. If successfully incorporated into VLPs, the target epitope will be displayed in the same conformation and density as the structural subunit it was fused to (Bárcena & Blanco 2013).

Nevertheless, generating chimaeric VLPs is still largely empirical. Current computational models of VLP formation can give an indication on how to design the chimaeric proteins, but it still is almost impossible to predict whether specific peptides will self-assemble into VLPs (Bárcena & Blanco 2013). The only method to confirm successful VLP assembly is by undergoing VLP characterization *in vitro* (Zeltins 2013).

Transmission electron microscopy (TEM) is the most used technique to assess VLP formation (Williams & Carter 2009); however, the use of purified samples is recommended for TEM visualization, because crude extracts contain large amounts of

unwanted proteins and other debris that can mask or interfere with VLP detection. Density gradient ultracentrifugation has been extensively used for the purification of both live viruses and VLPs (Zeltins 2013). Although in industrial-scale processes, the use of ultracentrifugation has some restrictions due to increased labor intensity and lack of scalability; at the laboratory level, ultracentrifugation is more than adequate for screening new constructs which are expected to lead to the formation of VLPs (Vicente et al. 2011).

In this section of the study, I investigated if the two plant-produced fusion proteins 5xM2e-HAstalk and 5xM2e-HAtrans, would successfully self-assemble into VLPs. Furthermore, I compared if these VLPs could be assembled solely using the M2e-HA fusions, as with the full-length HA protein, or if they required co-expression with M1. VLP characterization was performed by analyzing purified samples using transmission electron microscopy.

4.2. Materials and methods

4.2.1. Large scale infiltration

The proteins and respective expression vectors that were used for large scale infiltration were: pRIC-5xM2e-HAtrans, pEAQ-5xM2e-HAstalk and pRIC-M1. Furthermore, the wild-type HA protein (in the pEAQ-HT vector, (A/Viet Nam/1194/2004 H5N1)) was also used as a positive control for VLP formation and the empty pRIC vector was used as a negative control. An overview of the general procedure used in this sections is illustrated in Figure 1.

For vacuum infiltration, recombinant *Agrobacterium tumefaciens* was grown as described previously (Section 3.2.2) in LBB enriched medium (0.25 % tryptone, 1.25 % yeast extract, 0.5 % NaCl, 10 mM 2 L (NLMorpholino) ethanesulfonic acid (MES) pH 5.6), induced overnight with 20 µM acetosyringone and diluted to an OD_{600} of 0.5 in infiltration medium.

Large scale vacuum infiltration was performed as described by Marillonnet et al. (2005). Briefly, whole plants were submerged in 1 L of bacterial suspension, and placed in a vacuum chamber. Then, a vacuum of -90 kilopascal (kPa) was maintained for 5 seconds, and rapidly released (10-15 kPa.sec-1). This process would be repeated 2 to 3 times.

After infiltration, the plants were grown at 22 °C under 16 hrs/8 hrs light/dark cycles until harvested.

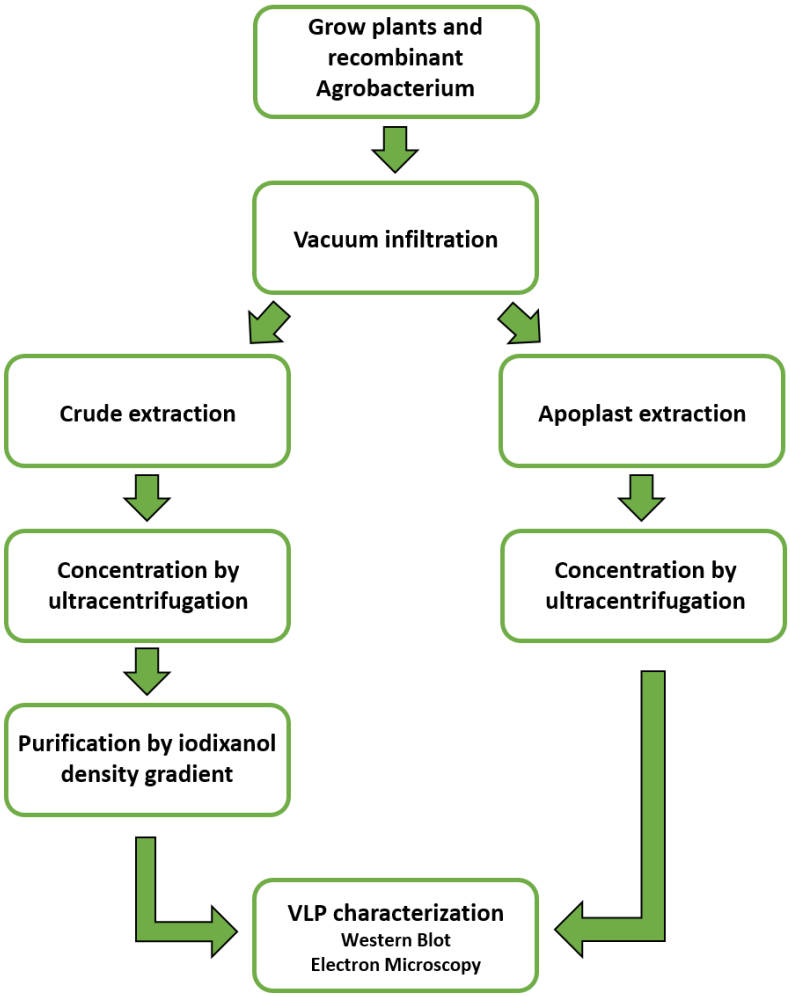

Figure 1| Overview of the general steps that were used for M2e-HA VLP purification and characterization.

4.2.2. Crude protein extraction

For protein extraction, whole leaves were harvested at 3 dpi and immediately weighed. Crude extracts were prepared in 3 v/w extraction buffer (1 x PBS composition: 137 mM NaCl, 1.8 mM KH2PO4, 10 mM Na2HPO4, 2.7 mM KCl, pH 7.4) using a T25 digital ULTRALTURRAX® homogenizer (IKA). Homogenized extracts were subsequently clarified by passing it through two folds of miracloth with a pore size of 22-25 µm (475855-IR, Millipore, Merck, Germany), followed by a centrifugation step at 15,000 x g for 10 min. The supernatant representing the crude leaf extract was collected for purification.

4.2.3. Apoplast extraction

To extract the apoplastic fluid from infiltrated plants, the infiltration-centrifugation technique described by Lohaus et al. (2001) was used. As previously, leaves from vacuum infiltrated plants were harvested at 3 dpi and weighed. Intact leaves were then infiltrated with 1 x PBS, using the vacuum infiltration method described above, except that the infiltration process was only performed once per plant batch. This prevented the loss of recombinant proteins.

PBS-infiltrated leaves were then carefully rolled and loaded into 50 mL syringes with the plungers removed. Syringes containing leaves were centrifuged twice for 20 min at 800 x g in a Beckman-Coulter centrifuge using a JA-14 rotor to extract crude apoplastic extract.

4.2.4. Iodixanol cushion pelleting

Iodixanol cushion ultracentrifugation was based on purification of influenza particles by Yang et al. (2009). After extraction, either crude or apoplastic extracts were overlaid onto 4 ml of 14 % iodixanol solution (Optiprep® Sigma-Aldrich, Germany) prepared in 38.5 mL Ultra-Clear™ centrifugation tubes (Beckman Coulter) using 1 x PBS. Sometimes, the apoplastic extraction volume was too low to completely fill the ultracentrifugation tubes; in these cases, 1 x PBS was simply added to fill tubes. Samples were ultracentrifuged for 90 min at 27,000 rpm (89,527 x g) at 4 ^{o}C in a SW 32 Ti rotor (Beckman). Pellets were re-suspended in 750 - 1000 µL 1 x PBS and kept at 4 ^{o}C for Western blot/TEM analysis and purification.

4.2.5. Density gradient purification

The pellets from crude extracts were further purified by density gradient purification. Briefly, re-suspended pellets were loaded on top of a 10 – 50 % iodixanol gradient (with 10 % increases) in a 5 mL Ultra-Clear™ centrifugation tubes (Beckman Coulter). The discontinous gradient was ultracentrifuged at 32,900 rpm (102,621 x g) for 2 hrs at 4^{o}C in a SW 55 Ti rotor (Beckman Coulter). After centrifugation, 0.5 mL fractions were collected from the bottom of the tube using a Foxy® Jr. Fraction Collector (Teledyne Isco, NE, United States of America). Collected fractions were analyzed by western blotting

and TEM. Density of iodixanol-containing solutions was measured using the Digital PAL-3 Pocket refractometer machine (Atago®, Japan).

4.2.6. Coomassie-stained SDS-PAGE gels and western blots

Samples from every purification step were analyzed by Coomassie-stained gels and western blots as described in section 3.2.2. For western blots, proteins were detected with either 1:5000 anti-M2 14C2 monoclonal IgG antibody (Abcam, UK), 1:5000 anti-M1 GA2B monoclonal IgG antibody (Abcam, UK), 1/5000 anti-H5 (H5N1) monoclonal IgG antibody [8D2] (Abcam, UK) or 1/10000 serum from rabbits immunized against M1 (Chapter 2). Antibodies produced in mice were detected with 1/10000 anti-mouse IgG (whole molecule) alkaline phosphatase conjugated antibody produced in goat (Sigma-Aldrich, Merck, Germany), whereas the rabbit serum was detected with 1/10000 anti-rabbit IgG (whole molecule) alkaline phosphatase conjugated antibody, also produced in goat (Sigma-Aldrich, Merck, Germany). Band densitometry analysis was performed using the ImageJ open-source software (ImageJ developers).

4.2.7. Transmission electron microscopy

TEM was carried on both crude and purified samples to analyze VLP formation. Before applying samples, copper grids were made hydrophilic by glow discharging at 25 mA for 30 s using a Model 900 SmartSet Cold Stage Controller (Electron Microscopy Sciences, United States of America). Glow-discharged grids were then placed on samples for 5 min and washed five times with distilled sterile water. Thereafter, samples were negatively stained on uranyl acetate for 30 s and again for 5 s and viewed using a Tecnai™ F20 Scanning Transmission Electron Microscope (FEI, OR, United States of America).

4.2.8. Immuno-gold labelling of VLPs

For immuno-gold labelling, glow-discharged grids were placed on samples for 30 min at room temperature, followed by six washes with sterile water. Thereafter, coated grids were incubated for 1 hr with either the 14C2 mouse anti-M2 antibody (Abcam, UK) or the 8D2 mouse anti-H5 (H5N1) antibody (Abcam, UK), both diluted to 1:100 in 20 mM 1 x TBS. After washing grids four times with sterile water, the anti-mouse gold conjugated IgG (10 nm gold particles) (Abcam, UK) was added at a 1/100 dilution in 20 mM 1 x TBS and left to incubate for another 15 min at room temperature. Finally, the

grids were washed four times and negatively stained as previously, before visualization using a Tecnai™ F20 Scanning Transmission Electron Microscope (FEI, OR, United States of America).

4.3. Results

4.3.1. Vacuum infiltration and purification

Using the expression conditions optimized previously, whole plants were vacuum infiltrated with recombinant *Agrobacterium*. Plants were either infiltrated with the fusion proteins alone or with the M1 protein. A positive control for VLP formation was also included by infiltrating plants with the full-length HA protein (A/Viet Nam/1194/2004 H5N1).

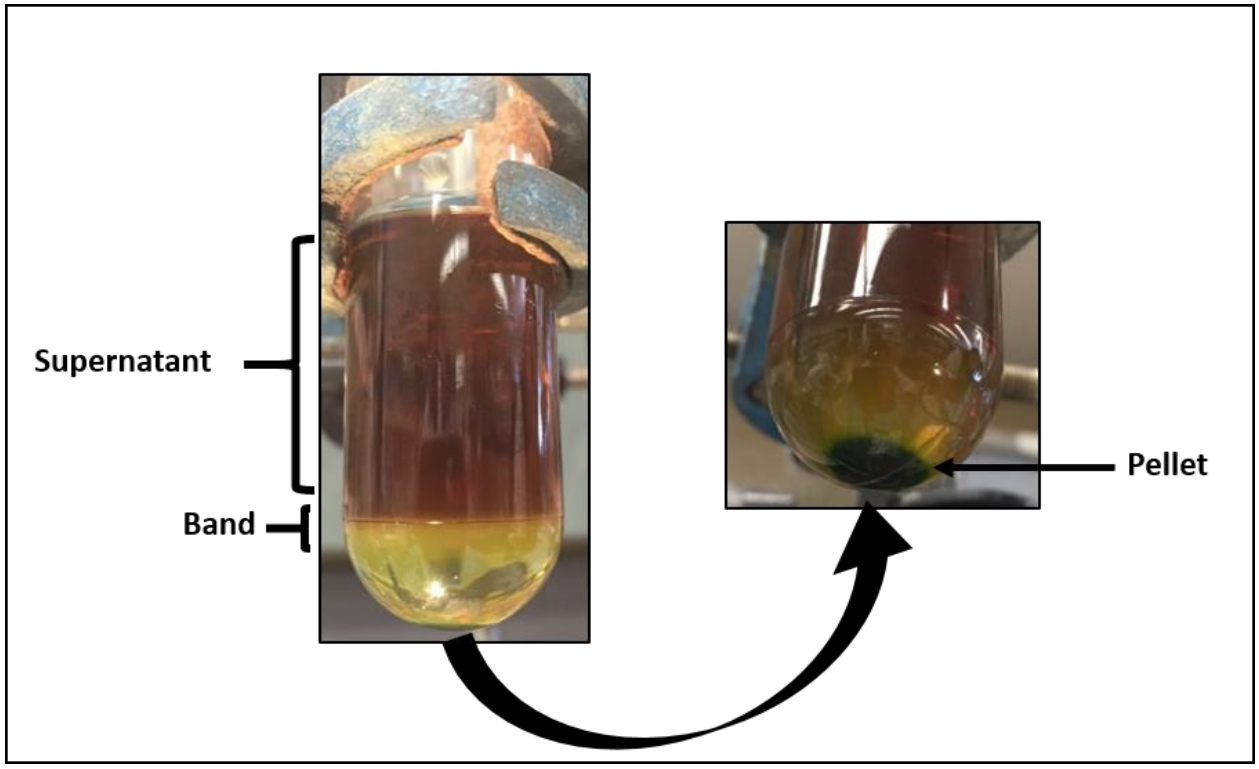

Figure 2| Iodixanol cushion step after ultracentrifugation showing the formation of a band and a pellet.

Following large-scale vacuum infiltration, whole leaves were harvested and homogenized using a mechanical blender. The homogenate was then centrifuged, and the supernatant collected and filtered through Miracloth to remove large particulates. The supernatant was then loaded onto a 14 % iodixanol cushion and ultra-centrifuged to pellet any particles that could be in the sample. This allowed me to concentrate the samples, thus reducing the working volume for the gradient step.

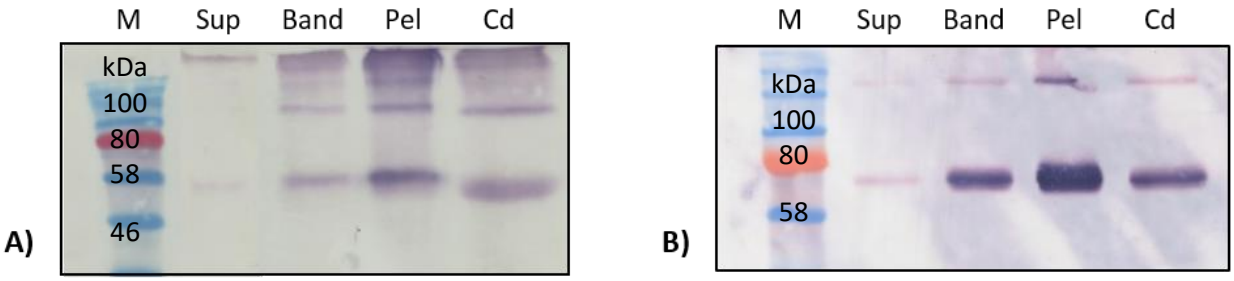

Figure 3| Western blots analysis of aliquots collected during the iodixanol cushion step. A) Analysis of 5xM2e-HAstalk after partial purification. Proteins were detected using the monoclonal anti-M2 antibody. B) Analysis of the full-length HA protein after partial purification. Detection was performed using the monoclonal anti-HA antibody. M – Molecular Marker; Sup – Supernatant fraction; Band – Band fraction; Pel – Pellet fraction; Cd – Crude extracts.

After centrifuging, a translucent band could be observed above the iodixanol cushion (Figure 2). This was observed for all samples, including plants infiltrated with an empty vector (negative control). An aliquot of the supernatant as well as the band was collected and the pellet re-suspended in PBS for western blot analysis (Figure 3). Immunoblot analysis revealed that both 5xM2e-HAstalk (Figure 3A) and 5xM2e-HAtrans (data not shown) fusion proteins, as well as, the recombinant HA (Figure 3B) accumulated mostly in the pellet, but were also present between the sample and iodixanol cushion (band). The supernatant also contained trace amounts of recombinant protein. Co-expression with M1 gave similar results (data not shown).

Since recombinant proteins were detected throughout the whole tube, I proceeded with analyzing the aliquots collected from the supernatant, the band and the pellet using TEM (Figure 4). Despite the background signal, TEM analysis of infiltrated leaf tissue expressing 5xM2e-HAstalk + M1 showed putative particles of around 80 - 120 nm diameter, in both the crude and pellet samples (Figure 4, red arrows). On the other hand, the extracts from the band fractions presented several structures of different shapes but nothing consistent with VLPs could be found. The supernatant samples where almost completely devoid of any particular structures. Similar results were observed for the remaining constructs (5xM2e-HAstalk/ 5xM2e-HAtrans/ 5xM2e-HAtrans + M1) (data not shown) and for the positive HA control (Figure 4). No particles were observed on extracts from leafs infiltrated with an empty pRIC 3.0 vector (negative control) (data not shown).

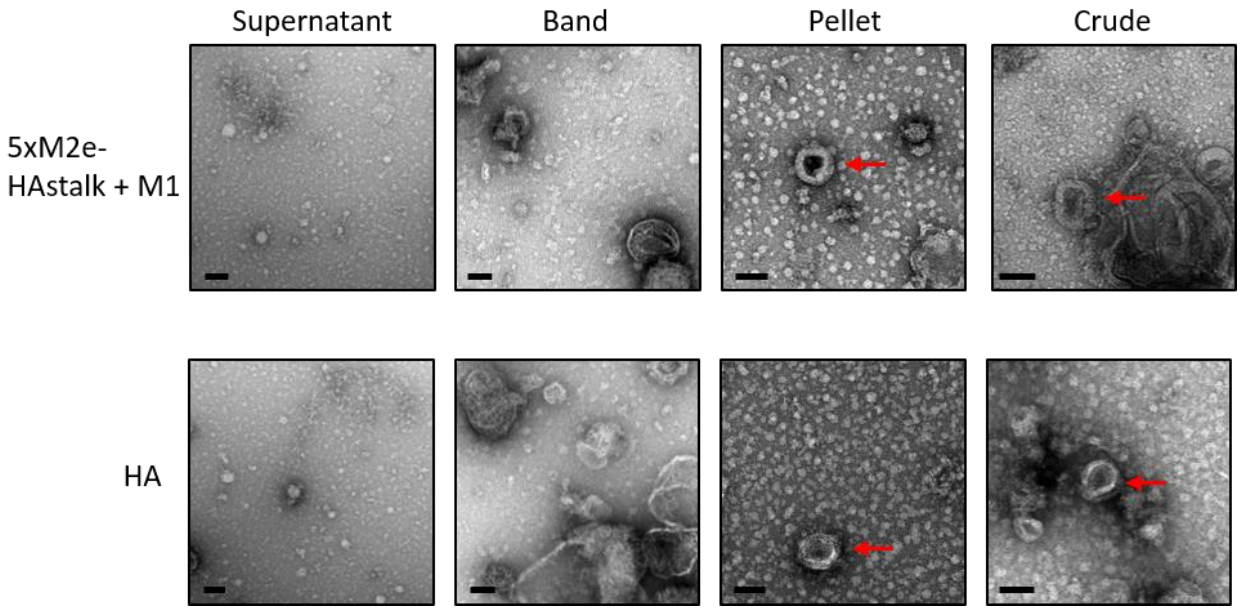

Figure 4|Transmission electron micrographs of partially purified extracts from leafs co-expressing 5xM2e-HAstalk + M1 or the HA protein alone. Aliquots from crude extracts or from the supernatant, band and pellet fractions following ultracentrifugation, were used to coat copper grids for VLP detection. Scale bars are 100 nm. Red arrows indicate putative VLPs.

Based on these results, the iodixanol cushion pellets fractions were further analyzed using a iodixanol density gradient ultracentrifugation consisting of 10 – 50 % iodixanol (in 10 % increments). This extra step served to concentrate the putative VLPs, while removing some of the background signal.

Following ultracentrifugation, fractions were collected from the density gradient and monitored for recombinant protein abundance using dot blots detected with anti-M2, anti-HA or anti-M1 antibodies and serum. Densitometry was used on dot blots to compare protein levels between different fractions. Densitometry analysis confirmed that all chimaeric proteins as well as M1 and HA, mostly accumulated between fractions 5 - 7(Figure 5A, C and E). These fractions represented an iodixanol density gradient ranging from 32 – 19 % iodixanol, as determined using the refractometer machine.

To confirm that the intensity peaks corresponded to the presence of desired recombinant proteins, western blots were performed for each fraction (Figure 5B, D and F). Detecting fractions containing the M2e fusions using an anti-M2 monoclonal antibody resulted in clear corresponding bands (± 53 kDa for 5xM2e-HAstalk/ ± 30 kDa for 5xM2e-HAtrans) between fractions 5 - 7. Faint bands could also be observed in

fractions 4 and 8; but no bands were observed in fractions 1 - 3 and 9. This was observed for single (data not shown) and co-expressed samples (Figure 5B and D). Furthermore, when the anti-M1 serum was used on western blots of co-expressed samples, bands corresponding to M1 (± 26 kDa) were also clearly visible between fractions 5 - 7; however, there were also fainter bands on fractions 8 and 9 (Figure 5B and D).

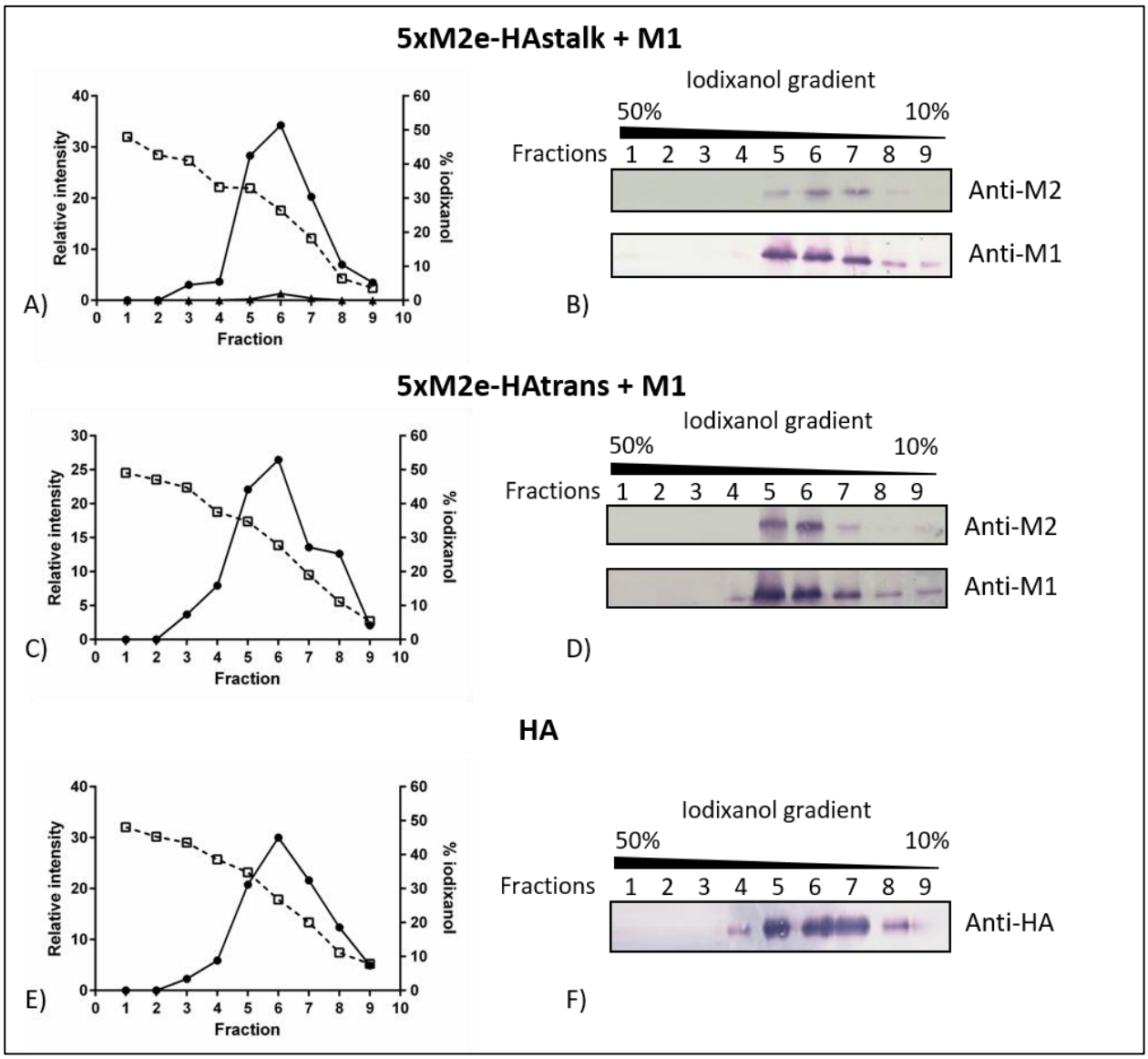

Figure 5| Analysis of the iodixanol gradient purification step. The iodixanol density (□) was compared with the relative intensity of recombinant proteins (●) from leaf tissue co-expressing (A) – 5xM2e-HAstalk + M1; (C) – 5xM2e-HAtrans + M1; or (E) – full-length HA, as determined by dot-blot using the anti-M2 antibody or the anti-HA antibody. The relative intensity of proteins from the negative control (empty pRIC) (▲) was also compared from dot blots in (A). (B), (D) and (F) show western blots of the fractions collected from the iodixanol gradient detect with the respective antibodies. Anti-M2 and anti-HA antibodies were used at a 1/5000 dilution; whereas the anti-M1 rabbit serum was used at a 1/10000 dilution.

Western blot analysis of the HA control also revealed strong bands around fractions 5 - 7, with some weaker bands in fractions 4 and 8 (Figure 5F). No bands corresponding to the desired recombinant proteins could be observed on SDS-gels stained with Coomassie (data not shown). Since fractions 5-7 seemed to contain most of the desired recombinant proteins for all samples, these fractions were pooled together and used to coat copper grids for TEM visualization (Figure 6).

Analysis of transmission electron micrographs of single expressed 5xM2e-HAstalk and 5xM2e-HAtrans revealed that putative VLPs (Figure 6, red arrows) ranging from 80 – 120 nm in size and with an oval shape, could be purified on the discontinuous gradient. These particles were in higher concentrations than with the samples analyzed before gradient purification. It was also possible to detect several particles that had not been completely assembled (Figure 6, black arrows). Moreover, irregular-shaped aggregates were also present in the samples (Figure 6, black arrows), possibly representing plant debris that was carried over the purification steps. Overall, there seemed to be no apparent difference in the shape, structure or size of particles from samples containing either 5xM2e-HAstalk or 5xM2e-HAtrans. These particles were similar in size and shape when compared to the HA control (red arrows); with the exception that the HA samples had clearly visible spikes that protruded from the surface of the particles whereas the M2e particles did not. Co-expression with M1 did not alter the morphology of particles, but it reduced the concentration of particles observed (Figure 6, red arrows). Analysis of the fractions from leaf tissue expressing the empty pRIC negative control vector did not find anything consistent with VLPs (Figure 6).

Previous studies have suggested that the cytoplasmic tail of the M2 protein is able to recruit M1 into the plasma membrane and thus promote viral assembly and budding (Chen et al. 2008; McCown and Pekosz 2006). Therefore, co-expression of the full-length M2 protein together with the fusion proteins and M1 was attempted (data not shown). However, despite several attempts, M2 expression could never be detected on western blots of crude extracts from infiltrated plants. Therefore, it was not possible to evaluate the effects of M2 co-expression.

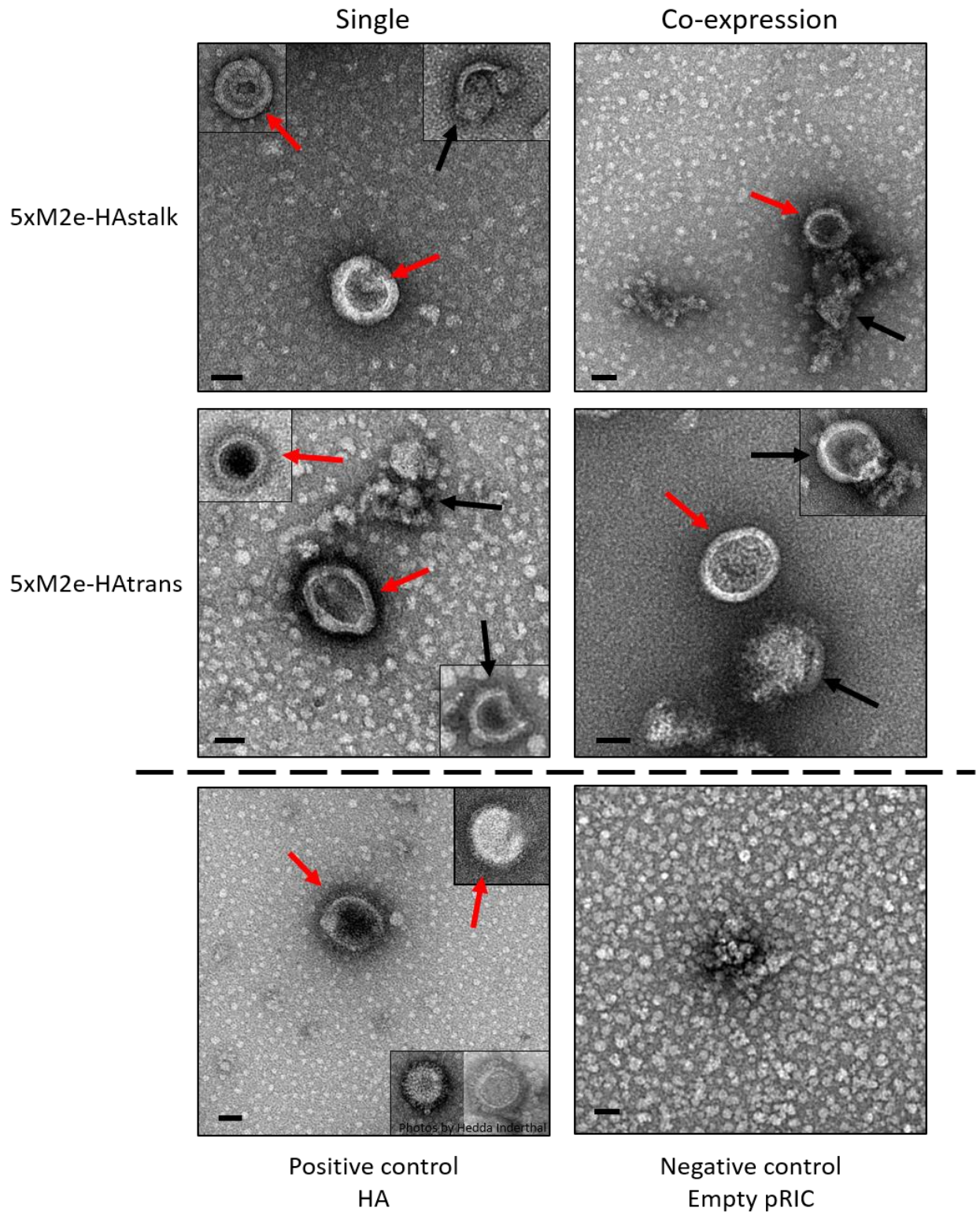

Figure 6| Transmission electron micrographs of pooled fractions 5 to 7 following iodixanol gradient ultracentrifugation. Corner images represent pictures taken in other regions of the copper grids. Red arrows indicate putative VLPs, black arrows indicate incomplete particles and other debris. Scale bars are 50 nm.

4.3.2. Apoplast extraction

Although some VLP-shaped particles could be observed for both 5xM2e-HAstalk and 5xM2e-HAtrans after iodixanol density gradient purification, their concentration was very low and they were not always fully assembled. Previous studies in our group using the full-length influenza A hemagglutinin protein have shown that most HA-VLPs were observed in the apoplast fractions of infiltrated plants. Hence, to confirm VLP identity, proteins from the apoplastic fraction were extracted and concentrated by ultracentrifugation through an iodixanol cushion.

Western blots of crude and apoplastic fractions were performed to confirm the presence of recombinant proteins (Figure 7). Bands corresponding to 5xM2e-HAstalk (data not shown), 5xM2e-HAtrans (Figure 7B) and HA (Figure 7A) could be observed in

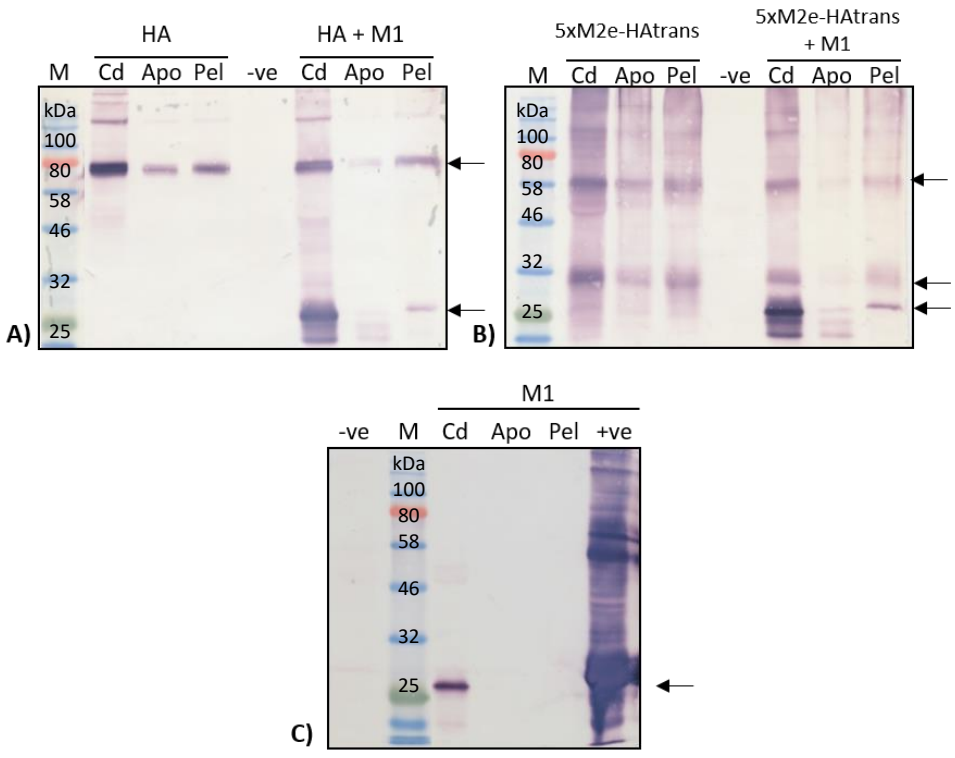

Figure 7| Western blot analysis of apoplast fractions. A) Analysis of leaves infiltrated with either HA alone or co-expressed with M1. Proteins were detected with a mixture of anti-HA antibody (1/5000) and anti-M1 antibody (1/5000). B) Analysis of leaves infiltrated with either 5xM2e-HAtrans alone or co-expressed with M1. Proteins were detected with a mixture of anti-M2 antibody (1/5000) and anti-M1 antibody (1/5000). C) Apoplast extraction of leaves infiltrated with only pRIC-M1. +ve – M1 expressed in *E. coli*. Proteins were detected with a monoclonal anti-M1 antibody (1/5000). M – Molecular Marker; Cd – crude extracts; Apo – Apoplastic fraction; Pel – pelleted apoplastic fraction; -ve – Apoplastic fraction of leaves infiltrated with an empty pRIC vector. Arrows indicate size of desired proteins.

both crude and apoplastic fractions. However, bands from the apoplast were generally fainter than those from the crude extracts. On the other hand, the M1 protein was only detected in the apoplastic fractions of co-infiltrated leaves; no bands corresponding to M1 could be observed in the apoplast of leaves infiltrated with M1 only (Figure 7A, B and C). Pelleting of the apoplast samples after a cushion ultracentrifugation step, resulted in higher protein concentration as shown by the increase in band intensity (Figure 7).

Once the presence of recombinant proteins was confirmed in the apoplastic fractions, I proceeded with visualization of the pelleted apoplastic fractions by TEM to analyze VLP formation. After coating with the samples, copper grids were immersed in either mouse anti-M2 or mouse anti-HA antibodies, followed by coating with an anti-mouse gold-labeled antibody. This would allow for identification and confirmation of influenza VLPs.

As described previously, HA apoplastic extracts examined under TEM showed circular particles of about 80 – 120 nm with regularly spaced spikes protruding from the VLPs (Figure 8). Most VLPs had small black dots attached on the surface, which corresponded to the gold beads that were covalently bound to the anti-mouse antibody. Co-expressing the HA protein with M1 resulted in particles that were less distinct and in lower amounts than those observed for single expressed HA.

Apoplastic fractions of leaves infiltrated with 5xM2e-HA-stalk or 5xM2e-HAtrans showed similar particles that were in higher number than the ones observed previously with density gradient purified extracts. Also, it is worth noting that, while for the density gradient purified samples, part of the structures observed corresponded to partially assembled particles, in the apoplastic fractions, particles were almost always complete, even after M1 co-expression (Figure 8). Immuno-gold experiments revealed that only single-expressed 5xM2e-HAstalk or 5xM2e-HAtrans samples displayed particles that had gold beads attached to them. However, these results could not always be reproduced and only a small proportion of the particles were gold immune-labeled, specially particles from 5xM2e-HAtrans expressed alone (Figure 8). It was never possible to visualize particles with gold beads for the co-expressed samples. Increasing the primary antibody concentration as well as its incubation time did not result in visible differences in the electron micrographs (data not shown). The negative control grids (apoplast

fraction of plants infiltrated with an empty pRIC vector) had few gold beads on the background but no particles could be observed.

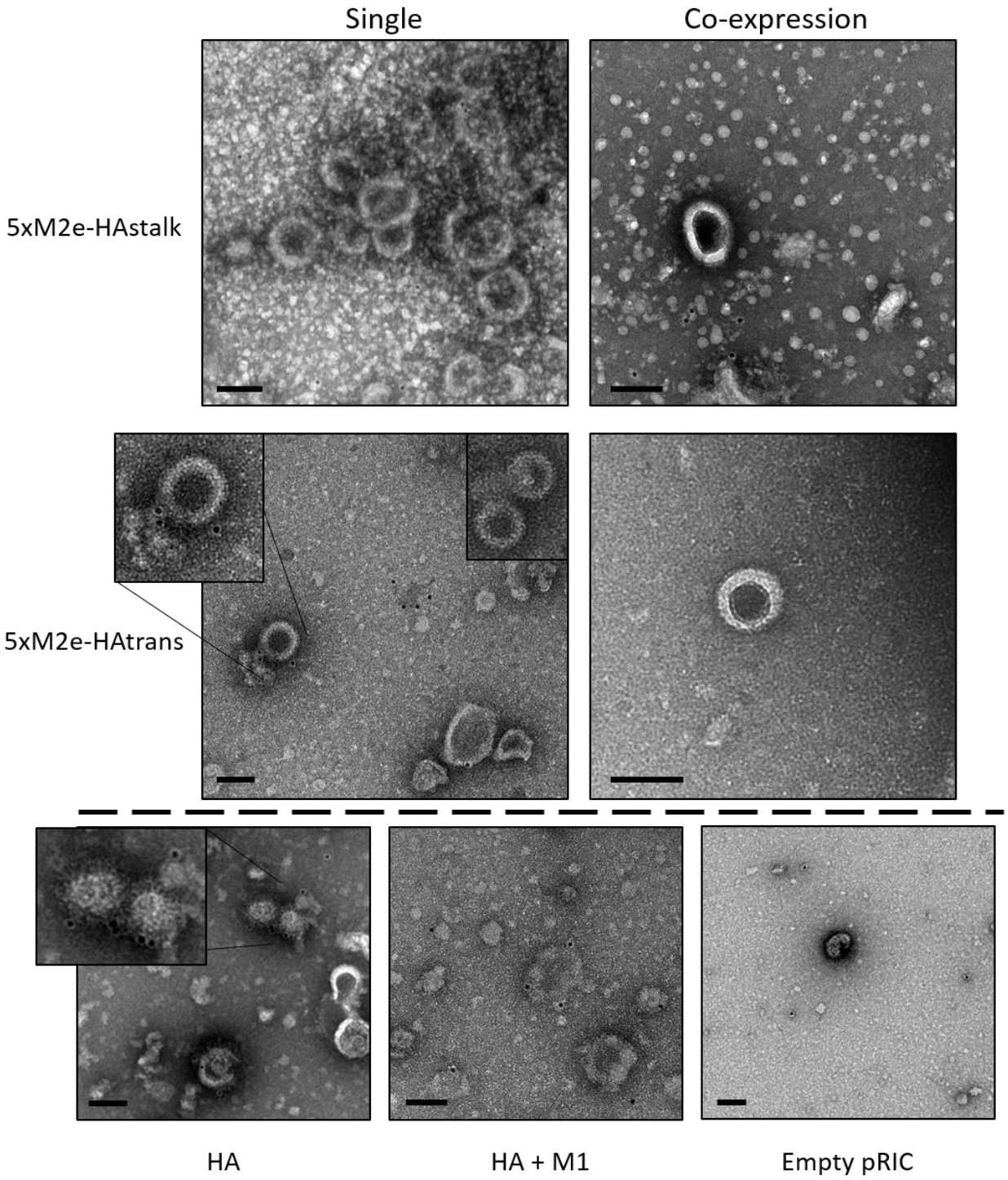

Figure 8| Immuno-gold labelling of VLPs in apoplastic extracts of infiltrated plants. The anti-M2 antibody was used to detect the M2e-HA VLPs and the negative control sample, whereas, the anti-HA antibody was used to detect HA VLPs. Gold beads are 10nm in diameter, scale bars are 100nm.

4.4. Discussion

In this section, I evaluated the ability of the 5xM2e-HAstalk and 5xM2e-HAtrans chimaeric proteins to self-assemble into VLPs using TEM analysis of purified samples. Producing enough plant material for VLP purification required the infiltration of whole plants as opposed to individual leaves. An alternative method using vacuum infiltration has been shown to be efficient at rapidly infiltrating multiple plants (Lai and Stahnke 2013). In this method, whole plants are first submerged in infiltration media containing the recombinant *Agrobacterium*. By creating a vacuum and suddenly releasing it, the pressure forces infiltration medium containing the *Agrobacterium* through the stomata and into the intercellular spaces, allowing for the entire plant to be infiltrated. This technique has been successfully used to produce influenza VLPs for clinical trials on a large scale (D'Aoust et al. 2010).

Crude extracts from vacuum infiltrated plants were loaded on top of an iodixanol cushion to pellet and concentrate possible VLPs before further purification steps. Any free HA-derived or small plant proteins in the supernatant should not be captured in the pellet containing VLPs, thereby also serving as a partial purification step. Western blots analysis of the different fractions collected confirmed that the majority of recombinant proteins accumulated in the pellet, including the HA positive control which is known to form VLPs. Previous work on purification of influenza VLPs, showed successful VLP pelleting after a cushion ultracentrifugation step (Young et al. 2015; Wu et al. 2010; Lai et al. 2011; Thompson et al. 2015). Most of these studies used sucrose for the preparation of the cushion. However, since the final purification step in this study was in an iodixanol gradient, I hypothesized that it would be less stressful for the VLPs to use the same density medium in the cushioning and gradient steps.

However, because recombinant proteins were not only detected in the pellet, but also between the iodixanol cushion and the supernatant fractions, I analyzed all fractions by TEM to confirm that the VLPs were being pelleted. As expected, TEM visualization of the band and pellet samples revealed large structures that probably corresponded to plant membrane-derived debris and other large protein aggregates (Figure 3). However, in both single and co-expressed M2e-HA fusion pellet fractions, it was possible to distinguish individual spherical particles, which were never visualized in either the

band or supernatant fractions. These particles ranged between 80 - 120 nm in diameter and despite the lack of characteristic HA spikes, were morphologically very similar to HA VLPs produced in plants (Figure 8; D'Aoust et al., 2008). These results provided preliminary evidence that both M2e-HA proteins could assemble into VLPs.

To confirm that the particles observed were VLPs, the pellets were applied to a discontinuous gradient. This step works by layering different concentrations of iodixanol (10/20/30/40/50 %) and then collecting fractions for analysis after ultracentrifugation. Each concentration of iodixanol has a different density: different particles are separated according to their density, allowing for the removal of undesired plant debris. Iodixanol has been widely used for the purification of influenza VLPs (Thompson et al. 2015; T. Latham & Galarza 2001; George & Aucoin 2015). Although being more expensive than conventional density solutions such as caesium chloride or sucrose, iodixanol offers certain distinct advantages (e.g. low viscosity, non-toxic to eukaryotic cells and it is suitable for direct TEM visualization) that makes it more suitable for screening new constructs which are expected to lead to the formation of VLPs (Gias et al. 2008).

In agreement with previous studies using live influenza virus (Hutchinson & Fodor 2014; Arora et al. 1973; Hutchinson et al. 2014), immunoblot analysis of the fractions collected after gradient ultracentrifugation, showed that both 5xM2e-HAstalk and 5xM2e-HAtrans accumulated between fractions 5 - 7 corresponding to 33 % and 19 % iodixanol respectively. However, although proteins could be detected on western blots, it was never possible to distinguish corresponding bands amongst the background signal on Coomassie-stained SDS-gels (data not shown).

The Coomassie Brilliant Blue R-250 reagent used here has been reported to be able to detect as few as 100 ng per band for most proteins. This would indicate that the concentration of influenza recombinant proteins after purification, was below 400 ng/mL and in terms of overall yield per gram of fresh weight leaves, this would be less than 5 mg/kg. In comparison, D'Aoust et al. 2008 have reported yields of approximately 50 mg/kg for the production of HA VLPs in plants. Therefore, further work on improving protein yield and purity must be performed for these plant-produced proteins to be commercially viable.

Nevertheless, since this was a preliminary study on the creation of new proteins that could form VLPs, the expression yields were not of major concern if sufficient amounts could be obtained for TEM analysis.

TEM of pooled fractions 5 to 7 displayed a higher concentration of particles that were similar in morphology compared to the ones observed in the pellet. However, despite being cleaner than the pellet, small protein aggregates could still be observed by TEM after gradient purification. These contaminants could potentially be excluded by additional specialized chromatography steps such as size-exclusion, ion exchange, and affinity chromatography (Zeltins 2013). Closer observation of the particles from 5xM2e-HAtrans and 5xM2e-HAstalk showed no major differences in size compared to HA VLPs (Figure 6), suggesting that the particles observed in the M2e-HA samples could probably be VLPs. Furthermore, as previously, despite the lack of spike projections, particles from M2e-HA fusions had a similar appearance to HA VLPs. These results were expected since the surface spike projections have been associated with the HA globular head domain (Howley 2013), which is lacking from the M2e-HA fusions. It is possible that there are some M2e spikes protruding from the M2e-HA fusion but due to their small sizes, they could not be visualized under the settings used for the TEM.

Surprisingly, no significant differences in VLP morphology, quantity or size were observed between the two M2e-HA fusion proteins: 5xM2e-HAstalk and 5xM2e-HAtrans. Since the only difference between these two proteins is the HA stalk domain present only in the 5xM2e-HAstalk construct, it can be hypothesized that the HA stalk domain does not have a significant structural impact in the formation of these VLPs, and that their formation is due mainly to the transmembrane domain. This would be in agreement with other studies that have used the HA transmembrane domain as a scaffold to mediate enhanced incorporation and display of enveloped proteins (Benen et al. 2014; Wang et al. 2007).

Although increased concentrations of VLP-resembling particles were observed in gradient-purified samples, an important number of these particles seemed to be incomplete (Figure 6, black arrows). Previously, D'Aoust et al. (2008) have shown that in plants, HA-VLP assembly takes place at the cell membrane of infiltrated plants, with most VLPs accumulating in the apoplastic spaces between the plasma membrane and

the cell wall. Therefore, I hypothesized that, if successfully assembled, M2e-HA VLPs would follow the same pathway as HA-VLPs, and accumulate at higher concentrations in the apoplastic spaces of infiltrated plants.

The apoplast is the extra-protoplasmic water-filled space of the plant cell: it is composed of secreted proteins like digestive enzymes, metabolites, ions and many other substances (Blinda et al. 1997). Proteins located in the apoplast can be easily extracted by vacuum infiltration with an extraction solution such as PBS, followed by a mild centrifugation step with leaves cut into strips to collect the apoplastic washing fluid (Witzel et al. 2011). Western blot analysis of apoplast extracts from infiltrated plants confirmed the presence of both M2e-HA fusions and the full-length HA when single or co-expressed. The lower protein yields observed from the apoplastic fractions (Figure 7) compared to crude samples are probably due to the relatively large volumes of extraction solution that had to be employed for harvesting of the apoplastic fluid. Nevertheless, TEM of apoplast fractions containing the M2e-HA fusions, showed a higher concentration of particles than previously observed for the purified crude extracts. The fact that no VLP-like structures could be observed on grids from leaves infiltrated with an empty vector adds strong evidence that these particles were M2e-HA VLPs. Interestingly, particles observed in the apoplastic fractions were almost always fully assembled, with very few that seemed incomplete. These findings provide tentative evidence that the M2e-HA VLPs follow the same pathway as wild-type HA VLPs by budding at the plasma membrane of infected cells. This could be confirmed with additional experiments by fixating infiltrated leaves with a cross-linking solution such as glutaraldehyde, and making ultra-thin sections for TEM analysis. This approach would allow for direct localization of the VLP budding process in plant cells (D'Aoust et al. 2008).

Immuno-gold labelling of M2e-HA particles using the monoclonal anti-M2 antibody was only partially successful as significant background signal was observed. Only the samples with the M2e-HA fusions expressed alone seemed to have VLPs that were successfully immune-labeled (Figure 8). However, given the strong background signal, it cannot be ruled out that the labeled particles observed could have been the result of non-specific antibody binding. Interestingly, M1 co-expressed samples never showed gold labeled

particles. This could be due to the low number of particles that were formed, or to the possibility that co-expression with M1 triggers a conformational change of the M2e-HA fusions that masks the M2e epitopes. To confirm these assumptions, further investigation is required using different M2 antibodies.

More interestingly, VLP-like particles were observed in higher numbers when the M2e-fusions were expressed on their own compared to when M1 was co-expressed. These results are consistent with the observations made in Chapter 3, where co-expression with M1 decreased fusion protein accumulation. During natural viral infection, the HA protein is targeted to the plasma membrane through the secretory pathways, whereas M1 collects in the nucleus/cytosol region (Sato et al. 2003). A number studies have demonstrated that VLPs without M1, can be successfully produced in different expression systems such as mammalian cells, insect cells or even plants (Chang et al. 2011; D'Aoust et al. 2008; Lai et al. 2011; Chen et al. 2007). However, for unknown reasons, this reduction in VLP concentration after M1 co-expression has only been reported when plants were used as expression systems (D'Aoust et al. 2008). It is therefore possible that plants lack certain components that are necessary for efficient budding of M1-contining VLPs. Identification and co-expression of these components with the recombinant influenza proteins could possibly increase VLP formation in plants.

Recently, the M2 protein has been found to promote the budding and release of the influenza virions, by interacting with the M1 protein (Wei et al. 2011; McCown & Pekosz 2006; Wang et al. 2010; Chen et al. 2007). There is also evidence that co-expression of M2 protein with certain HAs helps in VLP formation in plants (E.P. Rybicki, personal communication). Although the exact mechanisms for influenza budding formation remain unknown, it has been suggested that, interactions between structural proteins, such as M1 binding to the HA cytoplasmic tail, could prevent completion of viral budding until recruitment of other proteins, such as M2 (Iwatsuki-Horimoto et al. 2006; McCown & Pekosz 2005; Rossman et al. 2010; Wang et al. 2010; Kerviel et al. 2016). However, because of its highly insoluble nature, the M2 protein is relatively difficult to produce in a heterologous expression system (Czabotar et al. 2004; Mitraki et al. 1991). This could explain why there are so few influenza VLP studies that

include M2 in their VLP formulations, despite its reported ability to promote particle formation.

Here, I tried co-infiltrating both fusion proteins and M1, with the full-length M2 protein (data not shown). However, as anticipated from previous trials with *E. coli*, M2 expression could never be detected in plant extracts and thus it was not possible to investigate its effect on particle formation. Nevertheless, co-expression with the full-length M2 protein is extremely promising to increase particle formation and should therefore be investigated.

4.5. Conclusions

Thus, based on these results I can conclude that, when expressed in *N. benthamiana* plants, the 5xM2e-HAstalk and the 5xM2e-HAtrans fusion proteins, can form VLP-like particles on their own and to a lesser extent by co-expression with M1. These particles, were similar in size and shape to native HA-VLPs without the characteristic surface spikes. Furthermore, particles seemed to bud at the plasma membrane, finally accumulating in the apoplast, as previously described (D'Aoust et al. 2008). Nonetheless, further investigations to fully characterize these particles in terms of structural composition as well as immunogenic properties are required to confirm their potential as influenza vaccines.

Chapter 5: General conclusions

The aim of this project was to design and produce a new candidate influenza vaccine that could meet two major requirements: first, it would have to be rapidly produced using a system that could be easily scalable, to allow for a quick response in case of influenza pandemic. Second, because influenza A is constantly undergoing antigenic drifts/shifts, the vaccine would have to elicit broad immune responses that could provide protection against widely different Influenzavirus A strains. To meet these requirements, a transient expression system was utilized in *N. benthamiana* to rapidly produce virus-like particles (VLPs) displaying the M2e conserved ectopic region of the M2 viroporin protein. The plant expression platform has been shown to be favorable for the rapid production of highly immunogenic influenza virus HA-VLPs (D'Aoust et al. 2008). This made it conceivable to obtain similar VLPs, by replacing the highly variable head domain of the HA protein with several tandem copies of the M2e peptide. If successfully assembled, these M2e-HA VLPs would have the potential to elicit broader immune responses than any HA-VLP or current available vaccine.

Because available commercial antibodies against the influenza matrix proteins 1 (M1) and 2 (M2) are exceedingly expensive, both proteins were first expressed in *E. coli* in the form of insoluble inclusion bodies and subsequently injected into rabbits for antibody production. M1 expression in *E. coli* required little optimization and was shown to express at high yields, between 0.8 - 1.0 mg/mL. The rabbit serum raised from injecting *E. coli*-produced M1, could detect recombinant M1 produced in either bacteria or plants. This serum was used for subsequent immunoblot experiments in plants, thus reducing greatly the costs of the project.

On the other hand, because of its high insolubility, the M2 protein could only be produced in low amounts and its expression had to be optimized by resorting to the use of Terrific broth. Using this highly enriched media, I was able to reach 0.2 - 0.3 mg/mL of insoluble M2, which was enough for rabbit injection. Nevertheless, because of its weak immunogenicity, the recombinant M2 was not able to induce detectable amounts of M2-specific antibodies in the serum of injected rabbits. It is possible that increasing the amounts and the purity of recombinant M2 as well as the number and the time

interval between each boost could result in improved immune responses against the M2 protein, as suggested by (Feng et al. 2006). Additional M2 protein produced in this way could potentially be used for future animal trials to compare its immunogenicity against the plant produced M2e-HA chimaeric proteins.

To increase the chances of obtaining M2e-presenting VLPs, I designed six different M2e-HA fusion proteins based on the study by Kim, Lee, et al., 2013. After expression and sequence analysis, the two fusion proteins with the highest probability of forming immunogenic VLPs (5xM2e-HAstalk and 5xM2e-HAtrans) were selected for expression optimization and VLP characterization in *N. benthamiana* plants.

Both 5xM2e-HAstalk and 5xM2e-HAtrans fusion proteins could be readily expressed in plants after only 3 dpi. However, although protein accumulation was increased with a variety of optimizations, I was never able to produce sufficient amounts to make production commercially viable. Further optimizations strategies have been considered to improve recombinant protein yields in plants (Jung et al. 2015; Maclean et al. 2007; Mortimer et al. 2012; D'Aoust et al. 2008).

Such optimizations can be extremely time consuming and would be wasteful in the eventuality that the M2e-HA fusion proteins could not properly assemble into VLPs. Therefore, I decided to first evaluate VLP formation before trying any additional expression optimization.

Although Kim et al., 2013 have previously shown that M2e fused to the transmembrane domain of Influenzavirus HA could form VLPs in insect cells, these VLPs were only obtained when the M1 protein was included. In the present study, using transmission electron analysis of density-gradient purified samples, I showed that when expressed alone, the 5xM2e-HAstalk and 5xM2e-HAtrans proteins successfully assembled into putative VLPs that were similar in size and shape to HA VLPs without the characteristic spikes. Surprisingly, comparison between 5xM2e-HAstalk and 5xM2e-HAtrans particles showed no visible differences in morphology, suggesting that the formation of these particles was due mainly to the HA transmembrane domain. As anticipated, the highest concentration of fully assembled M2e-HA particles was found in the apoplastic space of infiltrated plants. This provides evidence that the M2e-HA proteins were still localized

to the plasma membrane despite having replaced the HA globular head with the five M2e tandem copies. No conclusions could be drawn from immune-gold labeling experiments because of the background signal observed, thus additional optimizations are probably required.

Furthermore, not only did co-expression with the M1 protein decrease the accumulation of 5xM2e-HAstalk and 5xM2e-HAtransin in crude extracts, but it also reduced the number of particles formed. These findings are contradictory to the study by Kim, Lee, et al., 2013, where the formation of M2e-HA VLPs in insect cells was only reported when the M2e-HA fusion was co-expressed with M1. These discrepancies could be attributed to the difference in expression systems used, as suggested by (Chen et al. 2007; Wang et al. 2010). The mechanisms leading to the synchronized buildup of the M2e-HA fusion proteins and M1 at the site of budding are complex, and could be very different depending on the expression system used. Moreover, it is possible that including other influenza structural proteins (such as M2) in the formulation of these particles, may help recruitment of M1 into the plasma membrane and promote the budding and release of influenza VLPs. Further work in comparing the expression of these M2e-HA fusions in different expression systems, as well as co-expressing with the M2 protein, would be of high interest.

In summary, this study provided preliminary data on the ability of plants to produce chimaeric influenza VLPs. To the best of my knowledge, this is the first report of M2e-HA chimeric VLP production using plants. Furthermore, these VLPs could be produced by expressing the M2e-HA proteins alone, which adds evidence that only the transmembrane and cytoplasmic domain of the HA protein are required for particle incorporation. This is also the first study that fused the two most promising conserved influenza peptides, M2e and the HA stalk domain, and showed that, when fused together, they could form VLPs in plants. Finally, this is the first proof that Influenzavirus M1 protein expressed in plants appears to be co-localized with HA or HA derivatives in VLPs when co-expressed.

It would be interesting to evaluate the immunogenicity of these VLPs to see if they can induce broad immune responses. However, given the low amount of VLPs observed, it is highly probable that any immunogenicity study performed using the conditions

of this project, would not accurately reflect the full potential of these VLPs. Therefore, to characterize the immunogenicity of the M2e-HA VLPs, future work should focus first on increasing the number VLPs formed. This could be achieved by several approaches, such as: i) increasing initial protein expression yields; ii) complementing density gradient purification with other purification methods, such as chromatography; and iii) co-expressing fusion proteins with both M1 and M2. This is by no means an exhaustive list and most probably, a combination of these approaches will have to be employed. It is to be hoped that others can use these suggestions to improve VLP formation and complete our team's goal of making a universal influenza A vaccine.

References

Ali, A. et al., 2000. Influenza virus assembly: effect of influenza virus glycoproteins on the membrane association of M1 protein. *Journal of virology*, 74(18), pp.8709–19.

Almeida, J.D. & Waterson, A.P., 1967. Some Observations on the Envelope of an Influenza Virus. *Journal of General Microbiology*, 46(1), pp.107–110.

Ameiss, K. et al., 2010. Delivery of woodchuck hepatitis virus-like particle presented influenza M2e by recombinant attenuated Salmonella displaying a delayed lysis phenotype. *Vaccine*, 28(41), pp.6704–13.

Ampofo, W.K. et al., 2012. Improving influenza vaccine virus selectionReport of a WHO informal consultation held at WHO headquarters, Geneva, Switzerland, 14-16 June 2010. *Influenza and Other Respiratory Viruses*, 6(2), pp.142–152.

Anon, 2014. WHO Influenza Fact sheet N°211. Available at: http://www.who.int/mediacentre/factsheets/fs211/en/ [Accessed July 7, 2016].

Antrobus, R.D. et al., 2014. Coadministration of Seasonal Influenza Vaccine and MVA-NP+M1 Simultaneously Achieves Potent Humoral and Cell-Mediated Responses. *Molecular Therapy*, 22(1), pp.233–238.

Arora, D.J., Pavilanis, V. & Robert, P., 1973. Two-step centrifugation method. A simplification of the density-gradient procedure for the purification of influenza virus. *Canadian journal of microbiology*, 19(5), pp.633–8.

Atsmon, J. et al., 2014. Priming by a novel universal influenza vaccine (Multimeric-001)—A gateway for improving immune response in the elderly population. *Vaccine*, 32(44), pp.5816–5823.

Ayllon, J., García-Sastre, A. & Hale, B.G., 2012. Influenza A viruses and PI3K. *Virulence*, 3(4), pp.411–414.

Bachmann, M.F. et al., 1993. The influence of antigen organization on B cell responsiveness. *Science (New York, N.Y.)*, 262(5138), pp.1448–51.

Baranovich, T. et al., 2010. Emergence of H274Y oseltamivir-resistant A(H1N1) influenza viruses in Japan during the 2008–2009 season. *Journal of Clinical Virology*, 47(1), pp.23–28.

Bárcena, J. & Blanco, E., 2013. Design of Novel Vaccines Based on Virus-Like Particles or Chimeric Virions. In pp. 631–665.

Barta, A. et al., 1986. The expression of a nopaline synthase - human growth hormone chimaeric gene in transformed tobacco and sunflower callus tissue. *Plant molecular biology*, 6(5), pp.347–57.

Beigel, J.H. et al., 2005. Avian influenza A (H5N1) infection in humans. *The New England journal of medicine*, 353(13), pp.1374–85.

Belshe, R.B. et al., 2007. Live Attenuated versus Inactivated Influenza Vaccine in Infants and Young Children. *New England Journal of Medicine*, 356(7), pp.685–696.

Belshe, R.B. et al., 1998. The Efficacy of Live Attenuated, Cold-Adapted, Trivalent, Intranasal Influenzavirus Vaccine in Children. *New England Journal of Medicine*, 338(20), pp.1405–1412.

Benen, T.D. et al., 2014. Development and immunological assessment of VLP-based immunogens exposing the membrane-proximal region of the HIV-1 gp41 protein. *Journal of Biomedical Science*, 21(1), p.79.

Bessa, J. et al., 2008. Efficient induction of mucosal and systemic immune responses by virus-like particles administered intranasally: implications for vaccine design. *European journal of immunology*, 38(1), pp.114–26.

Bhaskar, P.B. et al., 2009. Agrobacterium-Mediated Transient Gene Expression and Silencing: A Rapid Tool for Functional Gene Assay in Potato H. A. El-Shemy, ed. *PLoS ONE*, 4(6), p.e5812.

Black, R.A. et al., 1993. Production of the M2 protein of influenza A virus in insect cells is enhanced in the presence of amantadine. *Journal of General Virology*, 74(8), pp.1673–1677.

Blazevic, V., Trubey, C.M. & Shearer, G.M., 2000. Comparison of in vitro immunostimulatory potential of live and inactivated influenza viruses. *Human immunology*, 61(9), pp.845–9.

Blinda, A. et al., 1997. De novo synthesis and accumulation of apoplastic proteins in leaves of heavy metal-exposed barley seedlings. *Plant, Cell and Environment*, 20(8), pp.969–981.

Blokhina, E. a et al., 2013. A molecular assembly system for presentation of antigens on the surface of HBc virus-like particles. *Virology*, 435(2), pp.293–300.

Bommakanti, G. et al., 2010. Design of an HA2-based Escherichia coli expressed influenza immunogen that protects mice from pathogenic challenge. *Proceedings of the National Academy of Sciences*, 107(31), pp.13701–13706.

Brandenburg, B. et al., 2013. Mechanisms of Hemagglutinin Targeted Influenza Virus Neutralization P. Digard, ed. *PLoS ONE*, 8(12), p.e80034.

Bright, R. a et al., 2006. Adamantane resistance among influenza A viruses isolated early during the 2005-2006 influenza season in the United States. *JAMA : the journal of the American Medical Association*, 295(8), pp.891–894.

Bright, R. a. et al., 2005. Incidence of adamantane resistance among influenza A (H3N2) viruses isolated worldwide from 1994 to 2005: A cause for concern. *Lancet*, 366(9492), pp.1175–1181.

Broadbent, A.J. & Subbarao, K., 2011. Influenza virus vaccines: lessons from the 2009 H1N1 pandemic. *Current Opinion in Virology*, 1(4), pp.254–262.

Brown, I.H., 2000. The epidemiology and evolution of influenza viruses in pigs. *Veterinary Microbiology*, 74(1–2), pp.29–46.

Brunel, F.M. et al., 2006. Structure-Function Analysis of the Epitope for 4E10, a Broadly Neutralizing Human Immunodeficiency Virus Type 1 Antibody. *Journal of Virology*, 80(4), pp.1680–1687.

Butenko, A.M. et al., 1987. [Dhori virus--a causative agent of human disease. 5 cases of laboratory infection]. *Voprosy virusologii*, 32(6), pp.724–9.

Butt, K.M. et al., 2005. Human Infection with an Avian H9N2 Influenza A Virus in Hong Kong in 2003. *Journal of Clinical Microbiology*, 43(11), pp.5760–5767.

Center for Disease Control and Prevention (CDC), 2013. Prevention and control of seasonal influenza with vaccines. Recommendations of the Advisory Committee on Immunization Practices--United States, 2013-2014. *Mmwr*, 62(RR-7), p.1,5,28.

Centers for Disease Control and Prevention (CDC), 2013. Estimated influenza illnesses and hospitalizations averted by influenza vaccination - United States, 2012-13 influenza season. *MMWR. Morbidity and mortality weekly report*, 62(49), pp.997–1000.

Chan, P.K.S., 2002. Outbreak of avian influenza A(H5N1) virus infection in Hong Kong in 1997. *Clinical infectious diseases : an official publication of the Infectious Diseases Society of America*, 34 Suppl 2, pp.S58-64.

Chang, G.R.-L. et al., 2011. Production of immunogenic one-component avian H7-subtype influenza virus-like particles. *Process Biochemistry*, 46(6), pp.1292–1298.

Chen, B.J. et al., 2007. Influenza virus hemagglutinin and neuraminidase, but not the matrix protein, are required for assembly and budding of plasmid-derived virus-like particles. *Journal of virology*, 81(13), pp.7111–23.

Chen, B.J. et al., 2008. The Influenza Virus M2 Protein Cytoplasmic Tail Interacts with the M1 Protein and Influences Virus Assembly at the Site of Virus Budding. *Journal of Virology*, 82(20), pp.10059–10070.

Chen, R., 2012. Bacterial expression systems for recombinant protein production: E. coli and beyond. *Biotechnology Advances*, 30(5), pp.1102–1107.

Choi, J.-G. et al., 2013. *Protective efficacy of baculovirus-derived influenza virus-like particles bearing H5 HA alone or in combination with M1 in chickens*, Elsevier B.V.

Collins, T. et al., 2002. A novel family 8 xylanase, functional and physicochemical characterization. *The Journal of biological chemistry*, 277(38), pp.35133–9.

Collins, T. et al., 2013. Batch production of a silk-elastin-like protein in E. coli BL21(DE3): key parameters for optimisation. *Microbial Cell Factories*, 12(1), p.21.

Cox, M.M.J. et al., 2015. Safety, efficacy, and immunogenicity of Flublok in the prevention of seasonal influenza in adults. *Therapeutic Advances in Vaccines*, 3(4), pp.97–108.

Cox, N.J. & Subbarao, K., 2000. G LOBAL E PIDEMIOLOGY OF I NFLUENZA : Past and Present *. *Annu. Rev. Med.*, (51), pp.407–421.

Cox, R.J., Brokstad, K. a & Ogra, P., 2004. Influenza virus: immunity and vaccination strategies. Comparison of the immune response to inactivated and live, attenuated influenza vaccines. *Scandinavian journal of immunology*, 59(1), pp.1–15.

Czabotar, P.E., Martin, S.R. & Hay, A.J., 2004. Studies of structural changes in the M2 proton channel of influenza a virus by tryptophan fluorescence. *Virus Research*, 99(1), pp.57–61.

D'Aoust, M.-A. et al., 2008. Influenza virus-like particles produced by transient expression in Nicotiana benthamiana induce a protective immune response against a lethal viral challenge in mice. *Plant biotechnology journal*, 6(9), pp.930–40.

D'Aoust, M.-A. et al., 2010. The production of hemagglutinin-based virus-like particles in plants: a rapid, efficient and safe response to pandemic influenza. *Plant biotechnology journal*, 8(5), pp.607–19.

Darwish, I., Mubareka, S. & Liles, W.C., 2011. Immunomodulatory therapy for severe influenza. *Expert review of anti-infective therapy*, 9(7), pp.807–22.

Deng, L. et al., 2015. M2e-Based Universal Influenza A Vaccines. *Vaccines*, 3(1), pp.105–136.

Denis, J. et al., 2008. Development of a universal influenza A vaccine based on the M2e peptide fused to the papaya mosaic virus (PapMV) vaccine platform. *Vaccine*, 26(27–28), pp.3395–403.

DiazGranados, C.A. et al., 2014. Efficacy of high-dose versus standard-dose influenza vaccine in older adults. *The New England journal of medicine*, 371(7), pp.635–45.

DiazGranados, C. a., Denis, M. & Plotkin, S., 2012. Seasonal influenza vaccine efficacy and its determinants in children and non-elderly adults: A systematic review with meta-analyses of controlled trials. *Vaccine*, 31(1), pp.49–57.

Doherty, P.C. & Kelso, A., 2008. Toward a broadly protective influenza vaccine. , 118(10), pp.3–6.

During K., 1988. Wound-inducible expression and secretion of T4 lysozyme and monoclonal antibodies in Nicotiana tabacum. *Ph.D Thesis. Mathematisch-Naturwissenschaftlichen Fakultat der Universitat zu Koln*.

Edwards, M.J. & Dimmock, N.J., 2000. Two influenza A virus-specific Fabs neutralize by inhibiting virus attachment to target cells, while neutralization by their IgGs is complex and occurs simultaneously through fusion inhibition and attachment inhibition. *Virology*, 278(2), pp.423–35.

Fan, J. et al., 2004. Preclinical study of influenza virus A M2 peptide conjugate vaccines in mice, ferrets, and rhesus monkeys. *Vaccine*, 22(23–24), pp.2993–3003.

Feng, J. et al., 2006. Influenza A virus infection engenders a poor antibody response against the ectodomain of matrix protein 2. *Virology journal*, 3(1), p.102.

Fiers, W. et al., 2004. A "universal" human influenza A vaccine. *Virus research*, 103(1–2), pp.173–6.

Fiers, W. et al., 2009. M2e-based universal influenza A vaccine. *Vaccine*, 27(45), pp.6280–6283.

De Filette, M. et al., 2008. An influenza A vaccine based on tetrameric ectodomain of matrix protein 2. *The Journal of biological chemistry*, 283(17), pp.11382–7.

De Filette, M. et al., 2011. Antiserum against the conserved nine amino acid N-terminal peptide of influenza A virus matrix protein 2 is not immunoprotective. *Journal of General Virology*, 92(2), pp.301–306.

De Filette, M. et al., 2005. Universal influenza A vaccine: optimization of M2-based constructs. *Virology*, 337(1), pp.149–61.

Foppa, I.M. et al., 2015. Deaths averted by influenza vaccination in the U.S. during the seasons 2005/06 through 2013/14. *Vaccine*, 33(26), pp.3003–3009.

Frace, a. M. et al., 1999. Modified M2 proteins produce heterotypic immunity against influenza A virus. *Vaccine*, 17(18), pp.2237–2244.

Francis, T., 1940. A NEW TYPE OF VIRUS FROM EPIDEMIC INFLUENZA. *Science (New York, N.Y.)*, 92(2392), pp.405–8.

Fu, T.-M. et al., 2009. Characterizations of four monoclonal antibodies against M2 protein ectodomain of influenza A virus. *Virology*, 385(1), pp.218–226.

Gao, R. et al., 2013. Human Infection with a Novel Avian-Origin Influenza A (H7N9) Virus. *New England Journal of Medicine*, 368(20), pp.1888–1897.

García-Fruitós, E. et al., 2005. Aggregation as bacterial inclusion bodies does not imply inactivation of enzymes and fluorescent proteins. *Microbial cell factories*, 4, p.27.

García-Fruitós, E., 2010. Inclusion bodies: a new concept. *Microbial Cell Factories*, 9(1), p.80.

George, S. & Aucoin, M.G., 2015. Characterization of Alternative Promoters to Stagger and Control Protein Expression in the Baculovirus-Insect Cell System: From Intracellular Reporter Proteins to Fluorescent Influenza Virus-like Particles. *BMC Proceedings*, 9(Suppl 9), p.P49.

Gerhard, W., 2001. The role of the antibody response in influenza virus infection. *Current topics in microbiology and immunology*, 260, pp.171–90.

Gerhard, W., Mozdzanowska, K. & Zharikova, D., 2006. Prospects for universal influenza virus vaccine. *Emerging Infectious Diseases*, 12(4), pp.569–574.

Ghendon, Y., 1994. Introduction to pandemic influenza through history. *European journal of epidemiology*, 10(4), pp.451–453.

Gias, E. et al., 2008. Purification of human respiratory syncytial virus by ultracentrifugation in iodixanol density gradient. *Journal of Virological Methods*, 147(2), pp.328–332.

Goodwin, K., Viboud, C. & Simonsen, L., 2006. Antibody response to influenza vaccination in the elderly: A quantitative review. *Vaccine*, 24, pp.1159–1169.

Govorkova, E.A. et al., 2013. Antiviral resistance among highly pathogenic influenza A (H5N1) viruses isolated worldwide in 2002–2012 shows need for continued monitoring. *Antiviral Research*, 98(2), pp.297–304.

Grgacic, E.V.L. & Anderson, D.A., 2006. Virus-like particles: passport to immune recognition. *Methods (San Diego, Calif.)*, 40(1), pp.60–5.

Gross, P.A. et al., 1977. A controlled double-blind comparison of reactogenicity, immunogenicity, and protective efficacy of whole-virus and split-product influenza vaccines in children. *The Journal of infectious diseases*, 136(5), pp.623–32.

Guinea, R. & Carrasco, L., 1994. Influenza virus M2 protein modifies membrane permeability in E. coli cells. *FEBS Letters*, 343(3), pp.242–246.

Guo, L. et al., 2009. [Cloning and characterization of M1 gene of H3N2 subtype swine influenza virus]. *Sheng wu gong cheng xue bao = Chinese journal of biotechnology*, 25(5), pp.672–8.

Guo, Y.J. et al., 1983. Isolation of influenza C virus from pigs and experimental infection of pigs with influenza C virus. *The Journal of general virology*, 64 (Pt 1), pp.177–82.

Hanly, W.C., Artwohl, J.E. & Bennett, B.T., 1995. Review of Polyclonal Antibody Production Procedures in Mammals and Poultry. *ILAR Journal*, 37(3), pp.93–118.

Harbury, P.B. et al., 1993. RESEARCH ARTICLES A Switch Between Two- , Three- , and Four-Stranded Coiled Coils in GCN4 Leucine Zipper Mutants. , 262(November).

Hashem, A.M., 2015. Prospects of HA-Based Universal Influenza Vaccine. *BioMed Research International*, 2015.

Hashemi, H. et al., 2012. Immunization with M2e-displaying T7 bacteriophage nanoparticles protects against influenza A virus challenge. *PloS one*, 7(9), p.e45765.

Hass, J. et al., 2011. The role of swine as "mixing vessel" for interspecies transmission of the influenza A subtype H1N1: a simultaneous Bayesian inference of phylogeny and ancestral hosts. *Infection, genetics and evolution : journal of molecular epidemiology and evolutionary genetics in infectious diseases*, 11(2), pp.437–41.

Hayden, F.G. & de Jong, M.D., 2011. Emerging Influenza Antiviral Resistance Threats. *Journal of Infectious Diseases*, 203(1), pp.6–10.

Herzog, C. et al., 2009. Eleven years of Inflexal® V—a virosomal adjuvanted influenza vaccine. *Vaccine*, 27(33), pp.4381–4387.

Hiatt, A., Caffferkey, R. & Bowdish, K., 1989. Production of antibodies in transgenic plants. *Nature*, 342(6245), pp.76–78.

Hilsch, M. et al., 2014. Influenza A Matrix Protein M1 Multimerizes upon Binding to Lipid Membranes. *Biophysical Journal*, 107(4), pp.912–923.

Holland, J. et al., 1982. Rapid evolution of RNA genomes. *Science (New York, N.Y.)*, 215(4540), pp.1577–85.

Hood, E.E. et al., 1997. Commercial production of avidin from transgenic maize: characterization of transformant, production, processing, extraction and purification. *Molecular Breeding*, 3(4), pp.291–306.

Horn, M.E., Woodard, S.L. & Howard, J. a, 2004. Plant molecular farming: systems and products. *Plant cell reports*, 22(10), pp.711–20.

Houser, K. & Subbarao, K., 2015. Influenza Vaccines: Challenges and Solutions. *Cell host & microbe*, 17(3), pp.295–300.

Howley, B.N.F.D.M.K.P.M., 2013. *Fields virology* 6th editio. P. M. H. David M. Knipe, ed., Philadelphia : Wolters Kluwer Health/Lippincott Williams & Wilkins, ©2013.

Huafang Lai, Q.C. & Jake Stahnke, J.H., 2013. Agroinfiltration as an Effective and Scalable Strategy of Gene Delivery for Production of Pharmaceutical Proteins. *Advanced Techniques in Biology & Medicine*, 1(1).

Huang, Z. et al., 2013. Active inclusion bodies of acid phosphatase PhoC: aggregation induced by GFP fusion and activities modulated by linker flexibility. *Microbial Cell Factories*, 12(1), p.25.

Huleatt, J.W. et al., 2008. Potent immunogenicity and efficacy of a universal influenza vaccine candidate comprising a recombinant fusion protein linking influenza M2e to the TLR5 ligand flagellin. *Vaccine*, 26(2), pp.201–14.

Hurt, A.C. et al., 2009. Oseltamivir resistance and the H274Y neuraminidase mutation in seasonal, pandemic and highly pathogenic influenza viruses. *Drugs*, 69(18), pp.2523–31.

Hutchinson, E.C. et al., 2014. Conserved and host-specific features of influenza virion architecture. *Nature Communications*, 5, p.4816.

Hutchinson, E.C. & Fodor, E., 2014. Purification of influenza virions by haemadsorption and ultracentrifugation. *Protocol Exchange*.

Ibañez, L.I. et al., 2013. M2e-Displaying Virus-Like Particles with Associated RNA Promote T Helper 1 Type Adaptive Immunity against Influenza A P. Digard, ed. *PLoS ONE*, 8(3), p.e59081.

Imai, M. et al., 1998. Fusion of influenza virus with the endosomal membrane is inhibited by monoclonal antibodies to defined epitopes on the hemagglutinin. *Virus research*, 53(2), pp.129–39.

Impagliazzo, A. et al., 2015. A stable trimeric influenza hemagglutinin stem as a broadly protective immunogen. *Science*, 349(6254), pp.1301–1306.

International Committee on Taxonomy of Viruses, 2014. Virus Taxonomy: 2014 Release. Available at: http://www.ictvonline.org/.

Ito, T. et al., 1998. Molecular basis for the generation in pigs of influenza A viruses with pandemic potential. *Journal of virology*, 72(9), pp.7367–7373.

Iwatsuki-Horimoto, K. et al., 2006. The cytoplasmic tail of the influenza A virus M2 protein plays a role in viral assembly. *Journal of virology*, 80(11), pp.5233–40.

Jackson, L.A. et al., 2010. Safety, efficacy, and immunogenicity of an inactivated influenza vaccine in healthy adults: a randomized, placebo-controlled trial over two influenza seasons. *BMC Infectious Diseases*, 10(1), p.71.

Jackson, L.A., 2009. Using Surveillance to Evaluate Influenza Vaccine Effectiveness. *The Journal of Infectious Diseases*, 199(2), pp.155–158.

Jain, N.K. et al., 2015. Formulation and stabilization of recombinant protein based virus-like particle vaccines. *Advanced Drug Delivery Reviews*, 93, pp.42–55.

Jang, Y. & Seong, B., 2014. Options and Obstacles for Designing a Universal Influenza Vaccine. *Viruses*, 6(8), pp.3159–3180.

Jefferson, T. et al., 2005. Efficacy and effectiveness of influenza vaccines in elderly people: a systematic review. *Lancet*, 366(9492), pp.1165–74.

Jefferson, T. et al., 2009. Neuraminidase inhibitors for preventing and treating influenza in healthy adults: systematic review and meta-analysis. *BMJ (Clinical research ed.)*, 339, p.b5106.

Jefferson, T. et al., 2014. Vaccines for preventing influenza in healthy adults. *The Cochrane database of systematic reviews*, (3), p.CD001269.

Jefferson, T. et al., 2008. Vaccines for preventing influenza in healthy children. In T. Jefferson, ed. *Cochrane Database of Systematic Reviews*. Chichester, UK: John Wiley & Sons, Ltd.

Jefferson, T. et al., 2012. Vaccines for preventing influenza in healthy children. In T. Jefferson, ed. *Cochrane Database of Systematic Reviews*. Chichester, UK: John Wiley & Sons, Ltd.

Jevsevar, S. et al., 2005. Production of nonclassical inclusion bodies from which correctly folded protein can be extracted. *Biotechnology progress*, 21(2), pp.632–9.

Johnson, N.P. a. S. & Mueller, J., 2002. Updating the Accounts: Global Mortality of the 1918-1920 "Spanish" Influenza Pandemic. *Bulletin of the History of Medicine*, 76(1), pp.105–115.

Jung, S.-K.K., McDonald, K.A. & Dandekar, A.M., 2015. Effect of leaf incubation temperature profiles on agrobacterium tumefaciens-mediated transient expression. *Biotechnol Prog*, pp.783–790.

Kalthoff, D. et al., 2010. Immunization with Plant-Expressed Hemagglutinin Protects Chickens from Lethal Highly Pathogenic Avian Influenza Virus H5N1 Challenge Infection. *Journal of Virology*, 84(22), pp.12002–12010.

Kamionka, M., 2011. Engineering of therapeutic proteins production in Escherichia coli. *Current pharmaceutical biotechnology*, 12(2), pp.268–74.

Kanagarajan, S. et al., 2012. Transient expression of hemagglutinin antigen from low pathogenic avian influenza a (H7N7) in nicotiana benthamiana. *PLoS ONE*, 7(3), pp.1–10.

Kandun, I.N. et al., 2006. Three Indonesian Clusters of H5N1 Virus Infection in 2005. *New England Journal of Medicine*, 355(21), pp.2186–2194.

Kang, S.-M., Kim, M.-C. & Compans, R.W., 2012. Virus-like particles as universal influenza vaccines. *Expert review of vaccines*, 11(8), pp.995–1007.

Kato, N. & Eggers, H.J., 1969. Inhibition of uncoating of fowl plague virus by l-adamantanamine hydrochloride. *Virology*, 37(4), pp.632–641.

Kendall, P., 2007. Introduction to pandemic influenza. , (June), pp.240–244.

Kerviel, A. et al., 2016. Involvement of an Arginine Triplet in M1 Matrix Protein Interaction with Membranes and in M1 Recruitment into Virus-Like Particles of the Influenza A(H1N1)pdm09 Virus A. Pekosz, ed. *PLOS ONE*, 11(11), p.e0165421.

Khow, O. & Suntrarachun, S., 2012. Strategies for production of active eukaryotic proteins in bacterial expression system. *Asian Pacific Journal of Tropical Biomedicine*, 2(2), pp.159–162.

Kilbourne, E.D., 2006. Influenza pandemics of the 20th century. *Emerging Infectious Diseases*, 12(1), pp.9–14.

Kim, M.-C., Lee, J.-S., et al., 2013. Multiple heterologous M2 extracellular domains presented on virus-like particles confer broader and stronger M2 immunity than live influenza A virus infection. *Antiviral research*, 99(3), pp.328–35.

Kim, M.-C., Song, J.-M., et al., 2013. Virus-like Particles Containing Multiple M2 Extracellular Domains Confer Improved Cross-protection Against Various Subtypes

of Influenza Virus. *Molecular Therapy*, 21(2), pp.485–492.

Kissmann, J. et al., 2011. H1N1 influenza virus-like particles: physical degradation pathways and identification of stabilizers. *Journal of pharmaceutical sciences*, 100(2), pp.634–45.

Knipe, D.M. & Howley, P., 2001. *Fields Virology / Edition 4*,

Kosoy, O.I. et al., 2015. Novel thogotovirus associated with febrile illness and death, United States, 2014. *Emerging infectious diseases*, 21(5), pp.760–4.

Krammer, F. et al., 2013. Chimeric Hemagglutinin Influenza Virus Vaccine Constructs Elicit Broadly Protective Stalk-Specific Antibodies. *Journal of Virology*, 87(12), pp.6542–6550.

Krammer, F. et al., 2012. Hemagglutinin Stalk-Reactive Antibodies Are Boosted following Sequential Infection with Seasonal and Pandemic H1N1 Influenza Virus in Mice. *Journal of Virology*, 86(19), pp.10302–10307.

Krammer, F. & Palese, P., 2013. Influenza virus hemagglutinin stalk-based antibodies and vaccines. *Current Opinion in Virology*, 3(5), pp.521–530.

Krammer, F., Palese, P. & Steel, J., 2014. Advances in Universal Influenza Virus Vaccine Design and Antibody Mediated Therapies Based on Conserved Regions of the Hemagglutinin. In *Current topics in microbiology and immunology*. pp. 301–321.

Lagacé-Wiens, P.R.S., Rubinstein, E. & Gumel, A., 2010. Influenza epidemiology--past, present, and future. *Critical care medicine*, 38(4 Suppl), pp.e1–e9.

Lai, J. et al., 2011. Formation of virus-like particles from human cell lines exclusively expressing Influenza Neuraminidase. *BMC Proceedings*, 5(Suppl 1), p.P66.

Lamb, R.A., Zebedee, S.L. & Richardson, C.D., 1985. Influenza virus M2 protein is an integral membrane protein expressed on the infected-cell surface. *Cell*, 40(3), pp.627–33.

Landry, N. et al., 2010. Preclinical and Clinical Development of Plant-Made Virus-Like Particle Vaccine against Avian H5N1 Influenza R. A. M. Fouchier, ed. *PLoS ONE*, 5(12), p.e15559.

Latham, T. & Galarza, J.M., 2001. Formation of Wild-Type and Chimeric Influenza Virus-Like Particles following Simultaneous Expression of Only Four Structural Proteins. *Journal of Virology*, 75(13), pp.6154–6165.

Laver, W.G., Bischofberger, N. & Webster, R.G., 1999. Disarming flu viruses. *Scientific American*, 280, pp.78–87.

Leclerc, D. et al., 2013. A Novel M2e Based Flu Vaccine Formulation for Dogs M. Alsharifi, ed. *PLoS ONE*, 8(10), p.e77084.

Lee, Y.-T.Y.Y.-J. et al., 2014. New vaccines against influenza virus. *Clinical and experimental vaccine research*, 3(1), pp.12–28.

Leenaars, M. & Hendriksen, C.F.M., 2005. Critical Steps in the Production of Polyclonal and Monoclonal Antibodies: Evaluation and Recommendations. *ILAR Journal*, 46(3), pp.269–279.

Lim, H.K. et al., 2000. Production characteristics of interferon-alpha using an L-

arabinose promoter system in a high-cell-density culture. *Applied microbiology and biotechnology*, 53(2), pp.201–8.

Liu, W. et al., 2005. Sequence comparison between the extracellular domain of M2 protein human and avian influenza A virus provides new information for bivalent influenza vaccine design. *Microbes and Infection*, 7(2), pp.171–7.

Logrippo, A., 1960. Investigations of the use of beta-propiolactone in virus inactivation. *Annals of the New York Academy of Sciences*, 83, pp.578–94.

Lohaus, G. et al., 2001. Is the infiltration-centrifugation technique appropriate for the isolation of apoplastic fluid? A critical evaluation with different plant species. *Physiologia plantarum*, 111(4), pp.457–465.

Lomonossoff, G.P., 2016. Plant-produced biopharmaceuticals: A case of technical developments driving clinical deployment. *Science*, 353(6305), pp.1237–40.

López-Macías, C. et al., 2011. Safety and immunogenicity of a virus-like particle pandemic influenza A (H1N1) 2009 vaccine in a blinded, randomized, placebo-controlled trial of adults in Mexico. *Vaccine*, 29(44), pp.7826–7834.

Louie, J.K. et al., 2010. Severe 2009 H1N1 influenza in pregnant and postpartum women in California. *The New England journal of medicine*, 362(1), pp.27–35.

Lozano, R. et al., 2012. Global and regional mortality from 235 causes of death for 20 age groups in 1990 and 2010: a systematic analysis for the Global Burden of Disease Study 2010. *The Lancet*, 380(9859), pp.2095–2128.

Ma, W., Kahn, R.E. & Richt, J. a, 2008. The pig as a mixing vessel for influenza viruses: Human and veterinary implications. *Journal of molecular and genetic medicine : an international journal of biomedical research*, 3(1), pp.158–166.

Maassab, H.F. & Bryant, M.L., 1999. The development of live attenuated cold-adapted influenza virus vaccine for humans. *Reviews in medical virology*, 9(4), pp.237–44.

Maclean, J. et al., 2007. Optimization of human papillomavirus type 16 (HPV-16) L1 expression in plants: comparison of the suitability of different HPV-16 L1 gene variants and different cell-compartment localization. *The Journal of general virology*, 88(Pt 5), pp.1460–9.

Malik Peiris, J.S., Poon, L.L.M. & Guan, Y., 2009. Emergence of a novel swine-origin influenza A virus (S-OIV) H1N1 virus in humans. *Journal of Clinical Virology*, 45(3), pp.169–173.

Mallajosyula, V.V.A. et al., 2014. Influenza hemagglutinin stem-fragment immunogen elicits broadly neutralizing antibodies and confers heterologous protection. *Proceedings of the National Academy of Sciences*, 111(25), pp.E2514–E2523.

Malyala, P. & Singh, M., 2008. Endotoxin Limits in Formulations for Preclinical Research. *Journal of Pharmaceutical Sciences*, 97(6), pp.2041–2044.

Manderson, D., Dempster, R. & Chisti, Y., 2006. A recombinant vaccine against hydatidosis: production of the antigen in Escherichia coli. *Journal of industrial microbiology & biotechnology*, 33(3), pp.173–82.

Mardanova, E.S., Kotlyarov, R.Y., Kuprianov, V. V., Stepanova, L.A., Tsybalova, L.M., Lomonossoff, G.P., et al., 2015. High immunogenicity of plant-produced influenza

based on the M2e peptide fused to flagellin. *Bioengineered*, 5979(January 2016), pp.00–00.

Mardanova, E.S., Kotlyarov, R.Y., Kuprianov, V. V., Stepanova, L.A., Tsybalova, L.M., Lomonosoff, G.P., et al., 2015. Rapid high-yield expression of a candidate influenza vaccine based on the ectodomain of M2 protein linked to flagellin in plants using viral vectors. *BMC Biotechnology*, 15(1), p.42.

Marillonnet, S. et al., 2005. Systemic Agrobacterium tumefaciens–mediated transfection of viral replicons for efficient transient expression in plants. *Nature Biotechnology*, 23(6), pp.718–723.

Mason, H.S., Lam, D.M. & Arntzen, C.J., 1992. Expression of hepatitis B surface antigen in transgenic plants. *Proceedings of the National Academy of Sciences of the United States of America*, 89(24), pp.11745–11749.

Matić, S. et al., 2011. Efficient production of chimeric Human papillomavirus 16 L1 protein bearing the M2e influenza epitope in Nicotiana benthamiana plants. *BMC Biotechnology*, 11(1), p.106.

Mayor, S., 2010. Acute respiratory infections are world's third leading cause of death. *BMJ*, 341(nov09 1), pp.c6360–c6360.

McCown, M.F. & Pekosz, A., 2006. Distinct Domains of the Influenza A Virus M2 Protein Cytoplasmic Tail Mediate Binding to the M1 Protein and Facilitate Infectious Virus Production. *Journal of virology*, 80(16), pp.8178–8189.

McCown, M.F. & Pekosz, A., 2005. The influenza A virus M2 cytoplasmic tail is required for infectious virus production and efficient genome packaging. *Journal of virology*, 79(6), pp.3595–605.

Meyers, A. et al., 2008. Expression of HIV-1 antigens in plants as potential subunit vaccines. *BMC Biotechnology*, 8(1), p.53.

Miller, M.S. et al., 2013. 1976 and 2009 H1N1 influenza virus vaccines boost anti-hemagglutinin stalk antibodies in humans. *The Journal of infectious diseases*, 207(1), pp.98–105.

Mitraki, A. et al., 1991. Global suppression of protein folding defects and inclusion body formation. *Science (New York, N.Y.)*, 253(5015), pp.54–8.

Molinari, N.-A.M. et al., 2007. The annual impact of seasonal influenza in the US: measuring disease burden and costs. *Vaccine*, 25(27), pp.5086–96.

Monto, A.S. et al., 1999. Zanamivir in the prevention of influenza among healthy adults: a randomized controlled trial. *JAMA*, 282(1), pp.31–5.

Morell, M. et al., 2008. Inclusion bodies: Specificity in their aggregation process and amyloid-like structure. *Biochimica et Biophysica Acta (BBA) - Molecular Cell Research*, 1783(10), pp.1815–1825.

Morens, D.M., Folkers, G.K. & Fauci, A.S., 2004. The challenge of emerging and re-emerging infectious diseases. *Nature*, 430(6996), pp.242–9.

Mortimer, E. et al., 2012. Setting up a platform for plant-based influenza virus vaccine production in South Africa. *BMC biotechnology*, 12, p.14.

Nachbagauer, R. et al., 2014. Induction of Broadly Reactive Anti-Hemagglutinin Stalk

Antibodies by an H5N1 Vaccine in Humans. *Journal of Virology*, 88(22), pp.13260–13268.

Naffakh, N. & van der Werf, S., 2009. April 2009: an outbreak of swine-origin influenza A(H1N1) virus with evidence for human-to-human transmission. *Microbes and Infection*, 11(8–9), pp.725–728.

Neirynck, S., Deroo, T. & Saelens, X., 1999. A universal influenza A vaccine based on the extracellular domain of the M2 protein. *Nature medicine*.

Nelson, M.I. et al., 2009. The origin and global emergence of adamantane resistant A/H3N2 influenza viruses. *Virology*, 388(2), pp.270–8.

Nikbakht, G., Jahntigh, M. & Assadian, F., 2012. Generation of Egg Yolk Antibodies in Chicken Against Influenza M2 (M2e) Protein. *International Conference on Chemical, Biological and Medical Sciences*, 2, pp.25–27.

Noda, T., 2012. Native Morphology of Influenza Virions. *Frontiers in Microbiology*, 2(January), pp.1–5.

Obembe, O.O. et al., 2011. Advances in plant molecular farming. *Biotechnology advances*, 29(2), pp.210–22.

Ochocka, A.-M., Czyzewska, M. & Pawełczyk, T., 2003. Expression in Escherichia coli of human ARHGAP6 gene and purification of His-tagged recombinant protein. *Acta biochimica Polonica*, 50(1), pp.239–47.

Osterhaus, A.D. et al., 2000. Influenza B virus in seals. *Science (New York, N.Y.)*, 288(5468), pp.1051–3.

Osterholm, M.T. et al., 2012. Efficacy and effectiveness of influenza vaccines: a systematic review and meta-analysis. *The Lancet Infectious Diseases*, 12(1), pp.36–44.

Partridge, J. & Kieny, M.P., 2013. Global production capacity of seasonal influenza vaccine in 2011. *Vaccine*, 31(5), pp.728–731.

Pêra, F.F.P.G. et al., 2015. Engineering and expression of a human rotavirus candidate vaccine in Nicotiana benthamiana. *Virology Journal*, 12(1), p.205.

Petukhova, N. V et al., 2013. Immunogenicity and protective efficacy of candidate universal influenza A nanovaccines produced in plants by Tobacco mosaic virus-based vectors. *Current pharmaceutical design*, 19(31), pp.5587–600.

Pillet, S. et al., 2015. Plant-derived H7 VLP vaccine elicits protective immune response against H7N9 influenza virus in mice and ferrets. *Vaccine*, 33(46), pp.6282–9.

Pogue, G.P. et al., 2010. Production of pharmaceutical-grade recombinant aprotinin and a monoclonal antibody product using plant-based transient expression systems. *Plant Biotechnology Journal*, 8(5), pp.638–654.

Pope, B. & Kent, H.M., 1996. High Efficiency 5 Min Transformation of Escherichia Coli. *Nucleic Acids Research*, 24(3), pp.536–537.

Prasetyoputri, A. et al., 2010. The Development of A Bioassay Based on Heterologous Expression of M2 Ion-Channel Protein. , 14(2), pp.9–14.

Price, G.E. et al., 2010. Single-dose mucosal immunization with a candidate universal

influenza vaccine provides rapid protection from virulent H5N1, H3N2 and H1N1 viruses. *PloS one*, 5(10), p.e13162.

Rambaut, A. et al., 2008. The genomic and epidemiological dynamics of human influenza A virus. *Nature*, 453(7195), pp.615–619.

Rappazzo, C.G. et al., 2016. Recombinant M2e outer membrane vesicle vaccines protect against lethal influenza A challenge in BALB/c mice. *Vaccine*, pp.1–7.

Regnard, G.L. et al., 2010. High level protein expression in plants through the use of a novel autonomously replicating geminivirus shuttle vector. *Plant Biotechnology Journal*, 8(1), pp.38–46.

Richard, S.A., Viboud, C. & Miller, M.A., 2010. Evaluation of Southern Hemisphere influenza vaccine recommendations. *Vaccine*, 28(15), pp.2693–2699.

del Rio, C. & Guarner, J., 2010. The 2009 influenza A (H1N1) pandemic: what have we learned in the past 6 months. *Transactions of the American Clinical and Climatological Association*, 121(1), pp.128-37-40.

Rosano, G.L. & Ceccarelli, E.A., 2014. Recombinant protein expression in Escherichia coli: advances and challenges. *Frontiers in Microbiology*, 5.

Rossman, J.S. et al., 2010. Influenza virus M2 protein mediates ESCRT-independent membrane scission. *Cell*, 142(6), pp.902–13.

Ruigrok, R.W.H. et al., 2000. Membrane Interaction of Influenza Virus M1 Protein. *Virology*, 267(2), pp.289–298.

Rybicki, E.P., 2010. Plant-made vaccines for humans and animals. *Plant biotechnology journal*, 8(5), pp.620–37.

Rybicki, E.P. & Kightley, R., 2015. Influenza Virus. Introduction to a Killer. *Apple iBooks Store*, p.64.

Sainsbury, F. & Lomonossoff, G.P., 2008. Extremely high-level and rapid transient protein production in plants without the use of viral replication. *Plant physiology*, 148(3), pp.1212–8.

Sainsbury, F. & Lomonossoff, G.P., 2014. Transient expressions of synthetic biology in plants. *Current Opinion in Plant Biology*, 19, pp.1–7.

Sainsbury, F., Thuenemann, E.C. & Lomonossoff, G.P., 2009. pEAQ : versatile expression vectors for easy and quick transient expression of heterologous proteins in plants. , pp.682–693.

Saluja, V., 2010. *Novel perspectives for influenza vaccine formulation and administration*,

Sambrook, J., Fritsch, E.F. & Maniatis, T., 1989. *Molecular Cloning: A Laboratory Manual, Volume 1*, Cold Spring Harbor laboratory Press.

Samson, M. et al., 2013. Influenza virus resistance to neuraminidase inhibitors. *Antiviral Research*, 98(2), pp.174–185.

Sato, Y. et al., 2003. Localization of influenza virus proteins to nuclear dot 10 structures in influenza virus-infected cells. *Virology*, 310(1), pp.29–40.

Schillberg, S., Twyman, R.M. & Fischer, R., 2005. Opportunities for recombinant antigen

and antibody expression in transgenic plants--technology assessment. *Vaccine*, 23(15), pp.1764–9.

Scholtissek, C., Ludwig, S. & Fitch, W.M., 1993. Analysis of influenza A virus nucleoproteins for the assessment of molecular genetic mechanisms leading to new phylogenetic virus lineages. *Archives of Virology*, 131, pp.237–250.

Shaw, M.L., 2011. The host interactome of influenza virus presents new potential targets for antiviral drugs. *Reviews in Medical Virology*, 21(6), pp.358–369.

Shcherbik, S. et al., 2016. Implementation of new approaches for generating conventional reassortants for live attenuated influenza vaccine based on Russian master donor viruses. *Journal of Virological Methods*, 227, pp.33–39.

Shen, W.J. & Forde, B.G., 1989. Efficient transformation of Agrobacterium spp. by high voltage electroporation. *Nucleic acids research*, 17(20), p.8385.

Sheu, T.G. et al., 2008. Surveillance for neuraminidase inhibitor resistance among human influenza A and B viruses circulating worldwide from 2004 to 2008. *Antimicrobial agents and chemotherapy*, 52(9), pp.3284–92.

Shoji, Y. et al., 2015. Immunogenicity of H1N1 influenza virus-like particles produced in Nicotiana benthamiana. *Human Vaccines & Immunotherapeutics*, 11(1), pp.118–123.

Shoji, Y. et al., 2008. Plant-expressed HA as a seasonal influenza vaccine candidate. *Vaccine*, 26(23), pp.2930–2934.

Singh, A. et al., 2015. Protein recovery from inclusion bodies of Escherichia coli using mild solubilization process. *Microbial Cell Factories*, 14(1), p.41.

Singh, S.M. & Panda, A.K., 2005. Solubilization and refolding of bacterial inclusion body proteins. *Journal of Bioscience and Bioengineering*, 99(4), pp.303–310.

Sivashanmugam, A. et al., 2009. Practical protocols for production of very high yields of recombinant proteins using Escherichia coli. *Protein Science*, 18(5), pp.936–948.

Slepushkin, V.A. et al., 1995. Protection of mice against influenza A virus challenge by vaccination with baculovirus-expressed M2 protein. *Vaccine*, 13(15), pp.1399–402.

Smith, W., Andrewes, C.H. & Laidlaw, P.P., 1933. A VIRUS OBTAINED FROM INFLUENZA PATIENTS. *The Lancet*, 222(5732), pp.66–68.

Snyder, M.H. et al., 1988. Four viral genes independently contribute to attenuation of live influenza A/Ann Arbor/6/60 (H2N2) cold-adapted reassortant virus vaccines. *Journal of virology*, 62(2), pp.488–95.

Soema, P.C. et al., 2015. Current and next generation influenza vaccines: Formulation and production strategies. *European Journal of Pharmaceutics and Biopharmaceutics*, 94, pp.251–263.

Song, H. et al., 2010. In vitro stimulation of human influenza-specific CD8+ T cells by dendritic cells pulsed with an influenza virus-like particle (VLP) vaccine. *Vaccine*, 28(34), pp.5524–5532.

Song, J.-M., Wang, B.-Z., et al., 2011. Influenza Virus-Like Particles Containing M2 Induce Broadly Cross Protective Immunity E. J. Kremer, ed. *PLoS ONE*, 6(1), p.e14538.

Song, J.-M., Van Rooijen, N., et al., 2011. Vaccination inducing broad and improved cross protection against multiple subtypes of influenza A virus. *Proceedings of the National Academy of Sciences of the United States of America*, 108(2), pp.757–61.

Sridhar, S., Brokstad, K. & Cox, R., 2015. Influenza Vaccination Strategies: Comparing Inactivated and Live Attenuated Influenza Vaccines. *Vaccines*, 3(2), pp.373–389.

Staneková, Z. et al., 2011. Heterosubtypic protective immunity against influenza A virus induced by fusion peptide of the hemagglutinin in comparison to ectodomain of M2 protein. *Acta virologica*, 55(1), pp.61–7.

Staneková, Z. & Varečková, E., 2010. Conserved epitopes of influenza A virus inducing protective immunity and their prospects for universal vaccine development. *Virology Journal*, 7(1), p.351.

Steel, J. et al., 2010. Influenza Virus Vaccine Based on the Conserved Hemagglutinin Stalk Domain. *mBio*, 1(1), pp.e00018-10-e00018-10.

Stevenson, J.P. & Biddle, F., 1966. Pleomorphism of influenza virus particles under the electron microscope. *Nature*, 212(5062), pp.619–21.

Stills, H.F. et al., 2012. Polyclonal antibody production. *The laboratory rabbit, guinea pig, hamster and other rodents. Oxford, UK: Elsevier Inc*, pp.259–274.

Stiver, G., 2003. The treatment of influenza with antiviral drugs. *Canadian Medical Association Journal*, 168(1), pp.49–57.

Stokes, J. et al., 1937. RESULTS OF IMMUNIZATION BY MEANS OF ACTIVE VIRUS OF HUMAN INFLUENZA 1. *Journal of Clinical Investigation*, 16(2), pp.237–243.

Suarez, D.L. & Schultz-Cherry, S., 2000. Immunology of avian influenza virus: A review. *Developmental and Comparative Immunology*, 24(2–3), pp.269–283.

Syed, Z. et al., 2012. Prokaryotic expression and characterisation of recombinant M1 protein of an Indian H5N1 avian influenza virus. *The Indian Journal of Animal Sciences*, 82(12).

Tang, X.-C., Lu, H.-R. & Ross, T.M., 2011. Baculovirus-Produced Influenza Virus-like Particles in Mammalian Cells Protect Mice from Lethal Influenza Challenge. *Viral Immunology*, 24(4), pp.311–319.

Tartof, K.. & Hobbs, C.., 1987. Improved Media for Growing Plasmid and Cosmid Clones. *Bethesda research. Lab Focus*, 2(9), p.12.

Taubenberger, J. & Morens, D., 2006. 1918 Influenza: the mother of all pandemics. *Rev Biomed*, 17(1), pp.69–79.

Taubenberger, J.K., 2006. The origin and virulence of the 1918 “Spanish” influenza virus. *Proceedings of the American Philosophical Society*, 150(1), pp.86–112.

Taylor, R.M., 1949. Studies on survival of influenza virus between epidemics and antigenic variants of the virus. *American journal of public health and the nation’s health*, 39(2), pp.171–8.

Tegel, H., Ottosson, J. & Hober, S., 2011. Enhancing the protein production levels in Escherichia coli with a strong promoter. *FEBS Journal*, 278(5), pp.729–739.

Terpe, K., 2006. Overview of bacterial expression systems for heterologous protein

production: from molecular and biochemical fundamentals to commercial systems. *Applied Microbiology and Biotechnology*, 72(2), pp.211–222.

Thompson, C.M. et al., 2015. Critical assessment of influenza VLP production in Sf9 and HEK293 expression systems. *BMC Biotechnology*, 15(1), p.31.

Throsby, M. et al., 2008. Heterosubtypic Neutralizing Monoclonal Antibodies Cross-Protective against H5N1 and H1N1 Recovered from Human IgM+ Memory B Cells D. Unutmaz, ed. *PLoS ONE*, 3(12), p.e3942.

Thuenemann, E.C. et al., 2013. The Use of Transient Expression Systems for the Rapid Production of Virus-like Particles in Plants. *Curr Pharm Des*, 19(31), pp.5564–5573.

Tobita, K. et al., 1975. Plaque assay and primary isolation of influenza A viruses in an established line of canine kidney cells (MDCK) in the presence of trypsin. *Medical microbiology and immunology*, 162(1), pp.9–14.

Tran, T.H. et al., 2004. Avian influenza A (H5N1) in 10 patients in Vietnam. *The New England journal of medicine*, 350(12), pp.1179–88.

Traynor, K., 2012. First quadrivalent flu vaccine approved. *American journal of health-system pharmacy : AJHP : official journal of the American Society of Health-System Pharmacists*, 69(7), p.538.

Treanor, J.J. et al., 1990. Passively transferred monoclonal antibody to the M2 protein inhibits influenza A virus replication in mice. *Journal of virology*, 64(3), pp.1375–7.

Turley, C.B. et al., 2011. Safety and immunogenicity of a recombinant M2e-flagellin influenza vaccine (STF2.4xM2e) in healthy adults. *Vaccine*, 29(32), pp.5145–52.

Tyulkina, L.G. et al., 2011. New viral vector for superproduction of epitopes of vaccine proteins in plants. *Acta naturae*, 3(4), pp.73–82.

Varecková, E. et al., 2003. Inhibition of fusion activity of influenza A haemagglutinin mediated by HA2-specific monoclonal antibodies. *Archives of virology*, 148(3), pp.469–86.

Vicente, T. et al., 2011. Large-scale production and purification of VLP-based vaccines. *Journal of Invertebrate Pathology*, 107, pp.S42–S48.

Voinnet, O. et al., 2003. An enhanced transient expression system in plants based on suppression of gene silencing by the p19 protein of tomato bushy stunt virus. *The Plant journal : for cell and molecular biology*, 33(5), pp.949–56.

de Vries, R.D., Altenburg, A.F. & Rimmelzwaan, G.F., 2015. Universal influenza vaccines, science fiction or soon reality? *Expert review of vaccines*, 14(10), pp.1299–301.

Waheed, T.M. et al., 2016. Need of cost-effective vaccines in developing countries: What plant biotechnology can offer? Background. *SpringerPlus*, 5.

Walaza, S. & Cohen, C., 2015. Recommendations pertaining to the use of influenza vaccines and influenza antiviral drugs: Influenza 2015. *South African Medical Journal*, 105(2), p.90.

Wang, B.-Z. et al., 2007. Incorporation of High Levels of Chimeric Human Immunodeficiency Virus Envelope Glycoproteins into Virus-Like Particles. *Journal of Virology*, 81(20), pp.10869–10878.

Wang, D. et al., 2010. The Lack of an Inherent Membrane Targeting Signal Is Responsible for the Failure of the Matrix (M1) Protein of Influenza A Virus To Bud into Virus-Like Particles. *Journal of Virology*, 84(9), pp.4673–4681.

Wathen, M.W., Barro, M. & Bright, R. a., 2013. Antivirals in seasonal and pandemic influenza-future perspectives. *Influenza and other Respiratory Viruses*, 7(1 SUPPL.1), pp.76–80.

Wei, H.-J. et al., 2011. Fabrication of influenza virus-like particles using M2 fusion proteins for imaging single viruses and designing vaccines. *Vaccine*, 29(41), pp.7163–7172.

Weldon, W.C. et al., 2010. Enhanced Immunogenicity of Stabilized Trimeric Soluble Influenza Hemagglutinin R. Tripp, ed. *PLoS ONE*, 5(9), p.e12466.

WHO, 2015. Recommended composition of influenza virus vaccines for use in the 2016 southern hemisphere influenza season. *World Health*.

Wiersma, L., Rimmelzwaan, G. & de Vries, R., 2015. Developing Universal Influenza Vaccines: Hitting the Nail, Not Just on the Head. *Vaccines*, 3, pp.239–262.

Williams, D.B. & Carter, C.B., 2009. *Transmission Electron Microscopy*, Boston, MA: Springer US.

Wilson, I. a, Skehel, J.J. & Wiley, D.C., 1981. Structure of the haemagglutinin membrane glycoprotein of influenza virus at 3 A resolution. *Nature*, 289(5796), pp.366–373.

Witzel, K. et al., 2011. Comparative evaluation of extraction methods for apoplastic proteins from maize leaves. *Plant Methods*, 7(1), p.48.

Wohlbold, T.J. et al., 2015. Vaccination with soluble headless hemagglutinin protects mice from challenge with divergent influenza viruses. *Vaccine*, 33(29), pp.3314–3321.

Wong, S.S. & Webby, R.J., 2013. Traditional and new influenza vaccines. *Clin.Microbiol.Rev.*, 26(1098–6618 (Electronic)), pp.476–492.

Wroblewski, T., Tomczak, A. & Michelmore, R., 2005. Optimization of Agrobacterium-mediated transient assays of gene expression in lettuce, tomato and Arabidopsis. *Plant Biotechnology Journal*, 3(2), pp.259–273.

Wu, C.-Y. et al., 2010. Mammalian Expression of Virus-Like Particles for Advanced Mimicry of Authentic Influenza Virus C. Hauser, ed. *PLoS ONE*, 5(3), p.e9784.

Wu, Y. et al., 2014. Bat-derived influenza-like viruses H17N10 and H18N11. *Trends in microbiology*, 22(4), pp.183–91.

Yang, H. et al., 2011. A novel and convenient method to immunize animals: Inclusion bodies from recombinant bacteria as antigen to directly immunize animals. *African Journal of Biotechnology*, 10(41), pp.8146–8150.

Yang, L.P.H., 2013. Recombinant Trivalent Influenza Vaccine (Flublok®): A Review of Its Use in the Prevention of Seasonal Influenza in Adults. *Drugs*, 73(12), pp.1357–1366.

Yang, Y. et al., 2009. A Novel Method to Incorporate Bioactive Cytokines as Adjuvants on the Surface of Virus Particles. *Journal of Interferon & Cytokine Research*, 29(1), pp.9–22.

Yassine, H.M. et al., 2015. Hemagglutinin-stem nanoparticles generate heterosubtypic influenza protection. *Nature Medicine*, 21(9), pp.1065–1070.

Yasui, K. et al., 2010. Enhanced solubilization of membrane proteins by alkylamines and polyamines. *Protein Science*, p.NA-NA.

Young, K.R. et al., 2015. Generation and characterization of a trackable plant-made influenza H5 virus-like particle (VLP) containing enhanced green fluorescent protein (eGFP). *The FASEB Journal*, 2005, pp.1–11.

Zebedee, S.L. & Lamb, R.A., 1988. Influenza A virus M2 protein: monoclonal antibody restriction of virus growth and detection of M2 in virions. *Journal of virology*, 62(8), pp.2762–72.

Zeltins, A., 2013. Construction and Characterization of Virus-Like Particles: A Review. *Molecular Biotechnology*, 53(1), pp.92–107.

Zheng, W. & Tao, Y.J., 2013. Structure and assembly of the influenza A virus ribonucleoprotein complex. *FEBS letters*, 587(8), pp.1206–14.

Zhong, G.-Y. et al., 1999. Commercial production of aprotinin in transgenic maize seeds. *Molecular Breeding*, 5(4), pp.345–356.

Zou, P., Liu, W. & Chen, Y.H., 2005. The epitope recognized by a monoclonal antibody in influenza A virus M2 protein is immunogenic and confers immune protection. *International Immunopharmacology*, 5(4), pp.631–635.

van Zyl, A.R., Meyers, A.E. & Rybicki, E.P., 2016. Transient Bluetongue virus serotype 8 capsid protein expression in Nicotiana benthamiana. *Biotechnology Reports*, 9, pp.15–24.

Appendix A

Table A1|Compilation of the M2e sequences used to create the consensus M2e

Strain	Subtype	GenBank accession number
(A/Georgia/M5081/2012)	H1N1	CY148069.1
(A/Georgia/M5081/2012)	*	CY147988.1
(A/Brisbane/59/2007)	*	CY163841.1
(A/California/04/2009)	*	AEE69011.1
(A/Korea/01-2-2/2009)	*	CY110891.1
(A/Netherlands/602/2009)	*	CY148116.1
(A/Korea/01-2-9/2009)	*	CY110906.1
(A/Mexico/InDRE4487/2009)	*	GQ303341.1
(A/Niigata/749/2009)	*	GU138893.1
(A/India/P1114854/2011)	*	KF280666.1
(A/Cambodia/V1019320/2011)	*	KC118566.1
(A/swine/Geldern/IDT2888/04)	*	EU478821.1
(A/KOL/507/2007)	*	AEE68984.1
(A/swine/Hannover/1/81)	*	EU478795.1
(A/swine/Minnesota/SG1403/2011)	H1N2	CY159018.1
(A/swine/Colorado/02875/2009)	*	CY159450.1
(A/Singapore/1-MA12E/1957)	H2N2	CY087793.1
(A/Wisconsin/67/2005(H3N2))	H3N2	CY164001.1
(A/HaNoi/Q769/2007(H3N2))	*	CY105751.1
(A/swine/Quebec/01003/2006(H3N2))	*	CY160179.1
(A/swine/Italy/1553-2/98)	*	AJ293938.1
(A/blow fly/Kyoto/93/2004)	H5N1	AB212651.2
(A/chicken/Moscow/2/2007)	*	EF474449.1
(A/chicken/Kulon Progo/BBVet-XII-2/2004)	*	DQ492930.1
(A/Thailand/2(SP-33)/2004)	*	AY627893.1
(A/Viet Nam/1194/2004)	*	AY651387.1
(A/Viet Nam/1203/2004)	*	AAT70528.1
(A/Hong Kong/156/97)	*	AAC34266.1
(A/duck/Yangzhou/013/2008)	H6N5	ACZ54004.1
(A/Chicken/New York/8030-2/96)	H7N2	AF073190.1
(A/Nanjing/2/2013)	*	KF007047.1
(A/shearwater/Australia/2/1972)	H10N8	CY087761.1
M2e consensus sequence	-	(Fiers et al. 2004)